# INTERACTION OF SCRIBBLE WITH ZONULA OCCLUDENS AND INTERMEDIATE FILAMENT PROTEINS

**DOMINIC PHUA CHENG YANG**

**INSTITUTE OF MOLECULAR AND CELL BIOLOGY**

**DEPARTMENT OF PHYSIOLOGY**

**NATIONAL UNIVERSITY OF SINGAPORE**

**2008**

# INTERACTION OF SCRIBBLE WITH ZONULA OCCLUDENS AND INTERMEDIATE FILAMENT PROTEINS

**DOMINIC PHUA CHENG YANG**

**B.Sc. (Hons.), NUS**

**A THESIS SUBMITTED**

**FOR THE DEGREE OF DOCTOR OF PHILOSOPHY**

**INSTITUTE OF MOLECULAR AND CELL BIOLOGY**

**DEPARTMENT OF PHYSIOLOGY**

**NATIONAL UNIVERSITY OF SINGAPORE**

**2008**

## Acknowledgements

I would like to thank Dr. Walter Hunziker for giving me the opportunity to pursue this graduate programme in his laboratory. For his kind and patient guidance, encouragement and unwavering faith in me as a scientist, I am eternally grateful.

I am also grateful to my graduate programme committee members, Dr. Edward Manser and Dr. Tang Bor Luen for their continual support and insightful critique of this work throughout my candidature.

The progress of my project would not have been possible if not for the generous contributions of my collaborators. For their kind offering of reagents, I am thankful to Dr Ronald Liem, Dr Rudolf Leube, Dr Sachdev Sidhu and Dr Birgit Lane. For helping me with cell sorting, I am grateful to Lynnette Chen. For handling my IT affairs, my thanks go to Yap Kok Wee. To Dr Patrick Humbert, I am especially indebted not only for his generous contribution of reagents but also his support during the course of my project and advice throughout the writing and revision of the publication of my work.

My candidature in the Institute of Molecular and Cell Biology has been an eventful one and it is to this institute and the friends I have made here that I express my gratitude to. To my lab mates, both past and present, you all make it a daily joy for me to work and play in WH lab. These are the memories that I will cherish forever. To everyone else that I have had the pleasure to have known, thank you for taking part in this journey of mine.

Lastly, in no uncertain terms, my candidature will not be successful if not for the steadfast encouragement of my family. It is their undying support that has given me sustenance over these challenging years. To them and God, I owe everything.

# Table of Contents

## Summary

Cell polarization is defined by the asymmetric distribution of membrane and peripheral molecules, organelles and cytoskeletal networks into structurally, biochemically and functionally separate regions in the plasma membrane and cytoplasm. Such a distribution is fundamental to the progression of basic cellular processes like cell proliferation, growth, differentiation and movement, and is regulated by various hierarchical cellular events that are activated by coordinated spatial and temporal cues. The multidomain PDZ-containing scaffolding protein Scribble (Scrib) has been identified as a key polarity regulator and neoplastic tumor suppressor in *Drosophila* epithelial cells. The loss of Scrib results in the disruption of epithelial polarity and architecture, and unregulated cell proliferation. In addition, the mammalian Scrib homologue mediates cell-cell adhesion and controls the polarization of epithelial cells during directed cell migration.

In this study, we describe and characterize novel interactions between mammalian Scrib and the tight junction proteins Zonula Occludens (ZO) -2 and -3; and the intermediate filament vimentin. Scrib associates with both ZO-2 and ZO-3 via PDZ domain interactions. In fibroblasts, this interaction is responsible for Scrib recruitment to ZO-2 and ZO-3 positive vesicular structures. This may reflect a spatio-temporal role of these ZO proteins in the recruitment of Scrib during epithelial cell polarization since Scrib localizes substantially with its ZO interactors along the lateral membrane in non-polarized but not in polarized cells. Scrib interaction with vimentin is also PDZ domain-dependent. In epithelial cells, this interaction has a stabilizing effect on Scrib protein levels, with vimentin depletion resulting in the proteasome-dependent degradation of

Scrib. This consequently leads to defective epithelial cell-cell adhesion and randomized deregulated cell migration, closely phenocopying Scrib depletion. Double knockdown of Scrib and vimentin exhibits phenotypes similar to single silencing and suggests the function of both proteins in a single linear pathway. This stabilization of Scrib expression and function by vimentin relates well with previously reported observations of vimentin upregulation during epithelial wound healing and epithelial-mesenchymal transitions. Thus this implies a possible regulatory function of vimentin on Scrib homeostasis during epithelial migration.

# List of Figures, Table and Movies

# Abbreviations

| | |
|---|---|
| aa | Amino acid |
| ADP | Adenosine diphosphate |
| AJ | Adherens junction |
| APC | Adenomatous polyposis coli |
| Arf | ADP ribosylation factor |
| Arp | Actin-related protein |
| aPKC | Atypical protein kinase C |
| ATL | Adult T-cell leukaemia |
| ATP | Adenosine triphosphate |
| avl | Avalanche |
| CAM | Cell adhesion molecule |
| CD1 | Cyclin D1 |
| CDK4 | Cell division kinase 4 |
| CE | Convergent extension |
| Crc | Circletail |
| Crb | Crumbs |
| Crtam | Class-I MHC-restricted T-cell associated molecule |
| DNA | Deoxyribonucleic acid |
| Dlg | Discs large |
| DS | Desmosome |
| E6AP | E6-associated protein |
| ECM | Extracellular matrix |
| EGFR | Epidermal growth factor receptor |
| EMT | Epithelial-mesenchymal transition |
| FAK | Focal adhesion kinase |
| GAP | GTPase-activating protein |
| GDP | Guanosine diphosphate |
| GEF | Guanine nucleotide exchange factor |
| GFAP | Glial fibrillary acid protein |
| GIT | GRK-interacting protein |
| GMC | Ganglion mother cell |
| GMP | Guanosine monophosphate |
| GRK | G-protein-coupled receptor-kinase |
| GTX | Gtaxin |
| GTP | Guanosine triphosphate |
| GTPase | Guanosine triphosphatase |
| GSK | Glycogen synthase kinase |
| GUK | Guanylate kinase |
| GUKH | GUK-holder |
| HPV | Human papillomavirus |
| HTLV | Human T-cell leukaemia virus |
| Ig | Immunoglobulin |
| IF | Intermediate filament |
| IFN | Interferon |

| | |
|---|---|
| IS | Immunological synapse |
| JAK | Janus protein tyrosine kinase |
| JAM | Junctional adhesion molecule |
| JNK | Jun N-terminal kinase |
| K8 | Keratin 8 |
| K18 | Keratin 18 |
| LAP | LRR and PDZ |
| LAPSD | LAP-specific domain |
| Lgl | Lethal giant larvae |
| Lp | Loop-tail |
| LPP | LIM domain containing preferred translocation partner in lipoma |
| LRR | Leucine-rich repeat |
| MAGUK | Membrane-associated guanylate kinase |
| MAPK | Mitogen-activated protein kinase |
| MDCK | Madin-darby canine kidney |
| MHC | Major histocompatibility complex |
| MTOC | Microtubule-organizing centre |
| mTOR | Mammalian target of rapamycin |
| NES | Nuclear export signal |
| NF | Neurofilament |
| NFAT | Nuclear factor of activated T-cell |
| NLS | Nuclear localization signal |
| NMJ | Neuromuscular junction |
| NTD | Neural tube defect |
| NSF | *N*-ethylmaleimide-sensitive fusion protein |
| PA | Primordial adhesion junction |
| PAK | p21-activated kinase |
| PALS | Protein associated with Lin seven |
| Par | Partitioning-defective |
| PATJ | PALS1-associated tight junction protein |
| PBM | PDZ binding mutant |
| PCNA | Proliferating cell nuclear antigen |
| PCP | Planar cell polarity |
| PDZ | PSD-95/Dlg/ZO-1 |
| PI3K | Phosphatidylinositol 3-kinase |
| PIX | PAK-interacting exchange factor |
| PKC | Protein kinase C |
| PR | Proline-rich |
| PSD-95 | Post synaptic density protein 95 |
| Rb | Retinoblastoma |
| RNA | Ribonucleic acid |
| RTK | Receptor tyrosine kinase |
| SAF-B | Scaffold attachment factor-B |
| SAR | Sub-apical region |
| Scrib | Scribble |
| SH3 | Src homology 3 |

| | |
|---|---|
| SiRNA | Small interfering RNA |
| SJ | Septate junction |
| SNAP | Soluble NSF attachment protein |
| STAT | Signal transducer and activator of transcription |
| TBEV | Tick-borne encephalitis virus |
| TCR | T-cell receptor |
| TER | Transcellular electric resistance |
| TGFβ | Transforming growth factor β |
| Tiam | T-lymphoma invasion and metastasis |
| TJ | Tight junction |
| TNF | Tumor necrosis factor |
| TNFR | TNF receptor |
| TRADD | TNFR1-associated death domain |
| TRIP | Thyroid hormone receptor interactor |
| TSH | Thyroid stimulating hormone |
| TSHR | TSH receptor |
| t-SNARE | Target membrane-SNAP receptor |
| ULF | Unit-length filament |
| VAM | Vimentin-associated matrix adhesion |
| Vangl | Van Gogh-like |
| Vim | Vimentin |
| v-SNARE | Vesicle membrane-SNAP receptor |
| vps | Vesicular protein sorting |
| WASP/WAVE | Wiskott-Aldrich syndrome protein/ WASP family Verprolin-homologous protein |
| WT | Wild-type |
| Y2H | Yeast two-hybrid |
| ZA | Zonula adherens |
| ZO | Zonula Occludens |
| ZONAB | ZO-1-associated nucleic acid-binding protein |

# Chapter 1: Introduction

A common cellular feature of metazoans is the predominant presence of a specialized group of cells that form epithelia. These cells engage in various roles throughout the ontogeny of multicellular organisms, participating in physiological processes ranging from early embryonic development to organ function in adulthood. Epithelial cells play crucial roles in embryogenesis. During the onset of embryonic morphogenesis, primitive epithelial cells of the blastula migrate and change their shape to form the ectoderm, mesoderm and endoderm germ layers in the process of gastrulation. This initiates the formation of the body plan of the mature organism. The completion of gastrulation is followed by organogenesis. In this process, germ layers give rise to various rudimentary structures which eventually develop into organs. Epithelial cells of the germ layers are involved in various aspects of organogenesis, for example in neurulation where the neural plate of the ectoderm forms the neural tube which differentiates into the central nervous system (Colas and Schoenwolf, 2001). In developed organisms, epithelial cells line different internal compartments and cavities of organ systems and also the external body surface. Functionally, this provides protection of the body from the exterior environment, partitioning of distinct internal environments within the body and regulation of molecular exchange between environments. Aside from normal physiological functions, many pathological processes also involve epithelial cells. The dysregulation of epithelial cell function can lead to birth abnormalities like neural tube defects in which the epithelial cells of the neural plate fail to completely close and form the neural tube (Doudney and Stanier, 2005). Anomalous epithelial functions in developed organs are associated with various diseases. An example is the failure of kidney nephron epithelial cells to regulate reabsorption and secretion, thus resulting in

renal cystic diseases (Wilson, 1997). Of great modern medical significance and concern is the relationship between epithelial cell regulation and cancer. The majority of cancers are carcinomas. These originate from epithelial cells that have lost their epithelial characteristics and become tumorigenic (Wodarz and Nathke, 2007). With such wide ranging physiological functions and implications in human diseases, the understanding of epithelial cell biology has gained immense importance.

## 1.1 Epithelial Cell Polarity

Central to the function of epithelial cells, and to an extent cells in general, is the characteristic of cell polarization. Basic cellular processes like cell proliferation, growth, differentiation and movement essentially rely on various forms of polarization to progress. Epithelial cell polarization can be described by three modes of cell polarization: apical-basal, planar and anterior-posterior polarity (Fig. 1-1).

Apical-basal polarity of epithelial cells refers to the asymmetric distribution of membrane and peripheral molecules, organelles and cytoskeletal networks into two structurally, biochemically and functionally separate regions in the plasma membrane and cytoplasm, designated the apical and basolateral domains. Typically, polarized epithelial cells form a monolayered epithelial sheet by adhering laterally to each other and basally to the extracellular matrix (ECM), with the apical domain facing the lumen or external environment. Such a polarized sheet provides a permeability barrier with the two domains serving specialized functions of transcellular (through the cell) and paracellular (between adjacent cells) vectorial transport (Tsukita *et al.*, 2001).

Planar or tissue polarity is an extension to the concept of apical-basal polarity. The latter fundamentally describes polarity in an individual cell setting. However, planar polarity is a more global, tissue level concept which illustrates coordinated polarization of cells in an epithelial sheet such that orientation of polarity is uniform throughout the tissue. This is achieved by the transmission of spatial information among neighboring cells which then polarize as a unit (Zallen, 2007).

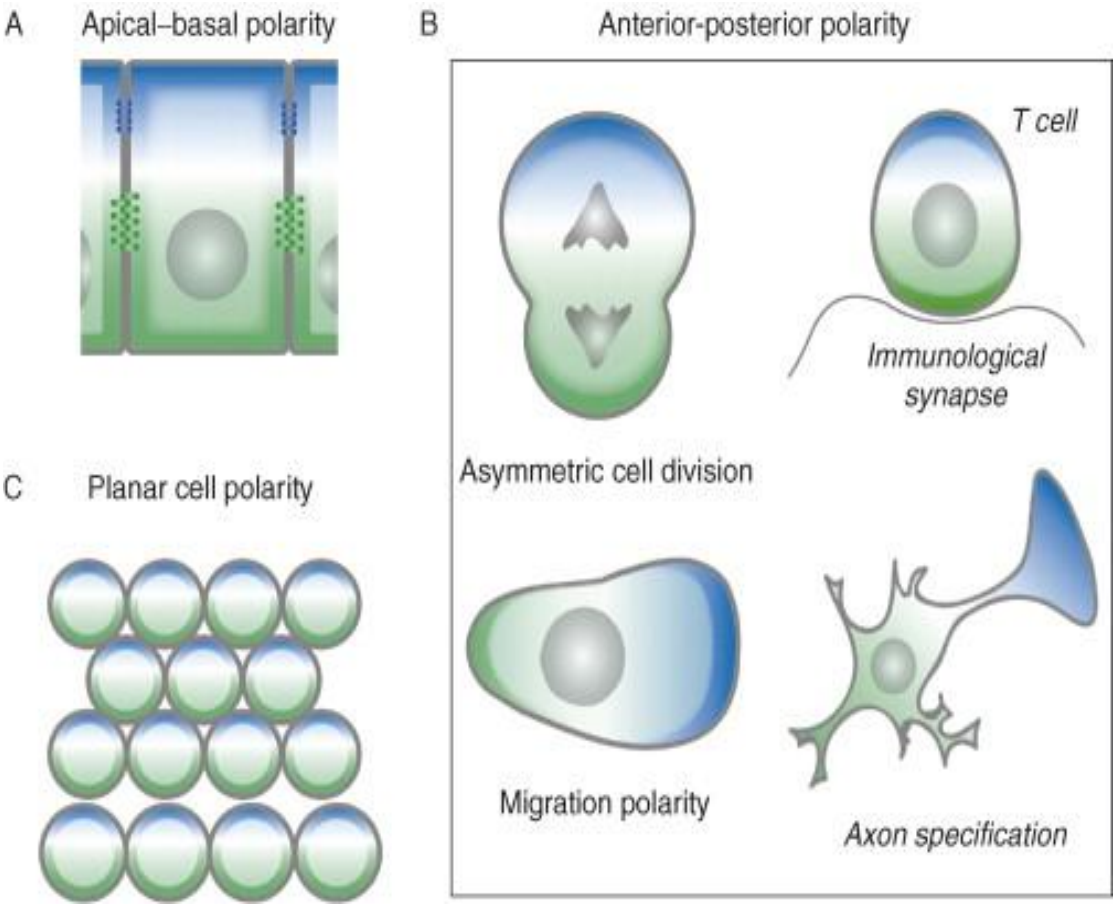


**Figure 1-1. Schematic diagram representing the various modes of cell polarity. (A)** Epithelial cell monolayer showing apical-basal polarization. **(B)** Anterior-posterior polarity exemplified by asymmetric division in neuroblast division, T-cell immunological synapse formation during antigen presentation, cell migration in wound healing and axon specification in neurogenesis. **(C)** Planar polarity presented as synchronized polarization and typified in cochlear sensory epithelium hair cell arrangement. Blue and green colors indicate polarized asymmetric distribution of cellular components. (Reprinted from International Review of Cytology, 262, 253-302, Dow, L.E., and Humbert, P.O., Polarity regulators and the control of epithelial architecture, cell migration, and tumorigenesis, (2007), with permission from Elsevier Ltd.)

The epithelial sheet is established and maintained by specialized cellular components. Crucial components include the cell-cell contact or junctional complexes that line the basolateral domains and the cytoskeletal networks that are linked to them. Cell-cell adhesion and cell polarity is initiated and sustained by the adherens junction (AJ) which encircles the sub-apical lateral membrane of cells in a belt-like manner. This consists of integral membrane cell adhesion molecules (CAMs) like cadherins and nectins which are anchored to the cortical actin cytoskeleton ring via peripherally-associated catenins and afadin respectively. The AJ serves as a trans-associating contact interface between counterpart CAMs of adjacent cells and the cytoskeletal network. Adhesion and polarity is further maintained by the encircling tight junction (TJ) located at the apicolateral boundary just above the AJ in vertebrate epithelia. This demarcates the apical and basolateral membranes and comprises principally of transmembrane CAMs claudins, occludin and junctional adhesion molecules (JAMs) and peripheral components like the zonula occludens 1 (ZO-1), ZO-2 and ZO-3. Similar to AJ, TJ CAMs are also trans-associating and linked to the underlying F-actin network via their submembranous components (Hartsock and Nelson, 2008) (Fig. 1-2). In addition, epithelial cell-cell adhesion is also mediated by cadherin-based junctions known as desmosomes (DS). These are located basal to the AJ and consist of desmosomal cadherins desmocollins and desmogleins associated with peripheral proteins plakoglobin, plakophilin and desmoplakin, which interacts intracellularly with keratin intermediate filaments (Garrod and Chidgey, 2008).

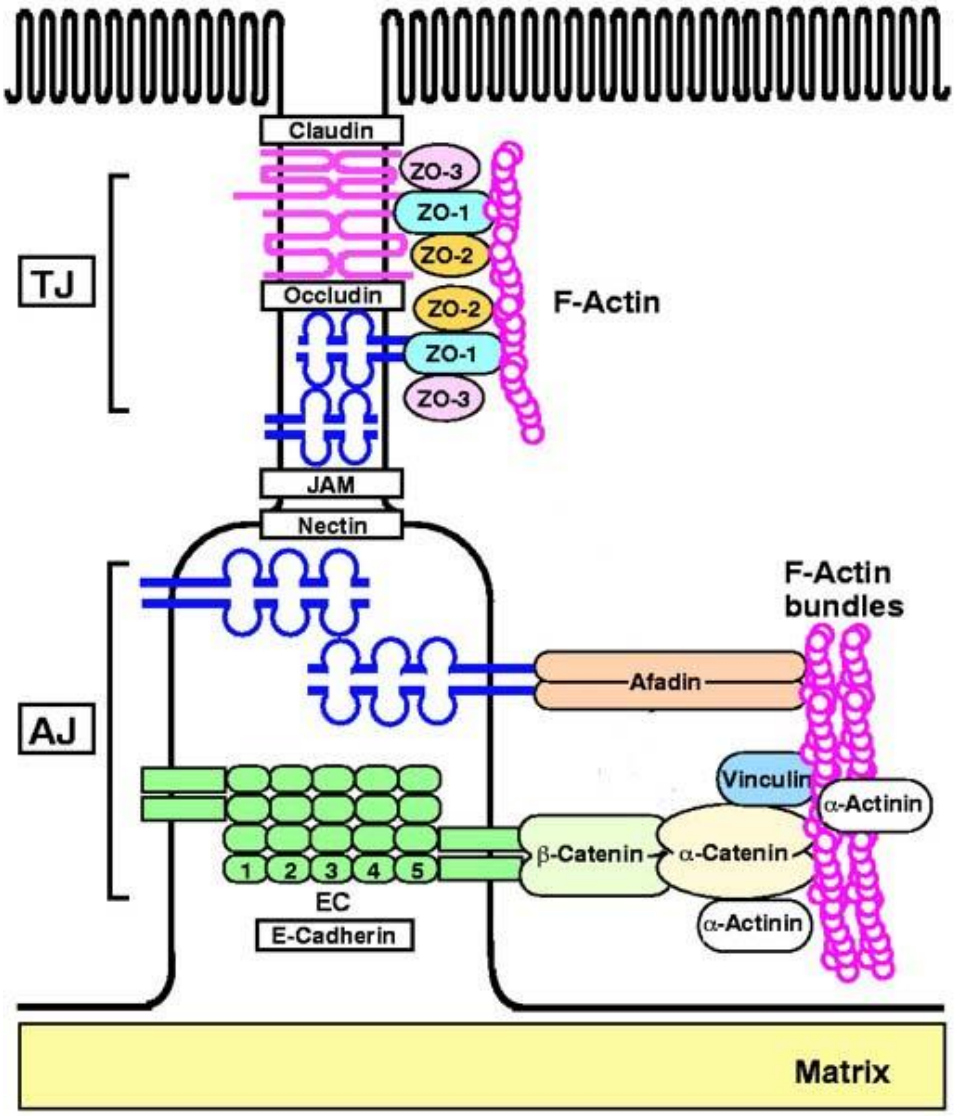


**Figure 1-2. Junctional components of apical-basal polarized epithelial cell**. The TJ and AJ are represented along the lateral membrane. The sub-apical AJ is composed of CAMs E-cadherin and nectin trans-associating at their extracellular domains and binding via their cytoplasmic domain to F-actin bundles through the mediation of interacting complexes consisting of catenins, afadin and actin-binding proteins vinculin and α-actinin. The TJ is apical of AJ and consists of CAMs claudins, occludin and JAMs. These associate intracellularly with the three ZO proteins which are in turn linked to F-actin. The apical pole is represented as microvilli typical of polarized intestinal epithelial cells while the basal membrane is apposed with the ECM. (Reprinted from Journal of Cell Science 116, 17-27, Takai, Y., and Nakanishi, H., Nectin and afadin: novel organizers of intercellular junctions. (2003), with permission from The Company of Biologists Ltd)

Anterior-posterior polarization is characterized by an asymmetric distribution of cellular components along a defined anterior-posterior axis of the cell. The concept of anterior-posterior polarity is illustrated in various cellular situations like asymmetric cell division, immunological synapse formation and neuronal axon specification, but in the context of epithelial cells, it is best described in the event of cell migration. The action of cell motility plays essential roles in many physiological and pathological situations. As mentioned before, epithelial cell migration regulates embryo morphogenetic processes like gastrulation. It is also crucial in tissue repair as illustrated in wound healing and contributes to the progression of carcinogenesis in invasive and metastatic tumors (Ridley *et al.*, 2003).

The process of directed cell migration can be triggered by specific extracellular migration stimuli like chemotactic cytokines, growth factors, ECM components or the free space of a wound. Migration often occurs as a coordinated cohesive movement of cell sheets which are uniformly polarized towards the stimuli. These cues align the axis of the cell parallel to the direction of movement, with the anterior facing the migration front and set off a series of processes that produces cell motility. Foremost of these is the generation of actin mediated lamellipodia and filopodia membrane protrusions at the anterior region or leading edge in the direction of migration. Polymerizing branched actin networks regulate the development of lamellipodia, which is a characteristic broad length membrane protrusion that thrusts the cell forward. The finger-like protrusions of filopodia are supported by long parallel bundled actin elongations and act as exploratory feelers that sense the immediate environment. Both protrusions are stabilized by actin-linked adhesion molecules adhered to the ECM or neighboring cells which act as

footholds for migration. In a cyclical manner, the cell propels itself forward in a posterior to anterior movement via actin cytoskeletal contraction in the posterior region, making new anterior footholds while coordinately disassembling previous adhesion sites which are posteriorly localized, thus mechanically driving the cell forward (Lauffenburger and Horwitz, 1996) (Fig. 1-3).

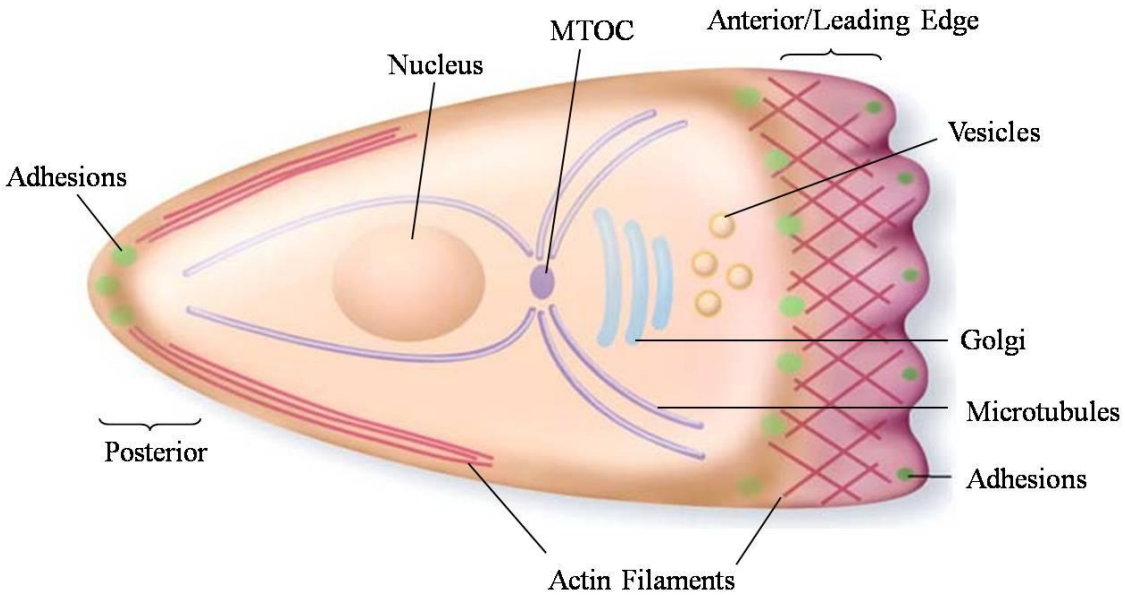


**Figure 1-3. Anterior-posterior polarization during cell migration.** Protrusion at the leading edge are driven by the anterior polarized actin filaments and stabilized by adhesions to the substratum. The microtubule-organizing centre (MTOC) and Golgi apparatus are polarized in front of the nucleus and vesicular trafficking oriented toward the anterior region (discussed in section 1.1.1.2). Adhesions and actin bundles at the posterior region are disassembled as the rear retracts with forward movement. (Reprinted from Science, 302, 1704-1709, Ridley, A.J., Schwartz, M.A., Burridge, K., Firtel, R.A., Ginsberg, M.H., Borisy, G., Parsons, J.T., and Horwitz, A.R., Cell migration: integrating signals from front to back. (2003), with permission from American Association for the Advancement of Science)

### 1.1.1 Mechanism of Cell Polarization

The establishment of both apical-basal and anterior-posterior polarity is regulated by various hierarchical cellular events that are activated by coordinated spatial and temporal cues. Both these aspects of polarization share many molecular mechanisms that control polarity. Studies of neuroblasts/neural progenitor cells, astrocytes, fibroblasts, endothelial and epithelial cells in both *Drosophila melanogaster* and mammalian model systems have revealed similar means of polarity regulation. A collation of information derived from these multiple cell systems will be discussed.

#### 1.1.1.1 Apical-Basal Polarity

The development of apical-basal epithelial cell polarity and junctional complexes is primarily regulated by three groups of evolutionarily conserved interacting protein complexes: 1) the Par complex consisting of Partitioning-defective 6 (Par6), Par3 and atypical protein kinase C (aPKC); 2) the Crb complex consisting of Crumbs (Crb), Protein associated with Lin seven 1 (PALS1) and PALS1-associated tight junction protein (PATJ); 3) the Scrib complex consisting of Scribble (Scrib), Discs large (Dlg) and Lethal giant larvae (Lgl). Upon activation by spatial and temporal cues, these complexes distribute asymmetrically. In polarized epithelial cells, the Par and Crb complexes localize to the apical surface and the tight junction region, while the Scrib complex distributes to the basal region of the lateral membrane. Although the precise mechanism of function remains undetermined, it is widely recognized that both the Par and Crb complexes confer apical activity which is repressed in the basal domain by the Scrib complex. Conversely, the basal activity of the Scrib complex is antagonized by the Par

and Crb complexes apically and therefore restricted to the basal domain. As such, opposing functions of the Par-Crb and Scrib complexes are regionally restricted and can thus coordinately control downstream effectors that consequently define and sustain the two cellular poles. With the exception of the cytoplasmic enzymatic aPKC, the other polarity complex components are non-enzymatic transmembrane or cortical membrane proteins possessing multiple protein-protein interaction domains and thus well placed to allow the complexes to coordinately interact with each other and act as scaffolds for the specific subcellular localization and control of effectors (Dow and Humbert, 2007) (Fig. 1-4).

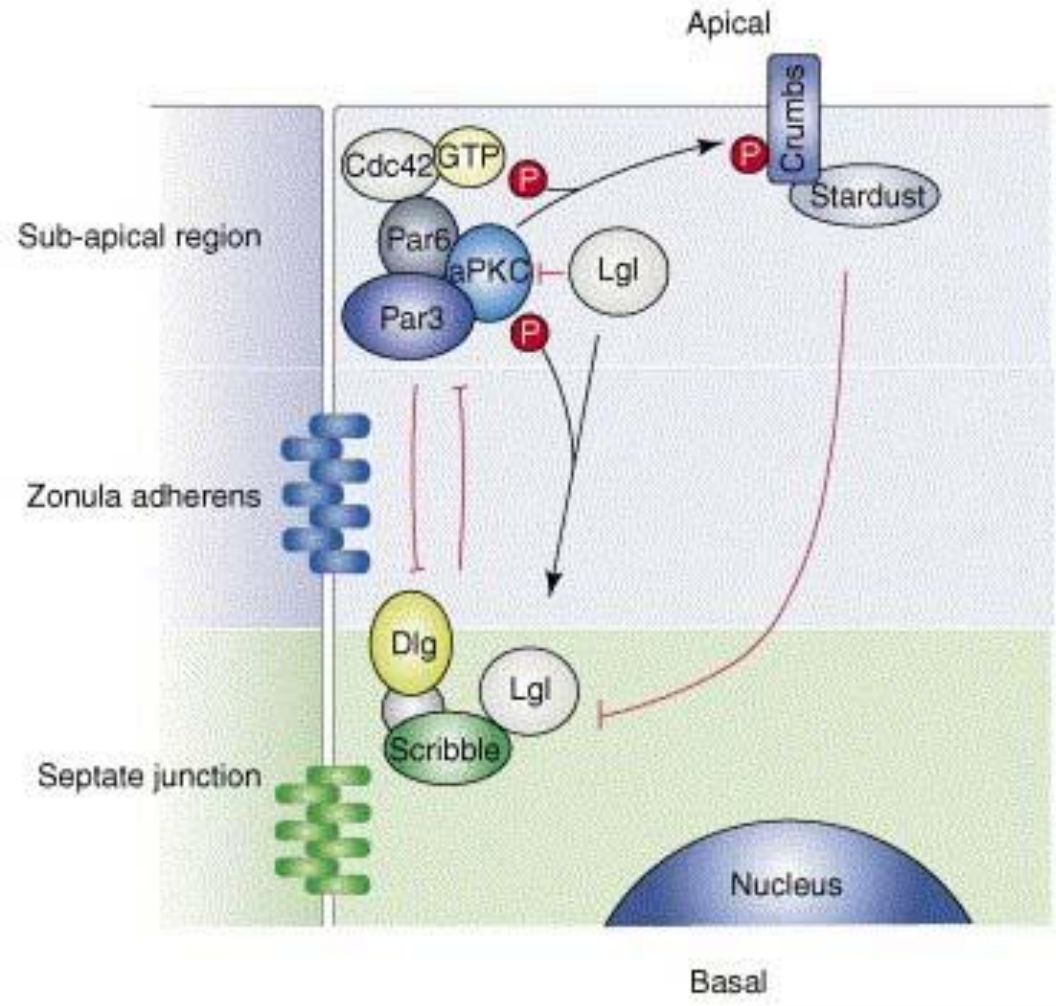


**Figure 1-4. Mechanistic interactions of polarity regulators in an apical-basal polarized *Drosophila* epithelial cell**. The Scrib complex Lgl association with Par6-aPKC inhibits their binding to Par3 thus rendering the Par complex inactive for apical polarizing function at the septate junction (SJ) region. At the sub-apical region (SAR) GTP-activated Cdc42 positively regulates the aPKC mediated phosphorylation of Lgl which leads to Lgl dissociation from Par6-aPKC. Thus the suppression of the Par complex is lifted at the apical domain and Par6-aPKC forms a tripartite with Par3. aPKC also phosphorylates Crumbs (Crb) and this modification is responsible for the apical localization of the Crb complex and its antagonism of the Scrib complex. Note that in vertebrate epithelial cells the equivalent to the *Drosophila* SJ is the TJ and this is located apical to the zonula adherens (ZA) i.e. AJ. Although the positions of these junctions are interchanged, the localization of the polarity regulators is conserved. Stardust is the *Drosophila* orthologue of vertebrate PALS1. (Reprinted from Trends in Cell Biology, 16, 622-630, Humbert, P.O., Dow, L.E., and Russell S.M., The Scribble and Par complexes in polarity and migration: friends or foes? (2006), with permission from Elsevier Ltd.)

The founding event of polarization is the initial cell-cell contact or primordial spot-like adhesion junctions (PA) between the basolateral sides of neighboring cells. This contact zone constitutes a polarization cue and is formed upon nectin and cadherin trans-associated clustering and throughout its maturation, sequentially recruits adherens junction and tight junction components, including catenins and afadin; and ZO-1, JAM and occludin in juxtaposed clusters respectively. The recruitment of these proteins during the formation of PA is followed by the later recruitment of claudins and members of the Par complex to the maturing junctional area (Suzuki *et al.*, 2002; Nakanishi and Takai, 2004). Through possible pathways involving local induction of phosphatidylinositol 3-kinase (PI3K) and its phosphoinositide products, Rho guanosine triphosphatase (GTPases) Cdc42 and Rac1 are recruited to and activated at this contact zone (Kim *et al.*, 2000b; Nakagawa *et al.*, 2001). These two small G-proteins are guanine nucleotide-binding proteins that regulate their activity by cycling between an inactive guanosine diphosphate (GDP) and an active guanosine triphosphate (GTP) bound form. Mechanistically, this molecular switch is regulated by a specific guanine nucleotide exchange factor (GEF) which dissociates GDP from the G-protein and allows GTP binding. Conversely the GTP bound form is inactivated by a GTPase-activating protein (GAP) which promotes the hydrolysis of GTP to GDP by the intrinsic GTPase activity of the G-protein (Jaffe and Hall, 2005). The recruitment and activation of Cdc42 and Rac1 is vital for initiation of epithelial polarization since it binds to and regulates Par complex signaling (Joberty *et al.*, 2000; Lin *et al.*, 2000). The Par complex aPKC kinase activity, in coordination with the other polarity complexes, crucially regulates downstream signaling processes involved in apical-basal polarity determination. Therefore, this

activity must be spatially and temporally controlled during the process of polarization and cell-cell contact maturation. This is achieved through its suppression by constitutive Par6 binding. The activity is restored to its basal state through the relief of this suppression by the binding of Cdc42-GTP to Par6 (Yamanaka *et al.*, 2001).

The coordinated spatial and temporal regulation of the Par complex activity and that of the other polarity complexes follows a hierarchical order. At the early stages of cell polarization, Lgl interacts with Par6 and aPKC at the cell-cell contact region along the basolateral domain. This competes off Par3 for Par6-aPKC binding and renders the Par6-aPKC inactive for apical polarizing function. However as polarization progresses, aPKC kinase is activated possibly by Rac1/Cdc42 regulation and lifting of the Par6 suppression. aPKC then phosphorylates the associated Lgl and triggers its dissociation from Par6-aPKC (Fig. 1-4). The free Par6-aPKC subsequently forms an active apical Par complex with Par3 (Plant *et al.*, 2003; Yamanaka *et al.*, 2003; Yamanaka *et al.*, 2006), whereas the phosphorylated Lgl is inactivated by exclusion from the apical membrane and cortical actin cytoskeleton (Musch *et al.*, 2002; Hutterer *et al.*, 2004; Betschinger *et al.*, 2005). Thus, the basal activity of Lgl is restricted from the apical domain and cannot antagonize the apical function of the Par complex.

In a parallel event at the initiation of cell polarization, PATJ is localized to the apical cortex and cell-cell contacts probably through recruitment by ZO-3. In addition, it also binds claudins (Roh *et al.*, 2002a). During junctional biogenesis, it binds and recruits PALS1 to transmembrane protein Crb at the maturing adhesions where the Crb complex is assembled with Crb indirectly binding PATJ via PALS1 mediation (Roh *et al.*, 2002b). This binding of PALS1 to PATJ has a stabilizing effect on the latter's expression and

together help target the newly assembled Par6-aPKC-Par3 complex to Crb through a Cdc42-enhanced Par6-PALS1 interaction (Hurd *et al.*, 2003; Straight *et al.*, 2004). In addition to this, the Par complex can also associate with the Crb complex through a direct Par6-Crb interaction (Lemmers *et al.*, 2004) or with TJ component JAM via Par3 binding (Ebnet *et al.*, 2001). Furthermore, aPKC can bind both Crb and PATJ and phosphorylates the former. Although this phosphorylation is not essential for aPKC binding, it is necessary for the proper apical localization of the Crb complex and its antagonism of the Scrib complex (Sotillos *et al.*, 2004). Through such multiple means, these complexes recruit each other to the apical domain and maturing PA where they mutually regulate the establishment of apical identity and both AJ and TJ biogenesis (Straight *et al.*, 2004; Michel *et al.*, 2005; Shin *et al.*, 2005; Wang *et al.*, 2007). This process is reliant on aPKC kinase and is initiated by the Par3 or PI3K-dependent recruitment and activation of Rac1-specific GEF T-lymphoma invasion and metastasis (Tiam1). Tiam then localizes activated Rac1-GTP to the maturing cell contact where it subsequently triggers the kinase activity of the Par complex. This activity mediates junctional differentiation and the various PA components are segregated to their respective polarized membrane domains where they are assembled into mature belt-like AJ and TJ anchored stably to cortical actin rings (Suzuki *et al.*, 2002; Chen and Macara, 2005; Mertens *et al.*, 2005).

The establishment of the apical domain by Par and Crb complexes is coordinated with the development of the basolateral region as regulated by Lgl, in conjunction with partners Dlg and Scrib. Unlike the aPKC-phosphorylated apical Lgl, un-phosphorylated basolateral Lgl is active and can thus function in basolateral definition. Like the apical restriction of Lgl activity by Par complex, this function includes the exclusion of Par and

Crb complex activity from the basolateral region. As mentioned, Lgl restricts basolateral Par complex formation by competing off Par3 binding. In addition, through an unknown mechanism, Lgl also regulates the localization of Par6 and PATJ, restricting their localization to the apical domain (Hutterer *et al.*, 2004). The basolateral defining function of Lgl has been widely suggested to involve two distinct but possibly related modes of action. One proposed model is the positive regulation of polarized exocytic vesicle fusion to the basolateral plasma membrane, involving Lgl interaction with plasma membrane vesicular fusion machinery, target membrane-soluble *N*-ethylmaleimide-sensitive fusion protein (NSF) attachment protein (SNAP) receptor (t-SNARE). The interaction of Lgl with the post-Golgi vesicular fusion core machinery is well conserved. Yeast Lgl orthologues Sro7/Sro77 associate with t-SNARE, Sec9 and loss of the latter results in accumulation of exocytic vesicles, suggesting a failure to fuse with the plasma membrane (Lehman *et al.*, 1999). Consistent with this, mammalian Lgl can bind to basolateral t-SNARE syntaxin 4 but not non-polar or apical t-SNAREs. Furthermore, another t-SNARE, SNAP23 appears to form a complex with Lgl-syntaxin 4 at the basolateral membrane (Musch *et al.*, 2002). The other model involves the modulation of actomyosin cytoskeleton via Lgl association with non-muscle myosin-II (Strand *et al.*, 1994; Strand *et al.*, 1995). Although, its mechanism of action remains unclear, it is thought that Lgl negatively regulates assembly of actomyosin cytoskeleton at the basolateral membrane, restricting it to the apical domain (Barros *et al.*, 2003). This modulation of actomyosin function is crucial in maintaining cell polarity and may be coupled to the Lgl coordinated vesicle fusion.

In addition to the establishment of polarity initiated by cell-cell contact cues as described above, epithelial cells also receive polarization cues from contact with the underlying ECM. Although less well understood, this is nonetheless crucial as it coordinates individual cell polarity with higher-order tissue architecture and ensures that the intracellular apical-basal axis is aligned with the overall multicellular tissue structure. Such coupling of polarity with the extracellular environment is initiated by the ECM component collagen I. Its binding to β1-containing integrins activates Rac1 and results in the basolateral assembly of an extracellular laminin-1 network, which in an autocrine loop, sends a polarizing signal that orients the apical domain (O'Brien *et al.*, 2001; Yu *et al.*, 2005). In all, these studies emphasize the fact that coordinated cues and activated regulatory proteins from both cell-cell and cell-ECM contacts are essential in creating a functional polarized epithelial cell layer.

Although the downstream activity of the three polarity regulator complexes, their effectors and the molecular mechanisms involved in perpetuating polarizing effects are unclear, it is certain that establishment of polarity necessitates the regulated sorting of cargo proteins into transport vesicles and translocation, docking and fusion of these vesicles to specific membrane domains. Parts of these processes are controlled by the dynamic remodeling of microtubule and actin cytoskeletons and the actions of membrane-tethered docking/fusion factors. Microtubules appear to be essential in regulating apical exocytosis while actin cytoskeleton is crucial for basolateral exocytosis. Microtubule and actin networks with their respective motor proteins dynein/kinesin and myosin can regulate transport of vesicles via cytoskeletal tracks. In addition, microtubule and actin cytoskeleton play a role in specifically positioning fusion machinery factors

syntaxin 3 and syntaxin 4 to the apical and lateral membrane respectively. These two factors together with SNAP23 form the exocytic docking and fusion machinery t-SNARE. t-SNAREs are localized to specific target membranes, with syntaxin 3-SNAP23 at the apical and syntaxin 4-SNAP23 at the basolateral membrane. These are complementary to the vesicle membrane SNARE (v-SNARE) of transport vesicles and the two groups of SNAREs on apposing membranes interact and mediate the docking and fusion of the vesicles to the plasma membrane. As mentioned, this mediation can be regulated by Lgl at the basolateral membrane. Likewise, the other polarity complexes along with additional regulators may play important roles in vesicular trafficking (Rodriguez-Boulan *et al.*, 2005).

### 1.1.1.2 Anterior-Posterior Polarity

The regulation of migrating cells is initiated by the perception of an extracellular cue. This directional sensing causes the polarization of migration promoting molecules to the leading edge of the cell i.e. the anterior pole. Local elevation of stimuli like growth factors and other ECM-associated ligands engage their cognate receptors like Epidermal Growth Factor Receptor (EGFR) and integrin adhesion molecules. Stimulation of these receptors leads to their physical association, clustering and phosphorylation of the cytoplasmic domains. Such modifications to the receptor cytoplasmic domains initiate a cascade of downstream events that activate the cell polarity machinery (Etienne-Manneville and Hall, 2001) (Fig. 1-5).

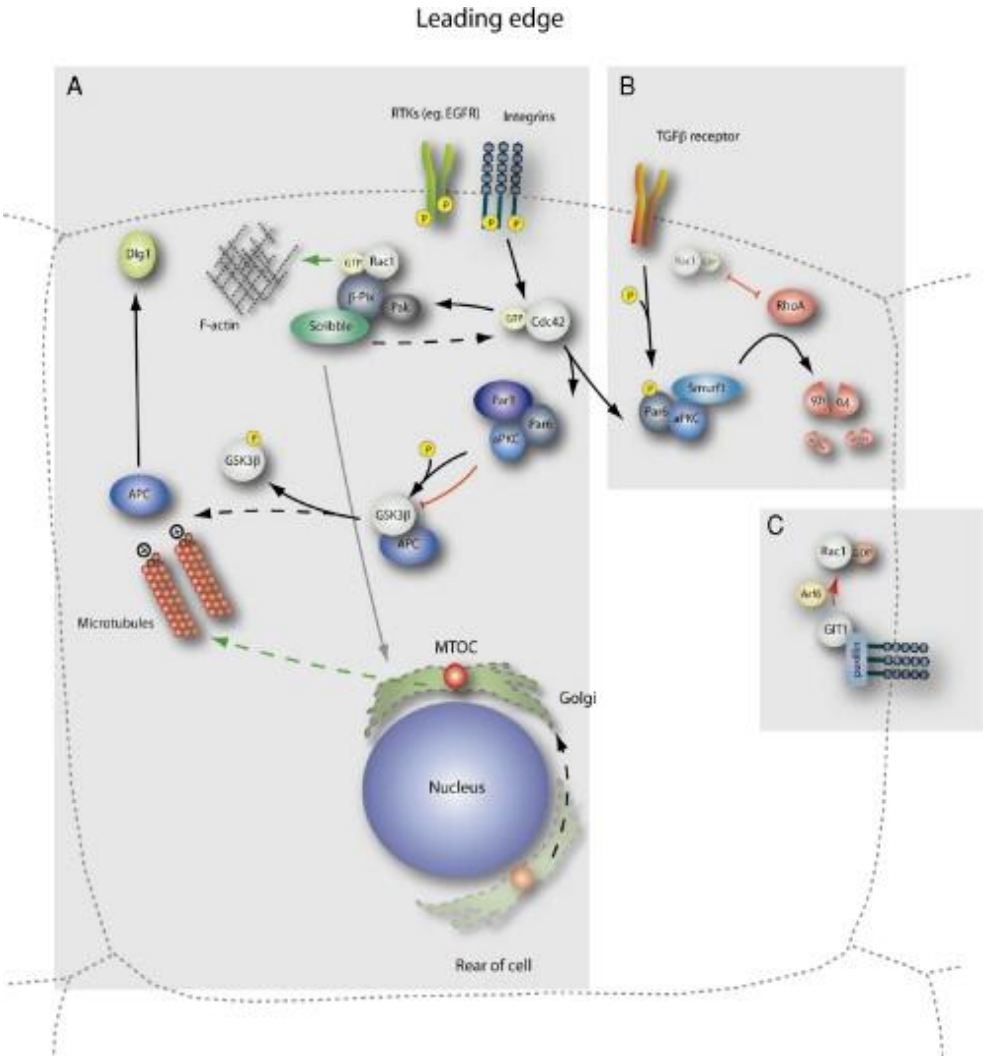


**Figure 1-5. Mechanistic interactions of polarity regulators in an anterior-posterior polarized migrating mammalian cell**. **(A)** At the leading edge, engagement of growth factor receptors e.g. receptor tyrosine kinase (RTK) EGFR and integrins locally activate Cdc42. Cdc42-GTP activation of PAK1 recruits βPIX which in turn recruits and activates Rac1 at the leading edge where it mediates polymerization of actin and membrane protrusion. Cdc42-GTP also activates aPKC of the Par complex which subsequently phosphorylates GSK3β, disrupting its association with APC and thus allowing APC to bind to microtubule positive ends. This APC is then recruited to the leading edge through interaction with Dlg1 and the anchored microtubules reposition the MTOC and Golgi towards the migration front. These events are dependent on Scrib localization at the leading edge as this recruits and activates Rac1/Cdc42 at the anterior membrane. **(B)** The rear retraction activity of RhoA and its Rac1/Cdc42 antagonistic effect is inhibited at the leading edge through the Cdc42-GTP and TGFβ-dependent phosphorylation of Par6 and activation of aPKC. This recruits Smurf1 at cellular protrusion where it mediates the degradation of RhoA. **(C)** At cell-cell contacts, the Arf6-dependent activation of Rac1is inhibited by the decrease of Arf6 activity caused by Arf-GAP GIT1. GIT1 is recruited to the nonphosphorylated integrins at cell-cell contacts through the mediation by paxillin. This thus restricts Rac1 activation to the leading edge. (Reprinted from International Review of Cytology, 262, 253-302, Dow, L.E., and Humbert, P.O., Polarity regulators and the control of epithelial architecture, cell migration, and tumorigenesis. (2007), with permission from Elsevier Ltd.)

Like in apical-basal polarity, Rac1 and Cdc42 Rho GTPases are key polarity regulators involved in the initiation of polarized migration and are locally activated at the leading edge. This localized stimulation can be driven by activated integrins and growth factor receptors. Away from the leading edge, nonphosphorylated integrins at cell-cell contacts bind G-protein-coupled receptor-kinase (GRK)-interacting protein 1 (GIT1) via paxillin. GIT1 is an adenosine diphosphate (ADP) ribosylation factor (Arf)-GTPase-activating protein (Arf-GAP) which inhibits Arf6 activity, leading to decreased Rac1activity. This therefore restricts active Rac1 GTP to the leading edge where integrin is phosphorylated (Nishiya *et al.*, 2005). As opposed to the GIT1 negative regulation of Rac1 activity, the GEF βPIX (p21-activated kinase (PAK)-interacting exchange factor) activates Rac1 and Cdc42. Scrib localization to the leading edge by an as yet unknown mechanism is responsible for the recruitment of its binding partner βPIX. This leads to a corresponding engagement and/or activation of Rac1 and Cdc42, thus ensuring the localized activation of Rac1/Cdc42 dependent downstream polarity events like actin polymerization at membrane protrusions. Consistent with this, the depletion of either Scrib or βPIX is coincident with a decrease in cell protrusions and migration (Cau and Hall, 2005; Osmani *et al.*, 2006; ten Klooster *et al.*, 2006; Dow *et al.*, 2007). Interestingly, Scrib can interact indirectly with GIT1 through a Scrib-βPIX-GIT1 tripartite complex (Audebert *et al.*, 2004). With the opposing roles of GIT1 and βPIX, Scribble could possibly also function to regulate the balance of their action on Rac1/Cdc42.

One functional aspect of localized Rac1/Cdc42 activation at the leading edge is the regulation of the initial migratory event of membrane protrusion via interaction with effector WASP/WAVE (Wiskott-Aldrich syndrome protein/ WASP family Verprolin-

homologous protein) proteins. Rac1 activity is traditionally linked directly to lamellipodia formation, whereas Cdc42 activity controls filopodia development (Hall, 2005). However, recent studies implicate both Rac1 and Cdc42 in lamellipodia induction. Rac1-induced lamellipodia is dependent on Cdc42-activated p21-activated kinase 1 (PAK1) recruitment of βPIX to the leading edge. βPIX subsequently recruits and activates Rac1, resulting in actin polymerization and membrane protrusion (Cau and Hall, 2005; ten Klooster *et al.*, 2006). Rac1 activated WAVE proteins stimulate the Arp2/3 (Actin-related protein 2 and 3) complex. The latter serves as nucleation sites that mediate the polymerization of actin filaments by promoting the branching of new filaments from existing ones, thus pushing the membrane into forming lamellipodia (Cory *et al.*, 2003). Similarly, Cdc42 binds to WASP proteins and induces actin filament branching via Arp2/3 (Welch and Mullins, 2002). However, this does not appear to involve filopodia induction since WASP null cells can still form filopodia (Snapper *et al.*, 2001). Membrane protrusions are characteristically stabilized by adhering to the surrounding ECM through actin filament-linked adhesion molecule integrin. The formation of adhesion clusters of integrin and its associated proteins, known as focal adhesion complexes, at the leading edge is dependent on Rac1/Cdc42 activity. Initial integrin engagement can activate and target Rac1 to the lamellipodia, at which Rac1 subsequently stimulates integrin recruitment and clustering in a positive feedback loop (del Pozo *et al.*, 2000; Kiosses *et al.*, 2001). These clusters confer tractional force to the migrating cell and also act as migration-regulating mechanosensors that transmit extracellular information into the cell through integrin-mediated signaling (Geiger *et al.*, 2001).

Aside from its role in regulating actin-dependent membrane protrusion, Cdc42 also plays a crucial function in the microtubule-dependent polarization of the microtubule organizing centre (MTOC) and Golgi apparatus in front of the nucleus, along the axis of migration. This represents the second aspect of migration polarization. The repositioning facilitates microtubule polymerization and the concurrent membrane trafficking through the Golgi complex via microtubule tracks towards the protruding lamellipodia, thus providing this with a supply of membrane components. Integrin-activated Cdc42 binds Par6-aPKC and activates aPKC kinase activity probably by lifting its suppression by Par6 like in apical-basal polarization as previously mentioned. aPKC then disrupts the interaction between glycogen synthase kinase 3β (GSK3β) and adenomatous polyposis coli (APC) by phosphorylating and deactivating the former. APC subsequently associates with the growing plus ends of microtubules and anchors them to the leading edge by interacting with anterior membrane polarized Dlg1. Dlg1 recruitment to the leading edge is also dependent on Cdc42-Par6-aPKC but this regulation does not involve GSK3β. Both these Cdc42-Par6-aPKC -dependent recruitments of APC and Dlg1 to the leading edge microtubule plus end clusters have been suggested to be mediated by Scrib (Osmani *et al.*, 2006; Takizawa *et al.*, 2006). With the anchoring of microtubules to the leading edge, pulling forces exerted can then facilitate the relocalization of MTOC and Golgi apparatus possibly by recruitment or activation of microtubule minus end-directed motor complex dynein-dynactin (Etienne-Manneville *et al.*, 2005). Interestingly, a recent study has revealed another upstream event in this relocalization. PATJ and PALS1 localization to the leading edge is necessary for the correct orientation of MTOC and microtubules during migration. This mediation is independent of Crb and appears to be through their

recruitment of aPKC and Par3 to the leading edge (Shin *et al.*, 2007). Thus, it seems that elements of both Scrib and Crb complexes are essential in targeting the Par complex to mediate cell migration.

The migration of a cell through forward membrane protrusion must be balanced with a simultaneous retraction of the rear. This is regulated by another Rho GTPase, RhoA via its stimulation of actin stress fiber assembly and contractile force at the side and rear of the cell. This retraction promoting function is antagonized by Rac1/Cdc42 at the leading edge and vice versa, thus separating the two disparate roles. The Cdc42 and transforming growth factor β (TGFβ)-dependent activation of the aPKC through Par6 phosphorylation has a role in this by promoting RhoA ubiquitin-mediated degradation at membrane protrusions via recruitment of E3 ubiquitin ligase Smurf1, thus negating its antagonistic effect (Wang *et al.*, 2003; Ozdamar *et al.*, 2005). The forward translocation of a migrating cell is driven by a cycle of adhesion assembly at new protrusions and disassembly at the retracting rear. This adhesion turnover is controlled by as yet unclear mechanisms that involve integrin-stimulated signaling networks regulating mitogen-activated protein kinase (MAPK), Rac1 and focal adhesion components focal adhesion kinase (FAK) and paxillin (Ishibe *et al.*, 2004).

## 1.2 Scribble: Polarity Regulator and Tumor Suppressor

The development of cancer involves the dysregulation of multiple processes like cell proliferation, apoptotic cell death, cell adhesion and motility. Consequently, this can lead to the characteristic malignant manifestations of cellular hyperproliferation, survivability, invasiveness and metastasis. A contributing factor to such impairment is the accumulative mutation of tumor suppressor genes which normally control these processes (Hanahan and Weinberg, 2000). In addition to these processes, epithelial-derived malignant tumors i.e. carcinomas also exhibit the hallmark characteristic of apical-basal polarity disruption, although a causal link between cell polarity loss and tumorigenesis remained uncertain. However the discovery of the Scrib tumor suppressor and cell polarity complex has bridged this and allowed a clearer understanding of cell polarity and cancer biology.

### 1.2.1 Discovery and Functions in *Drosophila melanogaster*

Classical genetic screens in *Drosophila melanogaster* over the years have identified various tumor suppressors. Two of these earlier discoveries are the *lgl* (Gateff, 1978; Mechler *et al.*, 1985) and *dlg* (Woods and Bryant, 1989) genes which function in cell shape, polarity and proliferation in larval epithelial imaginal disc and neuroblast (Manfruelli *et al.*, 1996; Woods *et al.*, 1996; Peng *et al.*, 2000). Interestingly, of all the previously identified *Drosophila* tumor suppressor genes, *lgl* and *dlg* are two of the few identified as neoplastic, whereas the others are hyperplastic. Hyperplastic mutants present tissue overgrowth but no loss of tissue structure and differentiation. In contrast, *Drosophila lgl* and *dlg* neoplastic mutants exhibit loss of cell polarity and adhesion,

structural disorganization, hyperproliferation, invasiveness and metastasis, eventually leading to host lethality (Gateff and Mechler, 1989). Such phenotypes display characteristic features of vertebrate neoplastic tumors, where loss of polarity and adhesion are hallmarks of malignancy (Bissell and Radisky, 2001) and thus *Drosophila* genetic studies have been widely used as a model for understanding cancer biology (Pagliarini and Xu, 2003).

More recently, a novel *Drosophila* neoplastic tumor suppressor was discovered in the form of the *scrib* gene. Genetic analysis on maternal and zygotic *scrib* mutations that impinge upon epithelial morphogenesis revealed a defect in embryonic epidermal organization and was reflected in a scribbled appearance to the secreted overlying cuticular surface. Analysis of *scrib* mutant embryonic development showed a progressively severe defective phenotype after gastrulation. The normally monolayered epidermis was disorganized into multilayered strips and interrupted by groups of round and irregular shaped cells with loose cell-cell contact. This corresponded with the misdistribution of AJ proteins Armadillo (*Drosophila* orthologue of vertebrate β-catenin) and E-cadherin throughout the membrane, leading to AJ formation at ectopic basolateral membrane locations. Linked to this defect, normally apical restricted proteins including the Crb polarity protein also showed aberrant localization to the basolateral membrane. Interestingly, basolateral proteins largely remained correctly localized, implying that mutant epithelial cells were not apolar (Bilder and Perrimon, 2000). Interestingly, consistent with the mislocalization of AJ, a subsequent study on *scrib* null wing imaginal disc epithelium revealed a loss of septate junction (SJ) (see below for definition of SJ) (Zeitler *et al.*, 2004). These studies therefore indicate that Scrib functions in the

restriction of apical polarity determinants to the apical membrane and together with these, is necessary for the proper assembly of cell junctions and separation of apical and basolateral membrane components.

Subsequent analyses of Scrib revealed a close physical and functional relationship with the neoplastic tumor suppressors, Lgl and Dlg. In mature *Drosophila* epithelial cells, Scrib and Dlg co-localize and overlap with cortical Lgl at the basolateral septate junction (SJ). This junction is located just basal to the adjacent AJ and is the functional equivalent of vertebrate TJ. In vertebrate epithelia, the lateral locations of the AJ and TJ are exchanged, with TJ being apical to AJ instead. However, the localization of Scrib complex is well conserved and in vertebrate epithelia appears at an identical lateral position as in *Drosophila*, thus co-localizing with the vertebrate AJ. To further elucidate the functional relationship between these three proteins, null mutations of *lgl*, *dlg* or *scrib* in *Drosophila* have been studied. Interestingly, mutant embryonic epidermis, larval brain and imaginal disc epithelium, and adult ovarian follicular epithelia revealed a failure to organize proper epithelial architecture and showed an expanded distribution of apical proteins, disruption of AJ and deregulation of epithelial proliferation. The similarity in protein localization and mutant phenotypes implied a physical and functional link between the three tumor suppressors. Tests for genetic interaction among the three proteins have indicated codependence for protein localization and dose-sensitivity in mutant phenotype, supporting the notion that these proteins act collaboratively in a common genetic pathway (Bilder *et al.*, 2000b).

Aside from its function in epithelial cell polarity and proliferation in *Drosophila*, Scrib, like Dlg and Lgl (Peng *et al.*, 2000), also plays a role in neuroblast asymmetric cell

division. During *Drosophila* neurogenesis, the undifferentiated dividing neuroblast develops distinct apical-basal cortical domains with specific cell fate determinants and an asymmetric mitotic spindle along the apical-basal axis. These allow it to divide unequally to generate a large apical neuroblast for self renewal and a smaller basal daughter cell called the ganglion mother cell (GMC), which subsequently divides to produce neurons or glia. Crucial aspects of this process of asymmetric cell division are regulated by the Scrib complex. The three proteins display a cortical distribution with apical enrichment from late interphase to metaphase i.e. early mitosis, but have a uniform cortical localization during anaphase and telophase. Here, Dlg is responsible for the cortical localization of Scrib and Lgl, unlike in epithelia where Scrib-Dlg-Lgl basolateral localization is interdependent. In metaphase neuroblasts, the Scrib complex is responsible for the correct basal cortical localization of cell fate determinants like Miranda and Prospero but not apically localized determinants. Investigations into s*crib* complex null mutants showed defect in this specific recruitment, displaying basal determinants with uniform cortical distribution and mislocalization to the cytoplasm and mitotic spindle. These mutants exhibited a smaller apical cortical domain relative to the basal cortex, resulting in symmetrical or inverted cell divisions at telophase. These aberrant divisions formed either two daughter cells of similar size or a small daughter neuroblast and a larger GMC respectively. In addition, the asymmetry of mitotic spindle was also disturbed. In wild-type telophase neuroblast, the apical spindle pole has a larger centrosome and astral microtubule length. However, like in the cortical domain size, this became either symmetrical or inverted (Albertson and Doe, 2003). Just like in the overproliferating epithelium of *scrib* complex mutants, the mislocalization of cell fate

determinants and dysregulation of neuroblast asymmetric division can lead to loss of differentiation and excessive proliferation of neuroblasts and GMCs, consequentially producing enlarged brain lobes (Gateff, 1978; Woods and Bryant, 1989).

Another neuronal-related Scrib function is its role in synaptic structure and function. Scaffolding proteins like Scrib and Dlg (Budnik *et al.*, 1996) are critical for the creation of networks of synaptic proteins and cytoskeleton at pre-and post synaptic membranes. The correct localization of specific synaptic proteins is essential for synaptic signaling, transmission and plasticity. At *Drosophila* neuromuscular junctions (NMJ) of *scrib* null mutants, synaptic ultrastructure was significantly altered. Three prominent structural defects were observed. This includes the ectopic distribution and increase in synaptic vesicle density at the presynaptic membrane. This vesicle pool represents the reserve pool which acts as a transmitter storage depot and constitutes the bulk of presynaptic vesicles. Also observed together with this at the presynaptic membrane is the decrease in the number of active zones, which are sites of synaptic vesicle clustering, docking and neurotransmitter exocytosis. Another structural defect is the thickening of the muscle basal lamina extracellular matrix coat between the pre- and post synaptic membranes. This basal lamina is responsible for the correct recruitment of synaptic components like neurotransmitter receptors. These synaptic structural alterations are associated with various physiological NMJ defects and include reduced synaptic transmission and faulty vesicle recycling, probably related to the inability to recruit vesicles of the reserve pool for exocytosis (Roche *et al.*, 2002).

### 1.2.2 Scribble: Polarity and Cancer in Mammals

While it is acknowledged that the Scrib polarity complex proteins are tumor suppressors in *Drosophila*, there is a caveat concerning its relevance in mammalian tumorigenesis. Though mammalian orthologues of *Drosophila* Scrib (dmScrib) and its complex members have been identified, it is uncertain if these mammalian counterparts possess similar tumor suppressive functions. Only mammalian Lgl has been implicated in the regulation of cell polarity and neoplastic transformation. Embryonic neuroepithelial cells in developing brains of *Lgl* null mice display tissue disorganization associated with disruptions in polarity, a failure to differentiate and overproliferation, eventually causing neonatal lethality. This phenotype histologically resembles brain cancer and is comparable to that determined in *Drosophila Lgl* null mutants, thus suggesting a similar tumor suppressive role of Lgl in mammals (Klezovitch *et al.*, 2004). Although no definitive mammalian *Scrib* or *Dlg* null study has been explored, there is circumstantial evidence to imply that like Lgl, lack of either has a causative role in cell proliferation and carcinogenesis.

The correlation of protein downregulation and mislocalization with progression of carcinogenesis is a suggestive indication of a tumor suppressive role. Human Scrib (hScrib) and/or Dlg (hDlg) exhibit such alterations in various cancers, including oesophaegal, gastric, human papillomavirus (HPV)-positive cervical and colon cancers (Hanada *et al.*, 2000; Liu *et al.*, 2002; Watson *et al.*, 2002; Nakagawa *et al.*, 2004; Gardiol *et al.*, 2006). Interestingly, both hScrib and hDlg are direct interactors of established vertebrate tumor suppressor APC, which also commonly exhibits loss or truncated expression in colorectal cancer (Matsumine *et al.*, 1996; Takizawa *et al.*, 2006).

In line with their presumed role in proliferation control, hScrib and hDlg have been implicated in epithelial cell cycle control. hScrib negatively regulates cell proliferation by inhibiting cell cycle entry from G1 to S phase. This is correlated with a concomitant upregulation of APC and downregulation of cyclin A and D1 (Nagasaka *et al.*, 2006). A similar inhibition of progression from G1 to S phase is also mediated by hDlg, in concert with its interacting partner APC (Ishidate *et al.*, 2000). As a further verification of tumor suppressive functional conservation, both hScrib and hDlg are able to substitute for their *Drosophila* counterpart and rescue *Drosophila* mutant phenotype. Exogenous expression of hScrib in *scrib* mutant imaginal disc epithelium was sufficient to restore apical-basal polarity and tissue architecture and suppress neoplastic overgrowth (Dow *et al.*, 2003). Similarly, rat Dlg expression in *Drosophila dlg* mutants rescued the overgrowth phenotype in imaginal disc epithelium and larval brains (Thomas *et al.*, 1997).

Perhaps the most convincing evidence of tumor suppressive function of mammalian Scrib and Dlg is their binding to and inactivation by viral oncoproteins. This infers a tumor suppressive role in mammalian cells since viral oncoproteins commonly transform mammalian cells by targeting tumor suppressors like p53 and Retinoblastoma (Rb) (Thomas *et al.*, 1999; Munger *et al.*, 2001). The viral transforming proteins high-risk HPV E6 and Human T-cell leukaemia virus type 1 (HTLV-1) Tax can target hScrib and hDlg for inactivation through degradative-dependent and independent mechanisms respectively. High-risk HPV E6 is an established aetiological agent of cervical cancer and is known to regulate the degradation of p53 in epithelium via the proteasome machinery. Although a critical step in oncoprotein-driven malignancy, it is insufficient and suggests that E6 has other targets. These additional targets include cell polarity and cell junction

proteins that contain the protein-protein interaction domain PDZ (PSD-95/Dlg/ZO-1), which both hScrib and hDlg possess. The C-terminal PDZ-binding motif of high-risk HPV E6 binds to the PDZ domain of these targets independent of its binding to p53. Interestingly, this motif is conserved only in high-risk HPV E6 and is absent in low-risk HPV E6 (non-carcinoma inducing), therefore correlating the degradation of these PDZ-containing targets with malignant progression. The E6 targeted degradation of hScrib and hDlg is regulated by the ubiquitination machinery, which transfers a series of ubiquitin proteins to lysine residues of hScrib and hDlg, In the case of hScrib, this transfer is mediated by a cellular ubiquitin-protein ligase, E6-associated protein (E6AP). E6AP interacts directly with E6 but not with hScrib, however E6 binding bridges an E6AP-E6-hScrib tripartite and directs E6AP substrate specificity towards hScrib. The ubiquitination of hScrib and hDlg specifically tags these proteins for subsequent inactivation by proteasome-mediated degradation (Gardiol *et al.*, 1999; Nakagawa and Huibregtse, 2000). The HTLV-1 Tax is another hScrib and hDlg interacting oncoprotein and contributes to the aetiology of adult T-cell leukaemia (ATL). It is known to stimulate cell transformation by deregulating the transcription of cellular genes encoding proteins involved in cell proliferation and apoptosis or inactivating cell cycle regulatory proteins by direct binding. Like high-risk HPV E6, Tax also contains a C-terminal PDZ-binding motif that interacts with the PDZ domains of hScrib and hDlg. However, unlike the modus operandi of E6, Tax does not inactivate these two proteins by targeted degradation. Instead, in HTLV-1-infected T-cells, Tax binds and inactivates hScrib and hDlg by sequestering them in cytoplasmic granular bodies, thus altering their normal cellular localization. Correctly localized hScrib and hDlg suppress T-cell proliferation by

negatively controlling the trans-activating nuclear factor of activated T-cell (NFAT) pathway. By sequestering them, Tax counteracts this suppression and thus promotes T-cell proliferation (Hirata *et al.*, 2004; Arpin-Andre and Mesnard, 2007). Moreover, Tax interaction with hDlg disrupts its binding to APC and lifts the hDlg-APC suppression of G1 to S phase cell cycle progression (Suzuki *et al.*, 1999).

In a more relevant patho-physiological context, Scrib tumor suppressive action has been explored in a study in *Drosophila* where *scrib* mutant clones were generated in the environment of surrounding normal tissue of the larval eye imaginal disc. This model mimics the clonal nature of mammalian tumor development as Scrib is removed in clones within a wild-type tissue context. As expected, mutant tissue lost their characteristic monolayered architecture and became multilayered, with rounded and overproliferating cells that exhibit upregulation of cyclin E. However, neighbouring wild-type tissue kept this overproliferation in check by inducing Jun N-terminal kinase (JNK)-mediated apoptotic cell death of the mutant tissue. Therefore, mutant tissue did not overgrow and cause host lethality. Remarkably, this apoptotic counter-balance could be overcome by the introduction of oncogenic forms of Ras or Notch. With these oncogenes in the *scrib* mutant background, the tissues continued to overgrow and formed massive amorphous tumors. The cooperative nature of tumor suppressor loss and oncogenic gain of function demonstrated in this *Drosophila* model closely resembles the process of mammalian tumor development and thus highlights the prospective applicability of Scrib function in mammalian carcinogenesis (Brumby and Richardson, 2003). Indeed in a recent study, loss of hScrib cooperated with oncogenic Ras to promote invasiveness of human epithelial cells. Constitutive Ras activation alone was insufficient to induce cell invasion

due to the negative regulation of Ras-MAPK signaling pathway by hScrib. Loss of hScrib conversely promoted activation of this pathway and synergistically induced cell invasion (Dow *et al.*, 2008).

Having established that Scrib polarity complexes act as tumor suppressors in Drosophila and probably in mammals too, the question remains as to how these two seemingly disparate processes of epithelial cell polarity and growth control are connected. This remains largely unanswered but a few general mechanisms have been proposed. A plausible mechanism would be the mislocalization of normally polarized growth factor receptors and signaling proteins that regulate cell proliferation or differentiation. Such mislocalization may lead to inappropriate activation of signaling pathways. The disruption of cell-cell adhesion is another likely mechanistic link. This would not only compromise contact inhibition-regulated proliferation but also release AJ peripheral components like β-catenin which may act as transcription activators of proliferation-related target genes (Bilder *et al.*, 2000b). These mechanisms represent concepts in which a general failure of polarization can affect cell growth control. However, the Scrib complex is the only polarity regulator that has been determined to mediate both polarity and proliferation. The Par and Crb complexes, although key players in cell polarity, have not been identified as being regulators of cell growth too. Therefore, it is likely that specific functional characteristics of the Scrib complex provide the mechanistic link between polarity and proliferation. One such characteristic would be the function in regulation of vesicle trafficking. As with Lgl, both Dlg and Scrib interact with basolateral t-SNARE syntaxin 4 in mammalian epithelial cells (Massimi *et al.*, 2008) and also have roles in trafficking dynamics. Dlg has been shown to directly interact with the

*Drosophila* t-SNARE guanylate kinase-interacting syntaxin, Gtaxin (GTX) at postsynaptic membranes of larval neuromuscular junctions. GTX is required for postsynaptic membrane expansion and Dlg directs its activity and distribution to defined sites of membrane addition (Gorczyca *et al.*, 2007). One role of Scrib in trafficking involves its direct interaction with basolateral membrane localized G protein-coupled thyroid stimulating hormone receptor (TSHR) in thyroid follicular cells. Through a Scrib-βPIX-GIT1-ARF6 pathway, Scrib regulates TSHR trafficking and signaling by promoting the recycling of thyroid stimulating hormone (TSH)-activated endocytosed TSHR back to the plasma membrane and inhibiting basal receptor endocytosis when TSHR is not ligand activated (Lahuna *et al.*, 2005). Although the trafficking function of Scrib complex has not as yet been determined to directly relate to proliferation control, recent discoveries of novel *Drosophila* neoplastic tumor suppressors has brought this link into prominence. Core endocytic trafficking machinery components *avalanche* (*avl*) and *vesicular protein sorting 25* (*vps25*) have been identified as neoplastic tumor suppressors. Mutant epithelium manifest properties similar to *scrib-dlg-lgl* phenotype, with expansion of apical domain to the basolateral membrane associated with dysregulation of epithelial architecture and proliferation (Lu and Bilder, 2005; Vaccari and Bilder, 2005).

### 1.2.3 Scribble: A LAP Family Member

According to its structural homology, Scribble has been classified as a member of a family of scaffolding proteins known as LAP (LRR and PDZ domain) proteins (Bilder *et al.*, 2000a). These proteins are structurally characterized by multiple conserved domains. The N-terminal encompasses sixteen LRRs (leucine-rich repeats), each consisting of a 20-29 amino acid (aa) residue motif containing a conserved 11 aa consensus sequence LxxLxLxxN/CxL (where 'x' is any aa, 'L' is leucine, isoleucine, valine or phenylalanine, 'N' is asparagine, threonine, serine or cysteine and 'C' is cysteine or serine) (Kajava, 1998). Immediately downstream to the sixteen LRRs are two LAPSDs (LAP-specific domains). The first LAPSD is designated LAPSDa and is a 38 aa LRR-like domain. Following this is the 24 aa LAPSDb, which is unrelated to LRR motifs. Residing at the C-terminus of LAP proteins are varying copies of PDZ domains. LAPs contain four, one or no PDZ domain and are designated as LAP4, LAP1 and LAP0 respectively (Santoni *et al.*, 2002). PDZ domains are one of the most common protein-protein interaction modules and are frequently present in multi-modular scaffolding proteins that contain several tandem PDZ domains and/or other protein binding domains. This domain is identified by the highly conserved 4 aa motif of GLGF (Glycine-Leucine-Glycine-Phenylalanine) and mainly recognize proteins with specific C-terminal peptide motifs, although internal peptides that structurally mimic C-terminal ligands can also be recognized. The PDZ domain is composed of six β strands (βA-F) and two α helices (αA and B). The ligand binding groove is structurally formed by a connecting loop between βA and βB, βB strand and αB helix. The connecting loop contains the conserved GLGF motif. These residues provide a cradle that crucially binds to and stabilizes the terminal

carboxylate group of ligands and thus the connecting loop is also known as the carboxylate-binding loop (Doyle *et al.*, 1996) (Fig. 1-6, see also Chapter 2 Fig. 2-3C).

The C-terminal PDZ-binding motif is usually 5 aa long and these residues have a particular positional nomenclature. Starting from the C-terminal residue towards the N terminus, the residues are referred to as $P_0$, $P_{-1}$, $P_{-2}$, $P_{-3}$, etc. Studies have determined that $P_0$ and $P_{-2}$ residues are crucial for PDZ binding and based on the type of aa residues preferred at these two sites, PDZ domains have been classified under three main classes. Class I PDZ domains recognize the consensus sequence S/T-X-Φ-COOH; Class II, the sequence Φ-X-Φ-COOH and Class III, the sequence D/E/K/R-X-Φ-COOH (where 'X' is any aa, 'Φ' is a hydrophobic aa, 'S' is serine, 'T' is threonine, 'D' is aspartic acid, 'E' is glutamic acid, 'K' is lysine and 'R' is arginine). In addition, outside these three classes, other ligands with the sequence X-X-C-COOH (where 'C' is cysteine) have also been discovered (Harris and Lim, 2001; Jelen *et al.*, 2003). Based on their aa sequence homology and ligand binding preference, LAP protein PDZ domains have been classified as Class I (Legouis *et al.*, 2000; Zhang *et al.*, 2006). As alluded to, internal peptide motifs represent an alternative mode of PDZ-ligand interaction. These internal motifs bind the same PDZ groove as C-terminal motifs and satisfy the PDZ recognition requirements by conformationally and biochemically mimicking a C-terminal peptide (Harris and Lim, 2001; Jelen *et al.*, 2003). This internal motif-mediated PDZ interaction is exemplified by the PDZ-PDZ homo or heterodimerization seen in the ZO proteins (Itoh *et al.*, 1999a; Itoh *et al.*, 1999b; Utepbergenov *et al.*, 2006).


**Figure 1-6. Ribbon diagram depiction of the tertiary structure of the PDZ3 domain of post synaptic density protein 95 (PSD-95).** The yellow insert represents a ligand in the binding groove. The binding groove is lined by the carboxylate-binding loop, βB strand and αB helix. (Reprinted from Cell, 85, 1067-1076, Doyle, D.A., Lee, A., Lewis, J., Kim, E., Sheng, M., and MacKinnon, R., Crystal structures of a complexed and peptide-free membrane protein-binding domain: molecular basis of peptide recognition by PDZ. (2007), with permission from Elsevier Ltd.)

LAP proteins have been discovered in various metazoans. Along with hScrib, four have been identified in vertebrates and include Densin-180, Erbin and Lano (Apperson *et al.*, 1996; Borg *et al.*, 2000; Saito *et al.*, 2001). Densin-180 and Erbin have only one PDZ domain and are LAP1 proteins whereas the LAP4 hScrib has four PDZ domains and LAP0 Lano is without PDZ domain. Lano however has a C-terminal PDZ-binding motif. In invertebrates, only the structurally conserved hScrib orthologue dmScrib has been identified as a LAP protein in *Drosophila*. Another LAP protein, the LAP1 LET-413 has been discovered in *Caenorhabditis elegans* (Legouis *et al.*, 2000) (Fig. 1-7). Aside from the neuron-specific Densin-180, the other LAP proteins are ubiquitous in expression. Like hScrib/dmScrib, Erbin, Lano and Let-413 are expressed in epithelia and localized to the basolateral membrane and the AJ. Interesting, Erbin and Let-413 also have roles in polarity regulation just like Scrib. Erbin (ERBB2 interacting protein) is named after its PDZ binding to the EGFR family member ERBB2. It associates with the non-activated unphosphorylated ERBB2 and abrogation of this interaction leads to the mislocalization of the receptor from its normal basolateral distribution to the apical membrane, leading to possible dysregulate of ERBB2 function (Borg *et al.*, 2000). In another relation to polarity regulation, *let-413 C. elegans* mutants strikingly display similar phenotypes to *scrib Drosophila* mutants. AJs of *let-413* mutant epithelial cells were absent or discontinuous. Furthermore, apical markers were also absent or mislocalized but basal marker remained unaffected (Legouis *et al.*, 2000). Together with Scrib, these two examples emphasize the common biological functions that LAP proteins play in epithelial cell polarization.

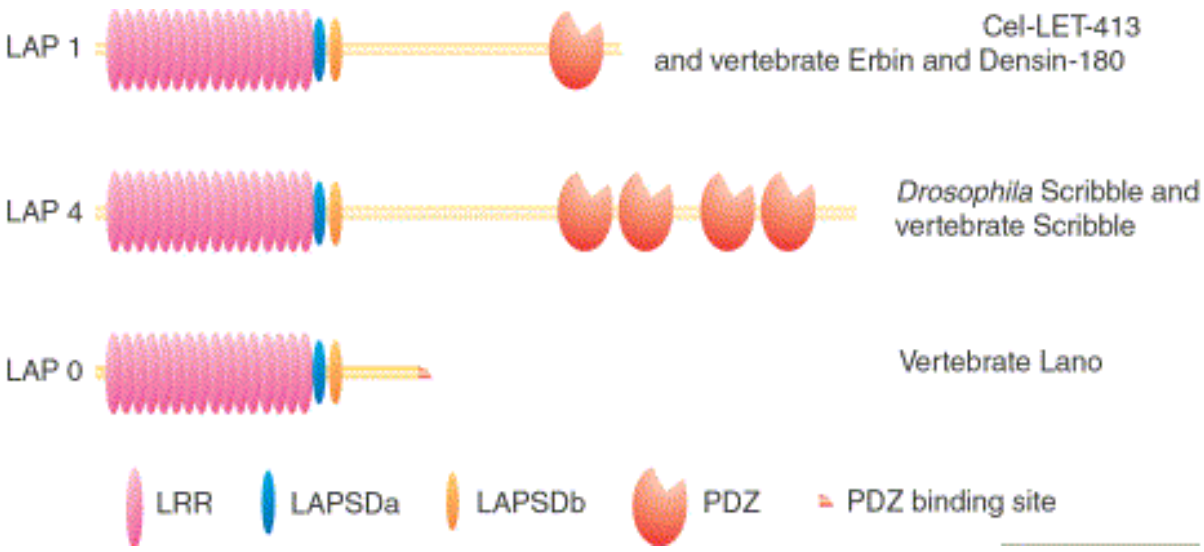


**Figure 1-7. LAP family conserved molecular structure.** All LAP members have sixteen LRR motifs, a LAPSDa and LAPSDb and variable numbers of PDZ domains. LAP 1 has one PDZ domain whereas LAP 4 has four PDZ domains. LAP 0 does not have any PDZ domain but member Lano has a C-terminal PDZ-binding motif. Members of each LAP subgroup are listed at the right hand end of the molecular structure. Cel - *Caenorhabditis elegans*. (Reprinted from Trends in Genetics, 18, 494-497, Santoni, M.J., Pontarotti, P., Birnbaum, D., and Borg, J.P., The LAP family: a phylogenetic point of view. (2002), with permission from Elsevier Ltd.)

### 1.2.4 Scribble Function

Genetic studies of *Drosophila scrib* mutant models have revealed the role of Scrib in epithelial and neuroblast polarity and proliferation and also neurological synaptic function. These seminal findings have been followed by studies which have identified Scrib function not only in apical-basal polarity but also in other polarity models of planar and anterior-posterior polarity. Other investigations have characterized Scrib at the molecular level and allowed for a better understanding of the mechanistic basis of its function in these polarity and proliferation processes.

#### 1.2.4.1 Interacting Partners of Scribble

The two main protein-protein interacting domains of Scrib are the sixteen LRRs and four PDZs. A number of Scrib interacting proteins have been identified and determined to bind its PDZ domains although only one Scrib LRR interacting protein has been discovered to date (Table 1).

The genetic interaction and co-localization of Scrib, Dlg and Lgl suggests a physical interaction among the three proteins. Studies in neuronal synaptic junctions and epithelial cells have confirmed such a relationship. At *Drosophila* larval NMJ, the GUK (guanylate kinase) domain of Dlg is essential for its binding to the synaptic protein GUKH (GUK-holder). GUKH also directly interacts with the second PDZ (PDZ2) of Scrib through its C-terminal PDZ-binding motif. While GUKH and Dlg are not necessary for each other's distribution, both are crucial for the synaptic localization of Scrib, therefore suggesting a tripartite complex with GUKH mediating the indirect interaction of Dlg with Scrib. Although Dlg (Budnik *et al.*, 1996) and Scrib (Roche *et al.*, 2002) are

required for synaptic structure and function, the role of Dlg-GUKH-Scrib interaction at NMJ has not been resolved (Mathew *et al.,* 2002). Lgl-Scrib interaction has been investigated in a polarized mammalian epithelial cell-line, Madin-Darby Canine Kidney (MDCK). Lgl interacts with the LRR domain of Scrib, and the majority of this complex localizes to the plasma membrane while a small fraction remains cytosolic. This interaction is suggested to be transient and is consistent with the regulatory role of Lgl (Kallay *et al.*, 2006).

As mentioned previously, Rac1 and Cdc42 are central initiators of epithelial cell polarity and migration. Also involved are their downstream effector PAK1 and upstream regulator βPIX. βPIX interacts with PAK1 and also activates Rac1/Cdc42 via its GEF activity and thus possibly creates a positive feedback loop (Manser *et al.*, 1998). A Scrib-βPIX interaction has been identified in mammalian epithelial and neuroendocrine cells. This interaction is mediated through the βPIX C-terminal PDZ-binding motif and Scrib PDZ domains. In addition, GIT1 associates with the GIT1 binding motif (GB) of βPIX and forms a tripartite complex with Scrib. In neuroendocrine cell-line PC12, interaction with membrane localized Scrib is necessary for the recruitment of cytosolic βPIX to the plasma membrane during membrane depolarization. This membrane targeted βPIX can form a complex with Rac1 and regulate hormone exocytosis through its GEF activity, probably via Rac1 stimulation. Together with their roles in cell migration, this highlights the conserved function of Scrib mediated recruitment of βPIX in various tissue types and polarity models (Audebert *et al.*, 2004).

In addition to βPIX, other polarity-related proteins have been identified as Scrib interactors. As alluded to previously, APC together with Dlg is involved in cell cycle

inhibition and the anterior-posterior polarization of microtubules in migrating cells. Furthermore, APC downregulates Wnt signaling pathway through its binding of β-catenin, leading to inhibition of cell proliferation (Senda *et al.*, 2007). APC has been identified as a direct interactor of Scrib in mammalian brain tissue and epithelial cell-lines. This binding is mediated through the C-terminal PDZ-binding motif of APC and the PDZ1 and 4 of Scrib and can exist in a complex containing β-catenin. This complex has been co-localized to epithelial basolateral membrane and protrusions and is thought to regulate E-cadherin adherens junction formation (Takizawa *et al.*, 2006). Like Lgl and Dlg in *Drosophila* apical-basal epithelial polarization, Scrib has also been found to genetically interact with planar polarity transmembrane protein Van Gogh-like 2 (Vangl2) during mouse neural tube development (Montcouquiol *et al.*, 2003). In polarized MDCK, Vangl2 interacts directly with Scrib PDZ2-3 through its C-terminal PDZ-binding motif and is localized to the basolateral membrane. This membrane localization appears to be diminished and becomes more vesicular when Vangl2 PDZ binding motif is deleted. Interestingly, Dlg has also been identified to bind Vangl2 in MDCK (Kallay *et al.*, 2006).

The establishment of cell polarity necessitates the integration of extracellular signals with intracellular response. The possibility that Scrib can mediate such a signal transduction has been highlighted by its interaction with two members of the zyxin family of scaffolding proteins in mammalian cells. This family of proteins localizes at cell-cell contacts and focal adhesions and can transiently translocate to the nucleus where they regulate transcription activation. Of the five zyxin family members, only LPP (Lin11, Isl-1 & Mec-3 (LIM) domain containing preferred translocation partner in

lipoma) and thyroid hormone receptor interactor 6 (TRIP6) directly bind to Scrib PDZ3 via their C-terminal PDZ-binding motif. Since Scrib does not localize to focal adhesions and the nucleus, this interaction likely occurs at cell-cell contacts where all partners co-localize. However, this localization does not appear to be dependent on the interaction. Although this interaction potentially links Scrib with cell-cell adhesion and nuclear signaling, the functional significance of the association has yet to be elucidated in the mammalian system (Petit *et al.*, 2005a; Petit *et al.*, 2005b).

As discussed earlier, one aspect of the transforming ability of oncogenic viral proteins high-risk HPV E6 and HTLV-1 Tax is their interaction with Scrib and inactivation of its tumor suppressive activity. Another viral protein, Tick-borne encephalitis virus (TBEV) NS5 has also been identified to directly interact with Scrib. Unlike the HPV and HTLV, TBEV is not associated with tumorigenesis but is instead neurovirulent and can result in lethal encephalitis. This infection can be controlled by the host innate immune response, initiated by interferon (IFN)-stimulated janus protein tyrosine kinase-signal transducer and activator of transcription (JAK-STAT) signal transduction, leading to the expression of genes involved in antiviral activities, cell cycle progression and apoptosis. Viral NS5 can circumvent this by inhibiting the formation of active phosphorylated STAT possibly via interaction with IFN receptor complexes at the plasma membrane. In order to localize to the membrane, NS5 uses the host cell membrane scaffolding system as an anchor by interacting with Scrib PDZ4. This PDZ association is unique among all Scrib PDZ interacting partners in that an internal binding site of NS5 mediates the binding instead of a canonical C-terminal PDZ-binding motif. The Scrib-mediated localization of NS5 JAK-STAT antagonism reveals an interesting

alternative function to the usual Scrib-viral activity relationship where Scrib interferes with virulence rather than promote it (Werme *et al.*, 2008).

| No. | Scrib Interactor | Interactor Binding Site | Scrib Binding Site | Subcellular Localization | Function |
|---|---|---|---|---|---|
| 1 | Lgl2 | N.A. | LRR | MDCK lateral membrane | Scrib complex localization |
| 2 | Vangl2 | ETSV-COOH | PDZ2-4 | MDCK lateral membrane | Vangl2 membrane localization |
| 3 | GUKH | ETAL-COOH | PDZ2 | *Drosophila* NMJ | Scrib synaptic localization |
| 4 | βPIX | TNL-COOH | PDZ domains | Neuronal presynaptic compartment and PC12 plasma membrane | βPIX localization to PC12 plasma membrane |
| 5 | APC | VTSV-COOH | PDZ1 and 4 | MDCK membrane protrusions and hippocampal neuron synaptic sites | AJ formation |
| 6 | Zyxin LPP and TRIP6 | STDL-COOH TTDC-COOH | PDZ3 | MDCK cell-cell contact | Possible cell-cell contact and nuclear signaling |
| 7 | Crtam | ESIV-COOH | PDZ3 | TCR | Scaffold for signal complexes in late T-cell activation |

| No. | Scrib Interactor | Interactor Binding Site | Scrib Binding Site | Subcellular Localization | Function |
|---|---|---|---|---|---|
| 8 | TSHR | TVL-COOH | PDZ1 and 3 | Thyroid follicular cell lateral membrane | TSHR recycling |
| 9 | High risk HPV E6 | Cter motifs | PDZ3 | Infected cervical epithelial cell cytosol | Scrib degradation |
| 10 | HTLV-1 Tax | ETEV-COOH | PDZ2 and 3 | Infected T-cell cytosolic granules | Scrib sequestration |
| 11 | TBEV NS5 | Internal site | PDZ4 | Infected mammalian cell plasma membrane | Scaffold for NS5 membrane localization |

**Table 1. Direct interacting partners of Scrib.** Note that all interactors except Lgl2 bind to Scrib PDZ domains. Lgl2 binds to Scrib LRR. Scrib PDZ binding interactions are mediated by C-terminal (Cter) binding motifs except for TBEV NS5 which uses an uncharacterized internal motif. All interactions reflect Scrib function as a membrane scaffold protein.

### 1.2.4.2 Functional Domains

The functional mapping of domains in the multi-modular Scrib helps dissect the specific molecular roles they play. This mapping can be done by rescue of *scrib* null mutant phenotype in *Drosophila* using full-length or domain constructs of wild-type (WT) *scrib* and have been investigated in epithelia and neuroblasts.

In the larval wing imaginal disc epithelium of *scrib* null mutants, expression of Scrib deletion mutants without the LRR domain but containing the rest of the C-terminal portion including the four PDZ domains exhibited no membrane localization. Instead, distribution was cytoplasmic and unpolarized. Furthermore, null mutant phenotype was not rescued. Additional investigations with Scrib deletion mutants expressing only the LRR and not the PDZ domains revealed broad non-polarized basolateral membrane localization. This could fully restore normal epithelial polarity and organization but showed only intermediate rescue of overgrowth. Complete rescue of mutant polarity by Scrib LRR is consistent with its ability to cortically localize Lgl, allowing it to perform its polarizing effect. Interestingly, deletion mutants encompassing the LRR and PDZ1 and 2 domains localized specifically to the apex of the lateral membrane and SJ as WT Scrib would, and fully rescued all null phenotypes. Taken together, these studies indicate that the LRR domain is necessary and sufficient to provide for the polarity and proliferation functions of Scrib. PDZ domains alone are non-functional but enhance LRR-regulated proliferation when combined with LRR. In addition, these two domains work in concert to correctly localize Scrib in a two step process. LRR domain mediates initial Scrib homogenous basolateral membrane distribution while PDZ domains

subsequently enrich it to the SJ (Zeitler *et al.*, 2004). This is also consistent with studies done in zebrafish embryos (Wada *et al.*, 2005).

Demarcation of Scrib domain function in *scrib* null neuroblast has also revealed a similar two step approach to Scrib localization. Localization of Scrib deletion mutants indicated that the LRR is necessary and sufficient for the uniform cortical distribution of Scrib. However, only in the presence of a functional PDZ2 domain was Scrib properly apical cortically enriched in metaphase neuroblast. This might be explained by the Dlg mediated Scrib recruitment via GUKH interaction with Scrib PDZ2. Additionally, both the LAPSDa/b and C-terminal tail (after PDZ domains) were not sufficient for proper neuroblast Scrib localization and this was also found to be true when *scrib* mutant epithelia were analyzed. As mentioned, basal determinants like Miranda are mislocalized in metaphase neuroblast of *scrib* null mutants. This was rescued by constructs encompassing both the LRR and PDZ domains. The LRR domain on its own could only restore Miranda to a uniform cortical distribution and needed the inclusion of the PDZ domains for full basal cortical enrichment. Additionally, restoration of mutant symmetrical or inverted mitotic spindle and cell size to normal asymmetry was only achieved by both LRR and PDZ domains in combination and not individually. Again like in Scrib localization, both LAPSDa/b and C-terminal tail were not required for any of these rescues (Albertson *et al.*, 2004).

The domain mapping of Scrib in epithelia and neuroblast illustrates the conserved functions of the LRR and PDZ domains in localization of Scrib in various cell polarity models. The absolute requirement of LRR in Scrib basolateral membrane localization is consistent with two other LAP proteins, Erbin and LET-413 (Legouis *et al.*, 2003). LRR-

mediated localization of LAP proteins is possibly regulated by its interaction with a tethering protein or a regulator of protein trafficking localized to the basolateral domain. The LRR domain of SUR-8 is known to bind the small G-protein Ras and is highly homologous to that of LET-413 (Sieburth *et al.*, 1998; Legouis *et al.*, 2000). This indicates that small G-proteins are potential interactors of LAP proteins and Rac1/Cdc42 are good candidates for this since they have been implicated in polarized basolateral trafficking (Cohen *et al.*, 2001; Wang *et al.*, 2005).

### 1.2.4.3 Mammalian Cell-Line Models

Although there is currently a lack of evidence for Scrib apical-basal polarity function in mammalian models, various studies have implicated Scrib in the regulation of other polarity models in mammalian systems. Such models include anterior-posterior polarization in T-cells and migrating astrocytes and epithelial cells. In spite of the morphological and functional differences between T-cell, glial and epithelial cell types, there remains a fundamental conservation of polarity regulation.

Aside from its roles in the widely studied mammalian epithelial cell system, Scrib function in adaptive immune system T-cells has also been studied. Migrating T-cells possess two identifiable poles. The leading edge defines the anterior pole and directs forward migration while the posterior pole is distinguished by a rear protrusion called the uropod. Similar to polarized epithelial cells, polarity proteins are asymmetrically distributed in uropod-containing T-cells. Scrib together with Dlg is localized in the uropod, where they regulate the asymmetric distribution of T-cell proteins to this structure and the exclusion of Par and Crb complex members. The abrogation or

depletion of Dlg function and Scrib levels respectively results in the failure of uropod formation and impeded cell migration. Scrib also regulates T-cell activation during antigen presentation. When T-cells are engaged by antigen-presenting cells, an immunological synapse (IS) is formed. This junction consists of clustered T-cell receptors (TCR) of the T-cell engaged with antigen-major histocompatibility complexes (MHC) of the antigen-presenting cell. In the early stages of engagement, T-cells disassemble their uropod and round up. This is coincident with a relocalization of Scrib and Dlg from the uropod to the interface of the T-cell and antigen-presenting cell and then to the opposite distal pole. Conversely Par and Crb complexes show a relocalization to the IS where IS proteins are like-wise polarized to. This repolarization and formation of IS is mediated by Scrib and depletion of this compromises IS formation during TCR activation (Ludford-Menting *et al.*, 2005). Interestingly, Scrib also functions in T-cell polarization after the initial TCR engagement. The TCR-activated late-expressing gene product Crtam (class-I MHC-restricted T-cell associated molecule) binds to Scrib at the TCR via its C-terminal PDZ-binding motif. This establishes T-cell polarity by providing a scaffold to anchor signal complexes, including Cdc42, that regulate later phases of T-cell activation such as cytokine production and cell proliferation (Yeh *et al.*, 2008).

Recent studies on various mammalian cell-line models have also revealed a role of Scrib in directed cell migration. This function has been linked to the regulation of E-cadherin-catenin AJ molecules and polarity-related proteins βPIX, Rac1/Cdc42 and PAK1. As discussed, Scrib localizes to the lateral membrane AJ of vertebrate epithelial cells. Further studies have shown this localization to be dependent on E-cadherin expression (Navarro *et al.*, 2005). This relation has been validated and revealed to affect

cell-cell adhesion and migration. Scrib silenced MDCK exhibited a morphological change characterized by a fibroblastic disorganized appearance. Furthermore, cells failed to migrate as a cohesive sheet but rather pulled away from the migration front, showing random and increased motility. Surprisingly, this aberration was not mediated by Scrib-βPIX or Rac but a defect in E-cadherin-catenin stabilization at AJ (Qin *et al.*, 2005). This is consistent with the discovery that Scrib degradation by caspase during apoptosis mediates the detachment of cell-cell contact (Sone *et al.*, 2008).

Studies on astrocytes have also discovered a role of Scrib in directed migration. However the mechanism in this system involves Cdc42 rather than E-cadherin-catenin. In migrating astrocytes, Scrib localizes to the leading edge and sequentially recruits its βPIX interacting partner and Cdc42 to the anterior membrane. Cdc42 is subsequently activated by βPIX GEF and thereafter regulates its downstream polarity pathway. Abrogation of Scrib-βPIX function results in the failure of Cdc42-dependent clustering of APC to the plus ends of microtubules and recruitment of Dlg1 to the leading edge of migrating cells, leading to impaired MTOC and Golgi apparatus reorientation, cytoskeletal organization and cell protrusion (Osmani *et al.*, 2006). Consistent with this, Scrib-dependent localization of Rac1/Cdc42 was also observed in human mammary epithelial cell-line MCF10A during directed cell migration. Depletion of Scrib similarly led to defects in Rac1/Cdc42 leading edge localization, cytoskeletal organization, lamellipodia formation and Golgi apparatus orientation. However, these aberrations appear to be unrelated to Rac1/Cdc42 activation since this, unlike in astrocytes, did not depend on Scrib. Furthermore, unlike migration defects in MDCK (Qin *et al.*, 2005), Scrib silenced MCF10A exhibited no abnormality in epithelial morphology and AJ structure. In fact,

epithelial migration was impeded instead of enhanced both in *in vitro* MCF10A and *in vivo* mouse embryo *scrib* mutant *rumz* (Dow *et al.*, 2007).

A more recent study on Scrib function in breast carcinoma cells and mouse embryonic fibroblast revealed a multimolecular complex of Scrib-βPIX-PAK/GIT1involved in regulation of directed cell migration. Like GIT1, PAK indirectly associates with Scrib through its βPIX interaction. In migrating cells, Scrib recruits both βPIX and PAK at nascent leading edge protrusions. Both Scrib and βPIX also positively regulate PAK phosphorylation, activating PAK and its polarization functions. Impairment of Scrib interaction with βPIX-PAK in turn results in the failure to form polarized protrusions and diminished cell migration. Interestingly, although Rac1/Cdc42 can mediate the activation of PAK, this Scrib-dependent PAK activation is independent of Rac1/Cdc42 (Nola *et al.*, 2008).

Taken together, these migration studies, although dissimilar mechanistically probably due to the uniqueness of cell models explored, point to a conserved function of Scrib in regulating directed cell migration.

### 1.2.4.4 Animal Models

Two vertebrate models have implicated Scrib in the regulation of planar polarity in mouse. Loop-tail (*Lp*) mouse is a mutant of planar cell polarity (PCP) gene *vangl2* and produces a gene product with a serine-to-asparagine point mutation. The Circletail (*Crc*) mouse has a mutation in *scrib* that expresses a truncated Scrib that terminates just before PDZ3. Both these mutants exhibit defects in cochlea, neural tube and heart formation.

*vangl2* is a mammalian orthologue of *Drosophila* PCP gene *strabismus*/*van gogh*. In the cochlear sensory epithelium hair cells, *Lp*/*Lp* homozygotes exhibit random orientation of stereociliary bundles. This phenotype is also observed in *Crc*/*Crc*, albeit to a less severe extent. Single heterozygous *Lp*/+ or *Crc*/+ mice are normal. However, mice double heterozygous for *Lp*/+ *Crc*/+ show comparable cochlear phenotype to *Lp*/*Lp* and thus indicate a genetic interaction in PCP regulation (Montcouquiol *et al.*, 2003).

Another PCP-related phenotype observed in *Lp*/*Lp* mice is the neural tube defect (NTD) craniorachischisis where the neural tube (NT) fails to close along the entire anterior-posterior axis during neurulation, thus resulting in lethality. This defect is similarly exhibited in *Crc*/*Crc* mutants. Moreover, compound double heterozygous *Lp*/+ *Crc*/+ embryos also exhibit severe NTDs similar to that of individual homozygotes, indicating genetic interaction (Murdoch *et al.*, 2001). Furthermore, Scrib and Vangl2 are both expressed in the neuroepithelium during NT formation. Although Scrib is an apical-basal polarity regulator in *Drosophila*, this axis is not disrupted in the neuroepithelium (Murdoch *et al.*, 2003). It is likely that Scrib and Vangl2 have roles in convergent extensions (CE) of the neural tissue. PCP signaling regulates the polarized cell movement of CE resulting in folding of the neural plate and formation of the NT (Zohn *et al.*, 2003).

As discussed, Scrib interacts directly with Vangl2. Except for PDZ1, all the PDZ domains of Scrib interact with Vangl2 and PDZ3 exhibits the strongest affinity. In *Crc*/*Crc* mice, although still membrane localized, Vangl2 asymmetric membrane distribution in cochlear hair cells is disrupted. Furthermore, Vangl2 expression in *Lp*/*Lp* cochlea is silenced. The Vangl2 mutation prevents targeting or anchoring of Vangl2 to the membrane and exposes it to post-translational degradation (Montcouquiol *et al.*, 2006). A similar disruption of Vangl2 localization is also seen in cardiomyocytes of *Crc*/*Crc* mice. Organization of these cells is abnormal and mutants develop heart malformations and cardiomyopathy. In the cardiomyocytes, Vangl2 is mislocalized from the membrane to the cytoplasm. This is concomitant with a mislocalization of N-cadherin and β-catenin from the lateral membrane AJ, resulting in defective cell-cell adhesion. Such a Scrib-associated AJ disruption has also been shown in mammalian epithelial cells (Qin *et al.*, 2005) and thus indicates the conserved function of Scrib among differing cell types (Phillips *et al.*, 2007). Mechanistically, these studies implicate Scrib in the targeting or maintenance of Vangl2 to membrane compartments where it mediates PCP.

In another vertebrate model, the zebrafish mutant *landlocked* (*llk*) has revealed a dual Scrib function in neural migration and CE movements in embryos, consistent with its role in *in vitro* cell migration (Qin *et al.*, 2005; Osmani *et al.*, 2006; Dow *et al.*, 2007; Nola *et al.*, 2008) and CE in mouse (Zohn *et al.*, 2003). However, no NTD was observed in *llk*. Two *llk* mutants where studied with one encoding Scrib with aa substitution in PDZ1 and another with a stop codon in the LRR domain. Zygotic *llk* embryos showed a complete loss of caudal migration of the nVII motor neurons of the hindbrain. Interestingly, *llk* embryos are viable, suggesting that Scrib is not essential for CE

movement. However, depletion of maternal *scrib* mRNA resulted in slight CE defects during gastrulation but this had no effect on migration of nVII motor neurons. The loss of maternal *scrib* can be compensated partially with zygotic *scrib* expression (Wada *et al.*, 2005). Interestingly, the Scrib-LPP interaction discovered in mammalian cells (Petit *et al.*, 2005b) was also indentified in zebrafish and both together mediate CE during embryogenesis (Vervenne *et al.*, 2008).

In all, these animal studies reveal a highly conserved Scrib function in cell motility essential for various aspects of embryogenesis and fetal development.

## 1.3 Tight Junctions and Epithelial Cell Polarity

Epithelial cell functions are highly dependent on the intercellular junctions that line the lateral membrane of apposing cells. These junctions include the AJ, TJ and DS and control various functions involved in epithelial homeostasis. The TJ is a characteristic epithelial junction and is crucially involved in the regulation of apical-basal cell polarity and paracellular transport. TJ acts as a fence or intramembrane diffusion barrier which divides the apical from the basolateral domains thus maintaining cell polarity by inhibiting intermixing of domain membrane components. It also plays gatekeeper or a paracellular seal by regulating the movement of ions and solutes across the epithelial sheet, hence establishing a permeability barrier (Tsukita *et al.*, 2001) (Fig. 1-8).

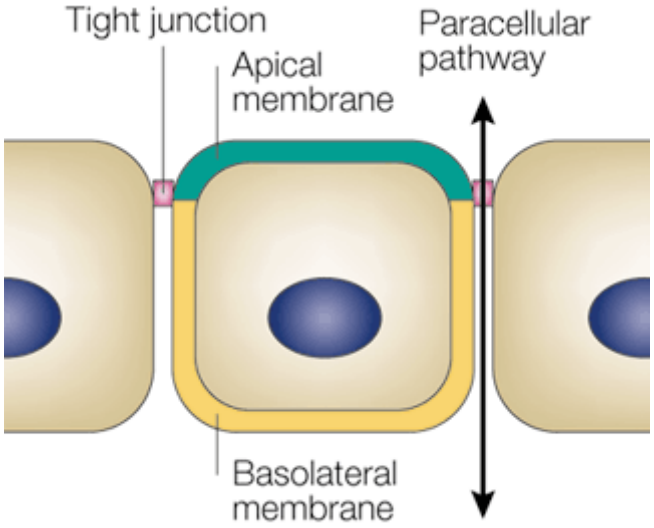


**Figure 1-8. Tight junctions regulate apical-basal cell polarity and paracellular transport.** The fence function of TJs prevents the intermixing of apical membrane (green color) and basolateral membrane (yellow color) components. Paracellular movement of solutes across the polarized epithelial sheet is also regulated by TJs. (Reprinted from Nature Reviews Molecular Cell Biology, 2, 285-293, Tsukita, S., Furuse, M., and Itoh, M., Multifunctional strands in tight junctions. (2001), with permission from Nature Publishing Group.)

### 1.3.1 Molecular Constituents of Tight Junctions

The TJ components can be categorized into integral transmembrane proteins and peripheral plaque proteins. Since TJ can contain a huge number of protein components (Tang, 2006), only the main players in structure and regulation of TJ will be discussed.

#### 1.3.1.1 Transmembrane Proteins

TJs consist of three main integral membrane proteins, occludin (Furuse *et al.*, 1993), claudin family (Furuse *et al.*, 1998a) and JAM family (Martin-Padura *et al.*, 1998) (Fig. 1-9). Both occudin and claudins are four transmembrane domain proteins with cytoplasmic N- and C-termini and two extracellular loops (Furuse *et al.*, 1998a; Feldman *et al.*, 2005). JAMs belong to the immunoglobulin (Ig) superfamily and are single transmembrane domain proteins characterized by two Ig-like extracellular motifs and a cytoplamic tail (Kostrewa *et al.*, 2001). These three transmembrane proteins function as CAMs and form adhesions with counterparts on adjacent cells. These adhesions create a tight seal or kissing points between apposing lateral membranes at the apical end and form a network of continuous anastomosing intramembranous strands i.e. TJ strands (Fig. 1-10). Occludin likely engages in homophilic associations (Van Itallie and Anderson, 1997) whereas claudins and JAMs employ both homophilic and heterophilic interactions with their family members. Notably, claudins interact with each other laterally within TJ strands and across adjacent cell TJ networks (Furuse *et al.*, 1999; Bazzoni *et al.*, 2000a; Arrate *et al.*, 2001).

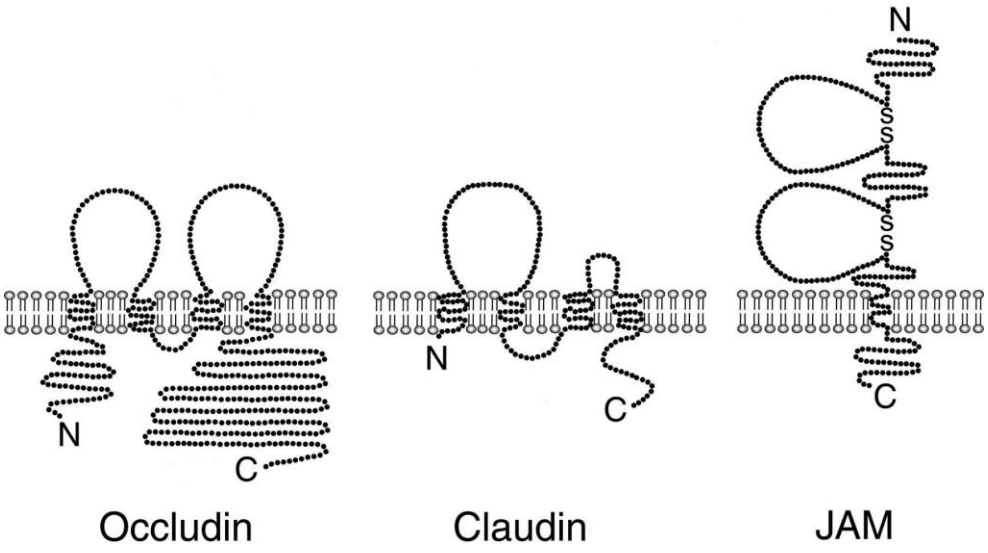


**Figure 1-9. Integral membrane proteins of tight junctions.** Both occludin and claudins are four transmembrane domain proteins with cytoplasmic N- and C-termini and two extracellular loops. JAMs are single transmembrane domain proteins characterized by two Ig-like extracellular motifs at the N-termini and a C-termini cytoplamic tail. (Reprinted from American Journal of Physiology: Cell Physiology, 286, C1213-C1228, Schneeberger, E.E., and Lynch, R.D., The tight junction: a multifunctional complex. (2004), with permission from The American Physiological Society.)

**A** **B**

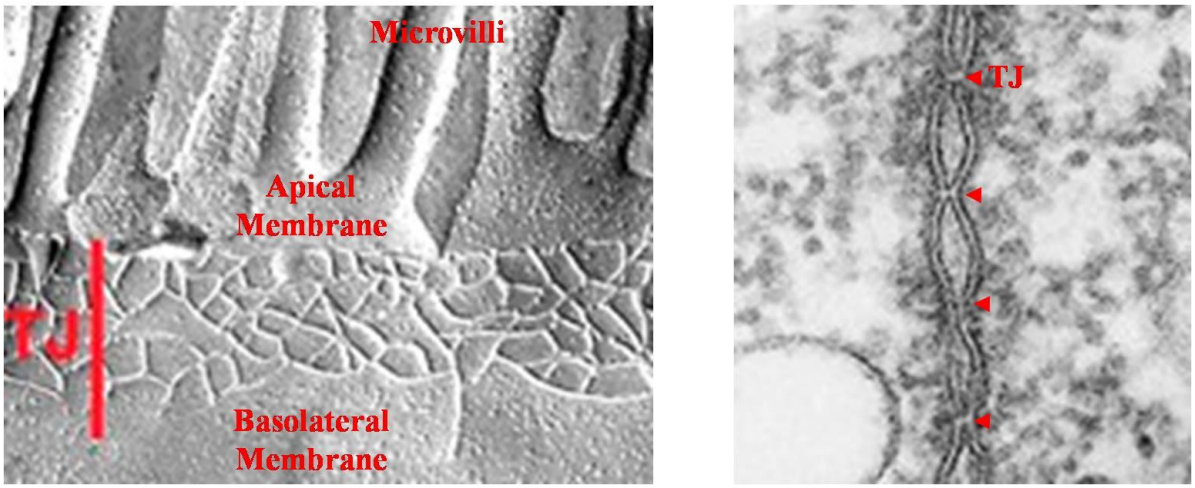


**Figure 1-10. Electron microscopic images of tight junctions in intestinal epithelial cells.** **(A)** Freeze-fracture replica image showing a network of continuous anastomosing intramembranous TJ strands. **(B)** Ultrathin sectional view depicting TJ kissing points (arrowheads) between apposing lateral membranes at the apical end. (Reprinted from Oncogene, 27, 6930-6938, Tsukita, S., Yamazaki, Y., Katsuno, T., Tamura, A. and Tsukita, S., Tight junction-based epithelial microenvironment and cell proliferation. (2008), with permission from Nature Publishing Group.)

The role of occludin in TJ function is inconclusive since studies have revealed conflicting results. The extracellular domains of occludin positively regulate cell-cell adhesion and permeability barrier function (Van Itallie and Anderson, 1997; Wong and Gumbiner, 1997). Permeability barrier function was evaluated using the transcellular electric resistance (TER) assay which measures electrical resistance across the epithelium and the flux of tracers across the paracellular space. Using these same assays, overexpression of occludin and C-terminal deletion mutants showed increase in transcellular electric TER, but paradoxically also an increase in paracellular flux (Balda *et al.*, 1996). Although these results point to occludin importance in TJ function, occludin knock out studies have shown that TJ assembly and permeability barrier function was independent of occludin expression (Saitou *et al.*, 2000).

Claudins are crucially involved in TJ strand formation and barrier function. Exogenously expressed claudins in fibroblast lacking TJ induced cell-cell adhesion and TJ network strands and readily recruited exogenous occludin to this structure (Furuse *et al.*, 1998b). The Claudin family consists of at least 24 members. These have specific tissue expression patterns and at least two members are expressed in most cells (Tsukita *et al.*, 2001). The different claudin isoforms expressed determine the ion and size selectivity of paracellular transport (Furuse *et al.*, 2001; Van Itallie *et al.*, 2001; Nitta *et al.*, 2003). This is dictated by the different charges and isoelectric points of the extracellular domains of various claudin members (Colegio *et al.*, 2002). Furthermore, phosphorylation of the C-termini of claudins by protein kinases can alter paracellular permeability (Yamauchi *et al.*, 2004; D'Souza *et al.*, 2005).

The JAM family comprises of four members, JAM-A, -B, -C and -4. Unlike claudins, JAMs are unable to form TJ strands in fibroblast but instead are concentrated at intramembrane strand-free cell-cell adhesions, implying that JAMs are not integral members of TJs (Itoh *et al.*, 2001). However, JAM extracellular domain is essential for the assembly of TJ and positively regulates barrier function (Liu *et al.*, 2000). Interestingly, JAMs play an important role in the apical-basal polarization of epithelial cells. During polarization, JAM is the first TJ integral membrane protein to recruit to the PA. This localization triggers the recruitment of the Par complex via interaction with Par3 and this allows regulation of junctional maturation of TJ and AJ (Ebnet *et al.*, 2001; Ebnet *et al.*, 2003).

### 1.3.1.2 Peripheral Proteins Zonula Occludens

Integral membrane proteins of the TJ are incorporated into a clustered network of intramembranous strands by their cytoplasmic associations with peripheral proteins that form a scaffold linking the TJ to actin cytoskeletal networks. The scaffold consists of many modular adaptor, polarity and signaling proteins that make up a submembranous plaque from which regulated intercellular communications emanate (Guillemot *et al.*, 2008).

The key scaffold molecules in this cytoplasmic TJ surface are the ZO proteins, ZO-1 (Stevenson *et al.*, 1986), ZO-2 (Gumbiner *et al.*, 1991) and ZO-3 (Balda *et al.*, 1993) (see Chapter 2 Fig. 2-1A). These ZO proteins have multi-modular protein-protein interaction domains and belong to a family know as membrane-associated guanylate kinase (MAGUK), which are characterized by one or more PDZ, a Src homology 3 (SH3) and a guanylate kinase (GUK) domain. The three ZO TJ MAGUKs have three N-terminal Class I PDZ domains, followed by a SH3 and GUK domain separated by a hinge region (Gonzalez-Mariscal *et al.*, 2000). PDZ domains have been described earlier. The non-catalytic SH3 domain is homologous to a region of the v-Src oncogene tyrosine kinase and mediates protein-protein interactions with ligands containing polyproline motifs (Dalgarno *et al.*, 1997). The GUK domain is homologous to an enzyme that uses adenosine triphosphate (ATP) to convert guanosine monophosphate (GMP) to GDP. However, the GUK domains lack critical aa essential for nucleotide binding and catalysis and is thus enzymatically inactive and binds neither GMP or ATP. Instead it can act as a protein interaction domain (Fanning *et al.*, 1998; Haskins *et al.*, 1998). Based on studies of other MAGUKs, SH3 can associate and establish an intramolecular interaction with

GUK in a non-polyproline motif manner (McGee and Bredt, 1999). Intermolecular homo or heterodimerization between SH3 and GUK of apposing MAGUKs can also occur (Masuko *et al.*, 1999). The balance between intra and intermolecular interactions is modulated by the hinge region between SH3 and GUK (McGee *et al.*, 2001). Indeed, it appears that SH3-hinge-GUK unit is necessary in the mediation of ZO1-ZO1 homodimer formation (Umeda *et al.*, 2006; Ikenouchi *et al.*, 2007) (discussed below).

Aside from the three typical MAGUK domains, ZO proteins distinctly have in addition an acidic and a proline-rich (PR) region towards the C-terminal but with the exception of ZO-3 which has its PR domain in between PDZ2 and 3. The PR region differs in length between the proteins and is alternatively spliced in ZO-1 and -2 (Willott *et al.*, 1992; Beatch *et al.*, 1996). Furthermore it also mediates protein interactions (Fanning *et al.*, 1998). Also, a basic domain is present between PDZ-1 and 2. Interestingly, all three ZO proteins possess nuclear sorting signals (Gonzalez-Mariscal *et al.*, 2000). The nuclear localization signal (NLS) and nuclear export signal (NES) located on proteins are sufficient to transport them into and out of the nucleus respectively (Izaurralde and Adam, 1998). ZO-1 has two NLSs located at PDZ1 and GUK domains and three NESs at SH3, acidic and proline-rich domains. ZO-2 has five functional NLS in PDZ1-basic domains and four NESs, with two each situated at PDZ2 and GUK domains. Two NLSs are located at the basic region and GUK domain of ZO-3 and an NES is found at the acidic domain. The nuclear sorting signals of ZO-1 and ZO-3 are putative since only those of ZO-2 have been investigated to be functional (Gonzalez-Mariscal *et al.*, 1999; Islas *et al.*, 2002; Jaramillo *et al.*, 2004; Gonzalez-Mariscal *et al.*, 2006). The

presence of these nuclear sorting signals in ZOs implies that they have more complex signaling functions other than being adaptor proteins.

As scaffold proteins, the ZO proteins establish direct interactions with transmembrane TJ proteins and participate in their assembly. The C-termini of claudins have a PDZ-binding motif which associates with PDZ1 of all three ZOs, although only the interaction with ZO-1 or ZO-2 but not ZO-3 is necessary for claudin recruitment and assembly into TJ strands (Itoh *et al.*, 1999a; Umeda *et al.*, 2006). Similarly, occludin binds to all three ZOs via its cytoplasmic C-terminal region (Furuse *et al.*, 1994; Haskins *et al.*, 1998; Itoh *et al.*, 1999b) and in ZO-1 this takes place specifically at the hinge-GUK region (Schmidt *et al.*, 2004). Furthermore, the C-terminal PDZ-binding motif of JAM can bind PDZ3 of ZO-1 (Bazzoni *et al.*, 2000b; Itoh *et al.*, 2001). With the binding of integral TJ proteins at their PDZ to GUK N-terminal half, ZOs link the transmembrane TJ to the underlying cortical cytoskeletal network by their C-terminal region association with F-actin (Fanning *et al.*, 1998; Wittchen *et al.*, 1999). Interestingly, in spite of their interaction with TJ integral membrane proteins, the PDZ and GUK domains are not sufficient to localize ZO-1 to the TJ. Instead, the SH3-hinge-GUK domain unit is necessary for this (Saitou *et al.*, 1998; Reichert *et al.*, 2000; Umeda *et al.*, 2006; Fanning *et al.*, 2007).

The ZO proteins themselves can interact with each other. Both ZO-1-ZO-2 and ZO-1-ZO-3 heterodimers form through PDZ2-PDZ2 interactions (Fanning *et al.*, 1998; Haskins *et al.*, 1998; Itoh *et al.*, 1999a; Itoh *et al.*, 1999b; Wittchen *et al.*, 1999). Moreover, ZO1 also forms homodimers via its PDZ2 (Utepbergenov *et al.*, 2006). Oligomerization of ZOs is an important feature since it mediates the formation of TJ

networks and this has been determined with ZO-1-claudin interaction. The SH3-hinge-GUK domain unit of ZO-1 mediates its localization to the membrane and this is probably via its catenin/afadin interaction (discussed below). Furthermore, this domain unit homodimerizes ZO-1 and together with the PDZ domains recruit and cluster claudin into TJ strands (Umeda *et al.*, 2006).

### 1.3.2 Zonula Occludens and Epithelial Cell Polarity

TJ proteins play various roles during the development of apical-basal polarity and junctional biogenesis. In non-polarized epithelial cells, ZO-1 localizes to nascent E-cadherin and nectin-based PA and interacts with α-, β-, γ-catenin (Rajasekaran *et al.*, 1996) and afadin (Yokoyama *et al.*, 2001) respectively via its SH3-hinge-GUK domain unit. JAM is subsequently recruited to the nectin-based PA via ZO-1 or afadin interaction (Bazzoni et al., 2000b; Itoh et al., 2001; Fukuhara et al., 2002a). JAM in turn recruits Par3 to the maturing adhesion site (Ebnet *et al.*, 2001; Ebnet *et al.*, 2003) and claudins and occludin recruitment follows (Fukuhara et al., 2002). These studies suggest that ZO-1 forms a complex with AJ proteins in non-polarized cells without assembled TJ. However upon polarization, ZO-1 proteins can recruit TJ structural proteins, segregate from PA and assemble into mature TJ strands. In parallel, mature belt-like AJ also evolve from the PA. Interestingly, ZO-1 through its positive regulation of Rac1 activity also plays a role in enhancing belt-like AJ formation from PA. The SH3-hinge-GUK-acidic domain unit of ZO-1 alone is necessary for this maturation of AJ and this is independent of claudin TJ assembly which requires the additional presence of the PDZ domains (Ikenouchi et al., 2007).

Although it is concluded that ZO-1 and ZO-2 are necessary and sufficient to assemble claudin TJ strands, the mechanism of ZO recruitment to nascent PA and mature TJ is yet unclear. However, it appears that apical polarity complexes play an important role in defining the site where ZOs and integral TJ proteins assemble. This is evident in several studies. The depletion of PATJ results in the delay of TJ assembly and mislocalization of ZO-3 and occludin to the lateral membrane (Michel *et al.*, 2005; Shin *et al.*, 2005). Furthermore, exogenous Crb mediates the formation of functional TJ and recruitment of claudin and occludin in TJ-deficient epithelial cell-line (Fogg *et al.*, 2005). Thus it appears that polarity complexes determine the apical-basal axis and construct landmarks where TJ form. Subsequently, the TJ reinforces polarity by acting as an intramembranous barrier preventing admixing of apical and basolateral membrane components. Consistent with this notion that polarity proteins define apical-basal polarity upstream of TJ assembly, the establishment of apical-basal polarity seems to be independent of TJ presence. In a ZO-3 expression-deficient epithelial cell system with knocked-out ZO-1and silenced ZO-2, although no TJ was formed, apical-basal polarity remained unaffected (Umeda *et al.*, 2006).

### 1.3.3 Zonula Occludens and Cell Signaling

In addition to their structural roles in junctional assembly, ZO proteins play various roles in cell signaling in relation to transcriptional regulation, cell proliferation and differentiation.

ZO-1 can exert its effect on these processes through its SH3 domain interaction with ZO-1-associated nucleic acid-binding protein (ZONAB), a Y-box transcription factor (Balda and Matter, 2000). In sparse and proliferating cell cultures where ZO-1 expression is low, ZONAB localizes both at the TJ and in the nucleus. Here it promotes cell proliferation through its interaction and nuclear accumulation with cell division kinase 4 (CDK4) and transcriptional activation of proliferating cell nuclear antigen (PCNA) and cyclin D1 (CD1). However in confluent, non-proliferative conditions, increased ZO-1expression negatively regulates ZONAB activity by sequestering it at the TJ and thus influencing its subcellular distribution (Balda *et al.*, 2003; Sourisseau *et al.*, 2006).

ZO proteins can also participate in signaling pathways through their nuclear localization. ZO-1and ZO-2 nuclear localization has been observed in inverse relation to cell-cell contact maturation in epithelial cells. This occurs during situations of subconfluency and cell-cell contact remodeling or loss e.g. during epithelium wounding or cell proliferation. This diminishes with increasing confluency as the ZOs relocalize to the cell boarders (Gottardi *et al.*, 1996; Islas *et al.*, 2002). ZO-2 nuclear function has been investigated in its interaction with several nuclear proteins. The deoxyribonucleic acid (DNA) binding protein, scaffold attachment factor-B (SAF-B) associates with ZO-2 PDZ1 and colocalizes in the nucleus as speckles (Traweger *et al.*, 2003). Though the

physiological importance of this interaction is not elucidated, it possibly involves transcription regulation since SAF-B binds scaffold or matrix attachment regions of DNA and participates in transcriptosome complex assembly near actively transcribed genes (Nayler *et al.*, 1998). Several transcription factors are also known to interact with ZO-2. The acidic-proline-rich domains of ZO-2 can bind transcription factors Jun-Fos AP-1 complex and C/EBP at the nucleus and TJ under sparse and confluent conditions respectively. These factors are known to regulate cell proliferation. Although it is not known which specific genes ZO-2-AP-1 interaction regulates, it is revealed through AP-1 promoter reporter gene assays that ZO-2 downregulates gene expression. Furthermore, these transcription factors could also be sequestered by ZO-2 at the TJ (Betanzos *et al.*, 2004).

Collectively, these studies indicate that ZOs are highly mobile and can act as mechanosensors of extracellular changes that impinge on TJ dynamics, coordinating cell polarization, junctional assembly and cell density with cell proliferation and differentiation. This is of significant importance considering that in cancer cells, ZO-1 has been detected in the nucleus (Takai *et al.*, 2005). Furthermore, both ZO-1 and ZO-2 loss or downregulated expression has been reported in breast cancer (Hoover *et al.*, 1998; Chlenski *et al.*, 2000).

# Chapter 2: Identification and Molecular Characterization of Scribble as a Zonula Occludens Interacting Protein

The function of ZO-1 and ZO-2 proteins on epithelial polarity, TJ assembly and cell signaling has been extensively investigated. However, not much is known about ZO-3 functions except from a few studies.

Exogenous expression of ZO-3 N-terminal PDZ1-3 in epithelial cell line MDCK exhibits dominant negative effects, delaying the membrane recruitment of endogenous junctional structural proteins like E-cadherin and ZO-1, and therefore impeding AJ and TJ assembly. Furthermore actin recruitment to the apical ring was delayed (Wittchen *et al.*, 2000) while other aspects of actin dynamics were also affected. The number of stress fibers and focal adhesions were also reduced in migrating cells, concomitant with an increase in cell migration (Wittchen *et al.*, 2003).

As discussed earlier, ZO-3 also has functions in apical-basal polarity definition. ZO-3 binds PATJ PDZ domains via its Class I C-terminal PDZ-binding motif. In MDCK, abolishment of the binding site on PATJ negates its localization to TJ but the converse is not true for ZO-3, indicating the ZO-3 dependent recruitment of PATJ (Roh *et al.*, 2002a). However, contrary to this, in a more recent study, PATJ silencing in human epithelial colorectal adenocarcinoma Caco 2 cells resulted in mislocalization of ZO-3 to the lateral membrane domain (Michel *et al.*, 2005). Nevertheless, these studies show an involvement of ZO-3 in epithelial polarization.

As the knowledge of ZO-3 function is still fragmentary, it was decided that a closer investigation was necessary. Although ZO-3 shares some binding partners with ZO-1 and ZO-2, there doesn't seem to be functional redundancy since ZO-3 does not

rescue ZO-1 null/ZO-2 silenced phenotype in epithelial cells, implying that ZO-3 may have some specialized functions (Umeda *et al.*, 2006). Furthermore, ZO-3 is exclusively expressed in epithelial cells unlike ZO-1 and ZO-2, thus emphasizing a specific importance to epithelial TJ function (Inoko *et al.*, 2003). A yeast two-hybrid (Y2H) system was employed to screen for potential binding partners of ZO-3 in order to gain a better perspective of its functions. The C-terminal portion of ZO-3 encompassing the SH3-hinge-GUK-acidic region was used as bait. This was chosen since it has thus far been poorly characterized. Moreover as discussed for ZO-1 and ZO-2, this region plays an important role in AJ and TJ assembly and also associates with various signaling proteins. Furthermore, unlike ZO-1, ZO-3 has a Class I C-terminal PDZ-binding motif which can prospectively bind to an array of PDZ domain proteins, of which many are polarity and junctional proteins.

## 2.1 Results

### 2.1.1 The ZO-2 and ZO-3 C-termini Directly Interact with Scrib

Novel ZO-3 interacting proteins were obtained by a Y2H screen of a mouse 17 day embryo cDNA library. The ZO-3 construct spanning the C-terminal region from SH3 to the C-terminal PDZ binding motif (SGC) was used as a bait. A BLAST search of positive cDNA library prey sequences revealed two clones that matched the mouse homologue of *Drosophila* Scribble. Both clones contained a partial PDZ1 domain and encompassed the entire PDZ2 and 3 domains before terminating within PDZ4. To determine the veracity of this interaction, the pACT2 partial mouse Scrib (mScrib) cDNA plasmid was co-transformed into AH109 yeast reporter strain with compatible pGBKT7

constructs containing various ZO C-terminal domains (Fig. 2-1A) . Co-transformants were selected on SD/-Trp/-Leu medium and positive interaction was monitored by X-α-Gal colorimetric assay (Fig. 2-1B). ZO-3SGC showed strong interaction with mScrib as indicated by intense blue staining. The interaction domain was mapped to the GUK and C-terminus (ZO-3 GC WT) which showed an equally intense staining. Staining was not observed with the ZO-3 SH3 construct. The exchange of the C-terminal PDZ-binding motif aa threonine (T), aspartatic acid (D) and leucine (L) ($P_{-2}$, $P_{-1}$, $P_0$) with alanines (AAA) (ZO-3 GC PDZ binding mutant (PBM)) abrogated this interaction suggesting a Class I PDZ binding dependency. mScrib interaction with the corresponding C-terminal domains of ZO-1and -2 was also investigated. Both ZO-1 and -2 GUK and acidic domains (ZO-1 GA and ZO-2 GA) did not register an interaction. However, ZO-2 proline-rich region (ZO-2 P) interacted with mScib, albeit weaker than ZO-3 GC and thus indicating a conserved interaction among some TJ MAGUKs. Interestingly, like ZO-3, the C-terminus of ZO-2 P has a threonine (T), glutamic acid (E) and leucine (L) ($P_{-2}$, $P_{-1}$, $P_0$) Class I PDZ-binding motif (Roh *et al.*, 2002a).

The interaction of ZO-2 and ZO-3 with mScrib was biochemically corroborated in the context of full-length mScrib in GST pull-down binding assays with *in vitro* translated (Fig. 2-1C panel a) and *in vivo* 293T cell line expressed (Fig. 2-1C panel b) HA-mScrib. Immobilized GST fusion proteins of the ZO-1 proline-rich region (ZO-1 P), ZO-2 P domain with intact TEL (WT) and TEL substituted with AAA (PBM), ZO-3 GC WT and ZO-3 GC PBM constructs (Fig. 2-1A) were incubated with $^{35}$S methionine ($^{35}$S Met) labeled *in vitro* translated full-length HA-tagged mScrib. Consistent with the Y2H assay, mScrib co-purified with GST ZO-2 P WT and ZO-3 GC WT, with a stronger

binding to ZO-3 GC WT. No or negligible binding was observed with ZO-2 and ZO-3 PBM respectively. ZO-1 C-terminus does not have a canonical Class I PDZ-binding motif and expectedly, no binding to mScrib was observed with GST ZO-1 P or the GST negative control (Fig. 2-1C panel a). To ensure proper folding of full-length HA-mScrib, this was exogenously expressed *in vivo* in 293T cells. Harvested cell lysates were incubated with the GST ZO fusion proteins and assayed. Similar to *in vitro* translated mScrib, exogenous mScrib bound strongly to GST ZO-3 GC and to a lesser extent to GST ZO-2 P in a PDZ-binding motif dependent manner. Again, no binding to GST ZO-1 P or GST as a negative control was observed (Fig. 2-1C panel b).

Collectively, these studies reveal a novel PDZ-mediated direct interaction between C-terminal PDZ-binding motif of the TJ peripheral proteins ZO-2 and ZO-3 and the PDZ domains of the mScrib polarity protein.

**A**

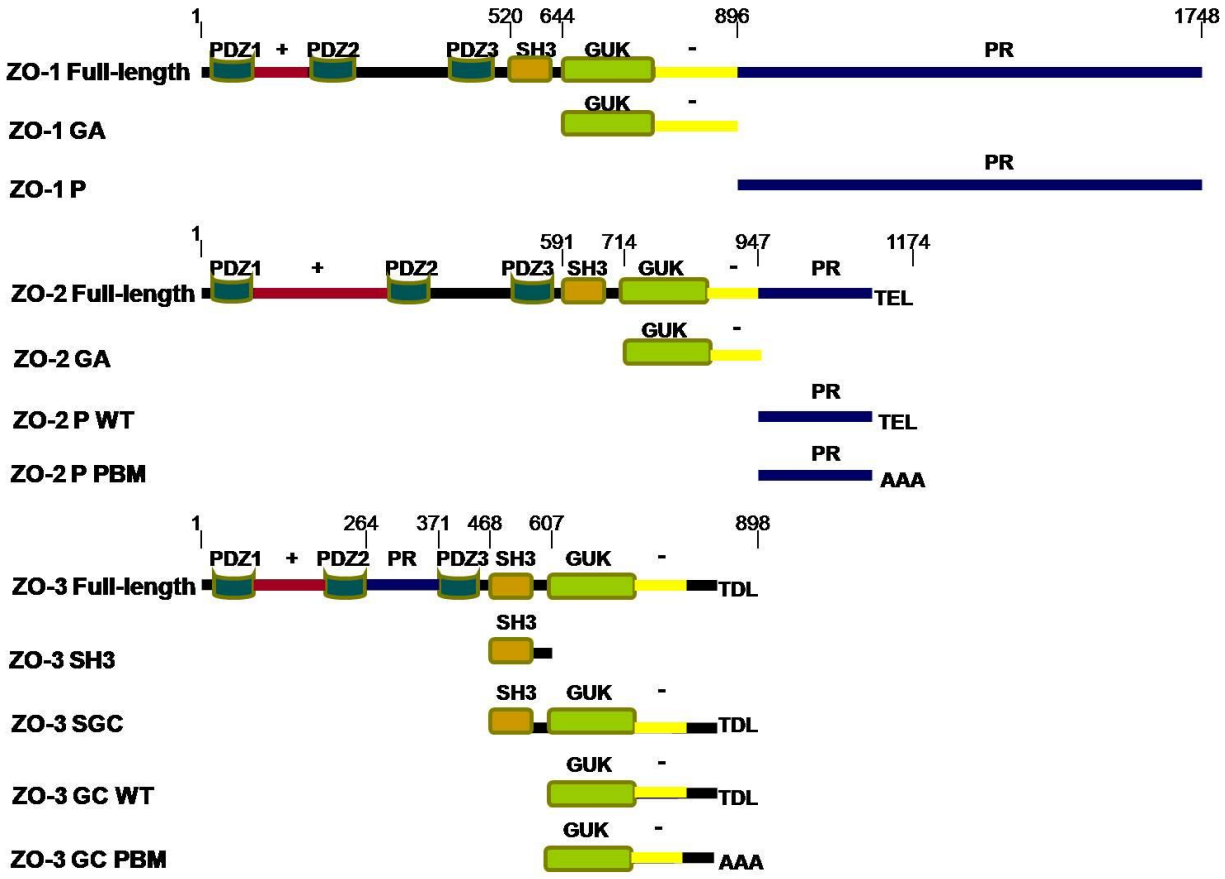
1
520
644
896
1748
PDZ1
+
PDZ2
PDZ3
SH3
GUK
-
PR
ZO-1 Full-length
GUK
-
ZO-1 GA
PR
ZO-1 P
1
591
714
947
1174
PDZ1
+
PDZ2
PDZ3
SH3
GUK
-
PR
TEL
ZO-2 Full-length
GUK
-
ZO-2 GA
PR
TEL
ZO-2 P WT
PR
AAA
ZO-2 P PBM
1
264
371
468
607
898
PDZ1
+
PDZ2
PR
PDZ3
SH3
GUK
-
TDL
ZO-3 Full-length
SH3
ZO-3 SH3
SH3
GUK
-
TDL
ZO-3 SGC
GUK
-
TDL
ZO-3 GC WT
GUK
-
AAA
ZO-3 GC PBM

**B**

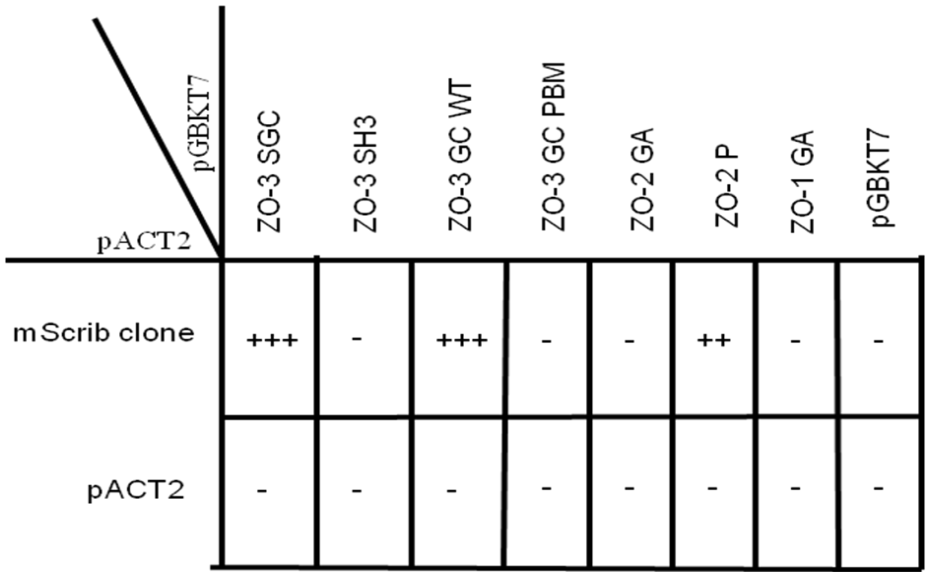
pGBKT7
pACT2
ZO-3 SGC
ZO-3 SH3
ZO-3 GC WT
ZO-3 GC PBM
ZO-2 GA
ZO-2 P
ZO-1 GA
pGBKT7
mScrib clone
+++
-
+++
-
-
++
-
-
pACT2
-
-
-
-
-
-
-
-

**C**

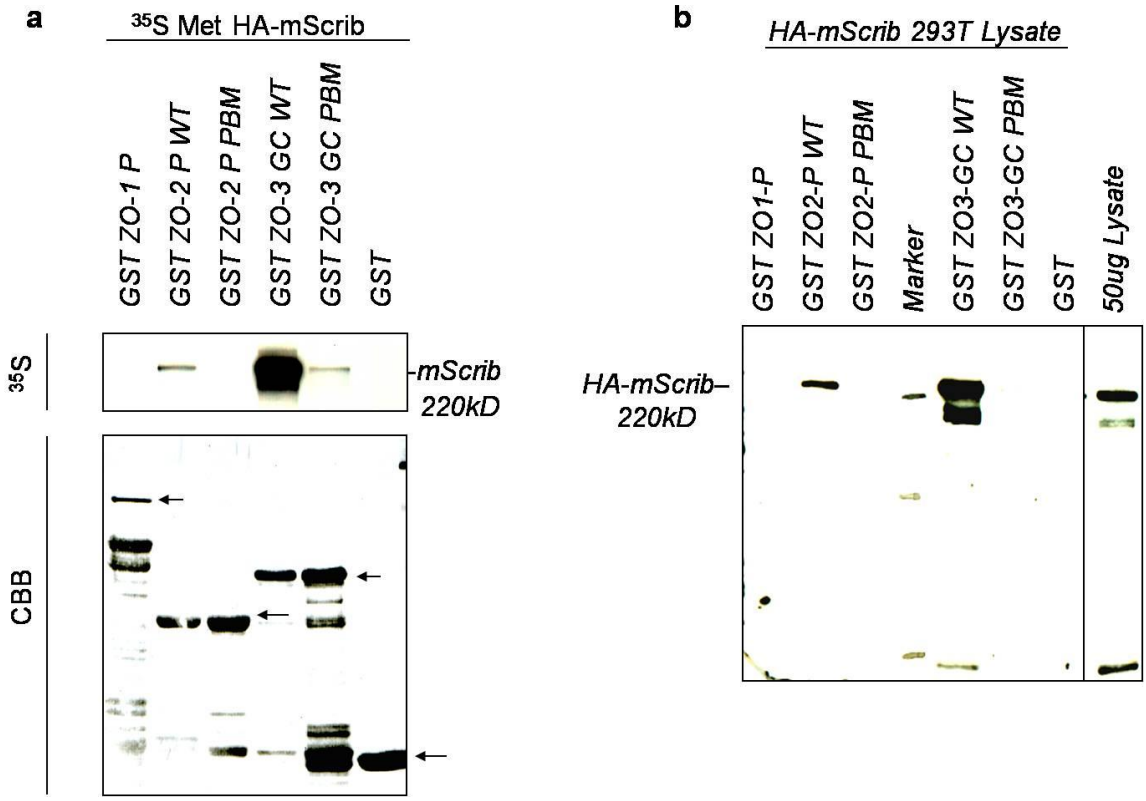


**Figure 2-1. Scrib directly interacts with the C-termini of ZO-2 and ZO-3. (A)** Schematic diagram of Zonula Occludens full-length and deletion mutants. GA constructs encode the GUK and acidic domains. P contructs contain the proline-rich region. SH3 constructs encode the SH3 domain. SGC constructs encompass the SH3, GUK, acidic domains and C-terminus, while the SH3 domain is deleted in GC constructs. Constructs with suffix WT represent a wild-type PDZ-binding motif whereas PBM signifies a replacement of this motif with three alanine residues. Amino acids demarcating the beginning or end of constructs generated are represented by numbers above each line. (+) and (-) represent the basic and acidic domains respectively. **(B)** Yeast two-hybrid assay. Various ZO pGBKT7 constructs (bait) or empty pGBKT7 vector (negative control) were co-transformed together with mScrib pACT2 library clone or empty pACT2 vector (negative control) in AH109 yeast reporter strain. Interaction was determined by monitoring the appearance and color intensity in an X-α-gal assay, with a blue colored appearance indicating positive interaction. Relative blue color intensity: +++, maximum; ++, intermediate; -, no blue coloring. **(C)** GST pull-down assay. *In vitro* translated $^{35}$S Met-labelled (panel a) or 293T expressed exogenous (panel b) HA-mScrib was applied to immobilized GST ZO fusion proteins. GST fusion proteins were precipitated and subjected to Western blot transfer. Co-purification of mScrib was detected either by autoradiography (panel a) or immunoblotting (panel b). Input of GST ZO fusion proteins was monitored by coomassie brilliant blue (CBB) (panel a). An aliquot (50ug) of lysate was analysed to monitor HA-mScrib expression level in 293T (panel b).

### 2.1.2 ZO-2 and ZO-3 Co-localize and Interact with Scrib in COS-1

To investigate the association of ZO-2/-3 and Scrib *in vivo*, full-length FLAG-tagged ZO-2 and ZO-3 WT and PBM and full-length HA-mScrib constructs were generated and expressed in COS-1 cells (Fig. 2-2A). Both ZO-2 WT and PBM exhibited a cytosolic distribution when exogenously expressed (Fig. 2-2A panels a and b). On the contrary, ZO-3 WT and PBM both displayed a vesicular-like localization (Fig. 2-2A panels c and d). Interestingly, mScrib showed a filamentous staining throughout the cytosol, radiating from a perinuclear region (Fig. 2-2A panel e). When co-transfected with full-length HA-mScrib, ZO-2 WT localized with mScrib in vesicular-like structures, thus re-localizing from their original cytosolic and filamentous distribution respectively (Fig. 2-2B, panels a-c). This co-localization was negated when the ZO-2 C-terminal PDZ-binding motif was mutated (PBM). This mutant redistributed back to the cytosol while mScrib assumed its filamentous localization (Fig. 2-2B panels d-f). A similar vesicular overlap was observed with ZO-3 WT and mScrib co-expression. Here, mScrib appeared to be de-localized from filaments and recruited to ZO-3 vesicles (Fig. 2-2C panels a-c). Again, mutation of the PDZ-binding motif disrupted this co-localization, with ZO-3 PBM remaining in the vesicular structures while mScrib redistributed back to filaments (Fig. 2-2C panels d-f). These localization studies imply a recruitment of mScrib by ZO-2 and ZO-3 from an uncharacterized filamentous location to vesicular-like structures. The identity of these vesicles has yet to be elucidated. However, a detailed investigation of the Scrib filamentous distribution will be discussed in Chapter 3.

The co-distribution of ZO-2/-3 with mScrib was further corroborated biochemically by immunoprecipitation. EGFP-tagged hScrib was co-expressed with

FLAG-ZO-2 WT or PBM (Fig 2-2D panel a), and FLAG-ZO-3 WT or PBM (Fig 2-2D panel b). Both ZO-2 and ZO-3 WT co-purified with hScrib immunoprecipitates, consistent with their co-localization. As expected, in line with their disparate distribution, ZO-2/-3 association with hScrib was abrogated in PBM. Thus, both full-length ZO-2 and ZO-3 physically interact with Scrib *in vivo* in a PDZ-binding motif-dependent manner.

**A**

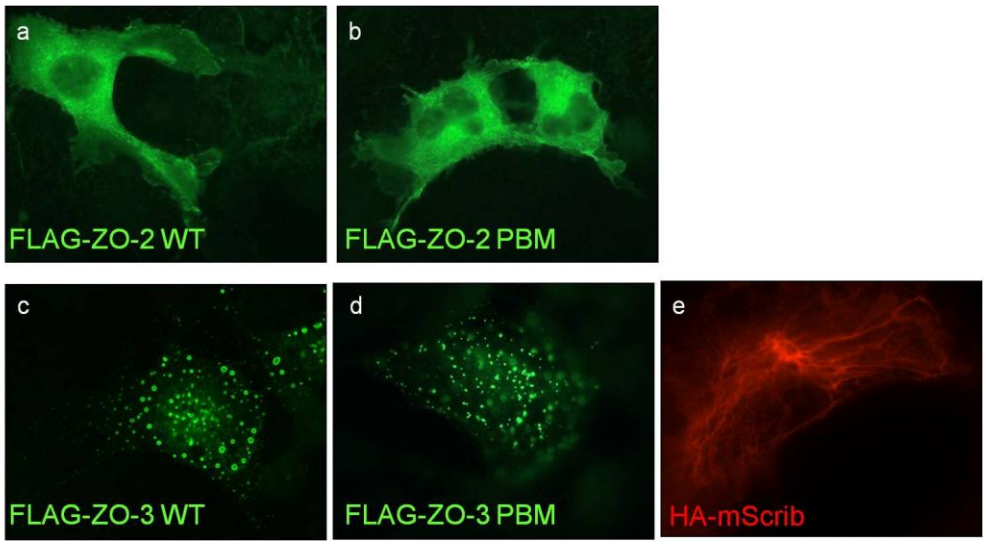
a
FLAG-ZO-2 WT
b
FLAG-ZO-2 PBM
c
FLAG-ZO-3 WT
d
FLAG-ZO-3 PBM
e
HA-mScrib

**B**

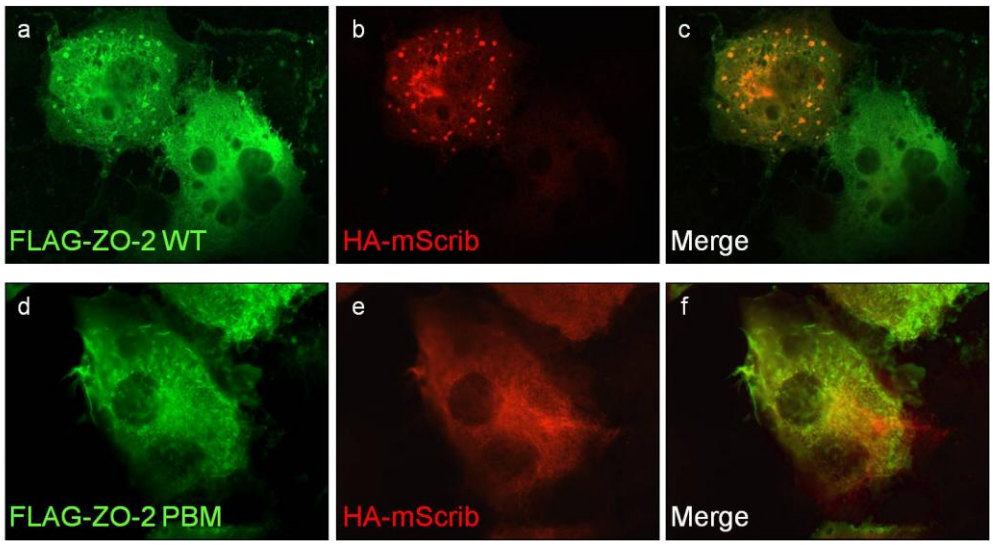
a
FLAG-ZO-2 WT
b
HA-mScrib
c
Merge
d
FLAG-ZO-2 PBM
e
HA-mScrib
f
Merge

**C**

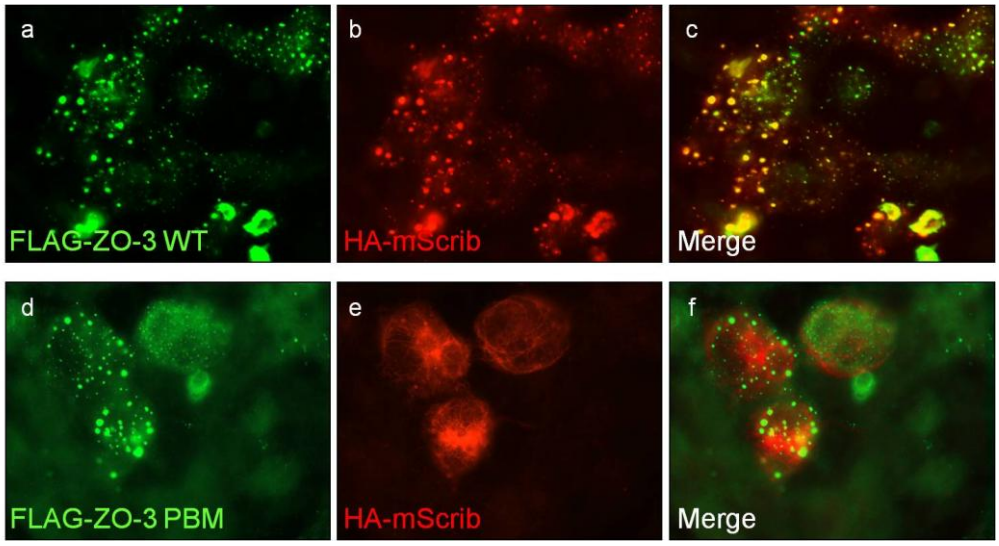
a
FLAG-ZO-3 WT
b
HA-mScrib
c
Merge
d
FLAG-ZO-3 PBM
e
HA-mScrib
f
Merge

**D**

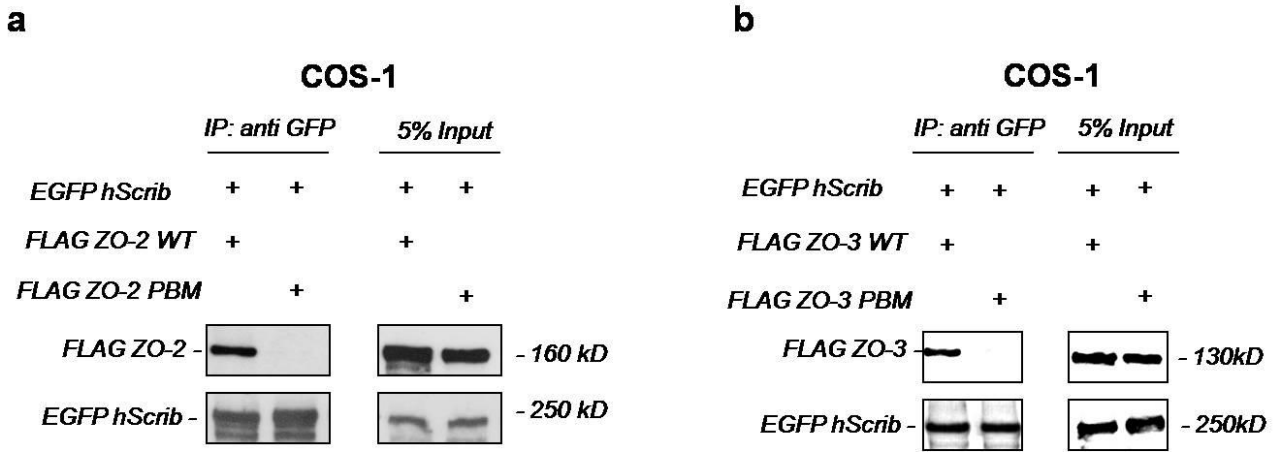


**Figure 2-2. Co-localization and interaction of ZO-2 and ZO-3 with Scrib in COS-1. (A)** Exogenous expression of epitope tagged ZO-2, ZO-3 and Scrib. Single transfections of FLAG-ZO-2 WT (panel a, green color) and PBM (panel b, green colour); FLAG-ZO-3 WT (panel c, green color) and PBM (panel d, green color); and HA-mScrib (panel e, red colour) were visualized in COS-1. Note the cytosolic, vesicular and filamentous distribution of ZO-2, ZO-3 and Scrib respectively. **(B)** ZO-2 and Scrib co-localize to vesicles. Co-expression of FLAG-ZO-2 WT (panel a, green) and HA-mScrib (panel b, red color) results in the recruitment of both proteins to vesicular structures. Yellow in the merged images indicate co-localization (panel c). Abolishment of the PDZ-binding motif of ZO-2 disrupts this co-localization (panel f) and FLAG-ZO-2 PBM (panel d, green color) and HA-mScrib (panel e, red color) return to their respective cytosolic and filamentous distributions. **(C)** ZO-3 recruits Scrib to ZO-3 containing vesicles. FLAG-ZO-3 WT (panel a, green color) co-expression with HA-mScrib (panel b, red color) re-localizes Scrib from its filamentous location to ZO-3 vesicles. Yellow in the merged image (panel c). Disruption of the interaction in FLAG-ZO3 PBM negates this recruitment (panels d-f). **(D)** ZO-2 and ZO-3 interacts with Scrib *in vivo*. Exogenous EGFP-hScrib co-expressed with FLAG-ZO-2 (panel a) or ZO-3 (panel b) was immunoprecipitated and subjected to Western blot. Co-precipitation with ZO-2 and ZO-3 WT was detected but not with PBM, indicating a PDZ-binding motif dependent interaction. Lysates representing 5% of input were analysed in parallel to monitor expression levels.

### 2.1.3 The Scrib PDZ Domains Interact Directly with ZO-2 and ZO-3

To ascertain a PDZ-dependent interaction and map the PDZ domain responsible for ZO-2/-3 binding, GST fusion of individual hScrib PDZ domains i.e. PDZ1 - 4 were employed in GST pull-down assays. Both *in vitro* translated (Fig. 2-3A and B panel a) and COS-1 exogenously expressed (Fig. 2-3A and B panel b) FLAG-ZO-2 (Fig. 2-3A) and ZO-3 (Fig. 2-3B) were applied to immobilized GST hScrib PDZs. ZO-2 WT but not PBM specifically bound hScrib PDZ1. No association to hScrib PDZ2-4 and GST negative control was observed (Fig. 2-3A). In contrast, ZO-3 WT does not interact with hScrib PDZ1 but instead binds PDZ3. Again, mutation of the ZO-3 C-terminal binding motif cancels this association. Furthermore, hScrib PDZ2, 4 and GST do not exhibit any binding to ZO-3 (Fig. 2-3B).

Although the mapping of ZO-3 interaction to PDZ3 of Scrib conforms well to the Y2H result using the mScrib library clone, it was surprising that ZO-2 associated only with Scrib PDZ1 in the pull-down assays since it displayed binding to the mScrib library clone that had only intact PDZ2 and 3 (Fig 2-1B). Therefore, unless the partial PDZ1 of the Y2H library clone could mediate this interaction, there lay a possibility that PDZ2 or 3 could also be involved. This discrepancy could be due to the dependence on the conformation of PDZ2 or 3 for ZO-2 interaction. To reconcile this, PDZ domain aa residues necessary for ligand binding were point mutated in the context of full-length hScrib, with the aim of preserving the overall hScrib native conformation while nullifying the binding capability of its PDZ domains (Fig 2-3C). The PDZ domain aa residues crucial for ligand binding have been identified in (Doyle *et al.*, 1996) using the PDZ domain of post synaptic density protein 95 (PSD-95) as a model. Point mutations of

these residues in ZO-1 PDZ domains have also been described previously (Kausalya *et al.*, 2004).

COS-1 exogenously expressed EGFP-hScrib WT and PDZ mutants (Fig. 2-3D panel c) were applied to GST ZO-2 P (Fig. 2-3D panel a) or ZO-3 GC (Fig. 2-3D panel b) in a pull-down assay. As expected, full-length hScrib with its PDZ1 mutated did not co-purify efficiently with ZO-2 P. However, a weak binding was still observed, indicating ZO2-P interaction with another PDZ domain. Interestingly, mutation of PDZ3 also diminished hScrib interaction with ZO2-P to a slight extent. Total abolishment of interaction was achieved with the double PDZ1 and 3 mutants, demonstrating sufficiency of these two domains in mediating ZO-2 interaction. Therefore, this has revealed PDZ3 as a ZO-2 interaction domain in addition to PDZ1 and is thus consistent with the earlier pull-down (Fig. 2-3A panels a and b) and Y2H results (Fig. 2-1B). hScrib PDZ3 mutation also expectedly abrogated interaction with ZO-3 GC, although not completely. Surprising, PDZ1 mutation slightly diminished this interaction and total negation was observed with both PDZ1 and 3 mutated. Taken together, these results reveal a strong interaction of ZO-2 to hScrib PDZ1 and a weaker one to PDZ3. Furthermore, hScrib PDZ3 binds ZO-3 with high efficiency while its PDZ1 mediates a less efficient interaction.

**A**

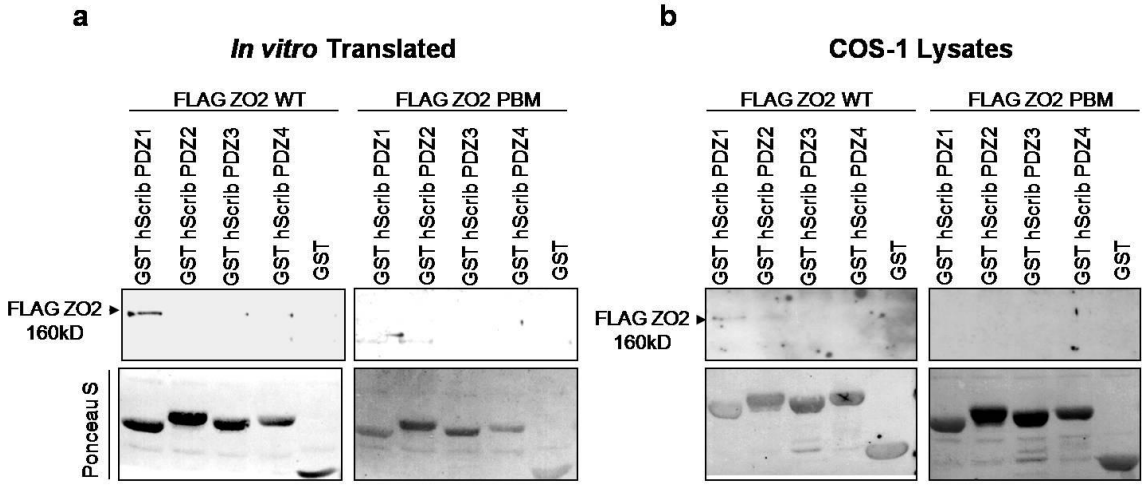
a
In vitro Translated
FLAG ZO2 WT
FLAG ZO2 PBM
GST hScrib PDZ1
GST hScrib PDZ2
GST hScrib PDZ3
GST hScrib PDZ4
GST
FLAG ZO2
160kD
Ponceau S
b
COS-1 Lysates
FLAG ZO2 WT
FLAG ZO2 PBM
GST hScrib PDZ1
GST hScrib PDZ2
GST hScrib PDZ3
GST hScrib PDZ4
GST
FLAG ZO2
160kD

**B**

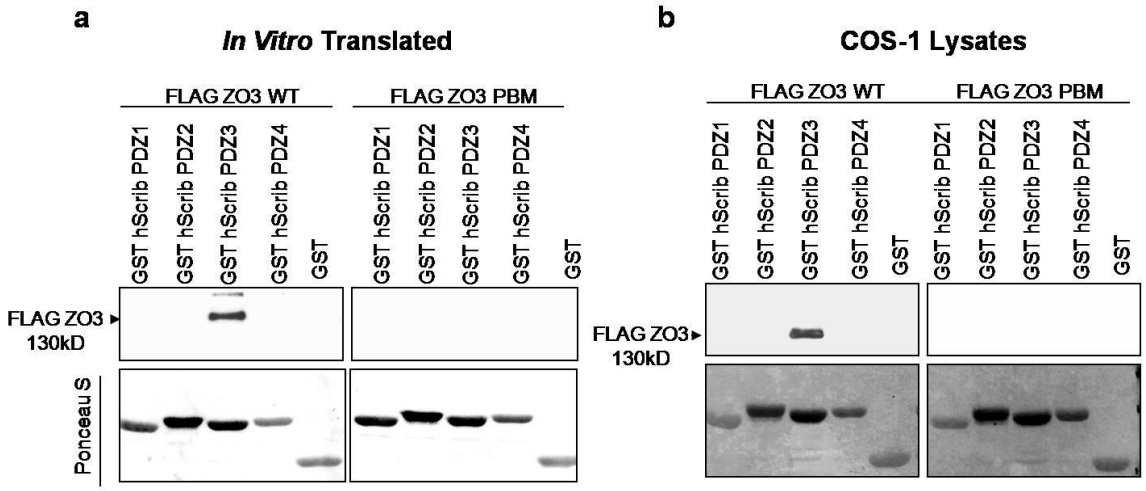
a
In Vitro Translated
FLAG ZO3 WT
FLAG ZO3 PBM
GST hScrib PDZ1
GST hScrib PDZ2
GST hScrib PDZ3
GST hScrib PDZ4
GST
FLAG ZO3
130kD
Ponceau S
b
COS-1 Lysates
FLAG ZO3 WT
FLAG ZO3 PBM
GST hScrib PDZ1
GST hScrib PDZ2
GST hScrib PDZ3
GST hScrib PDZ4
GST
FLAG ZO3
130kD

**C**

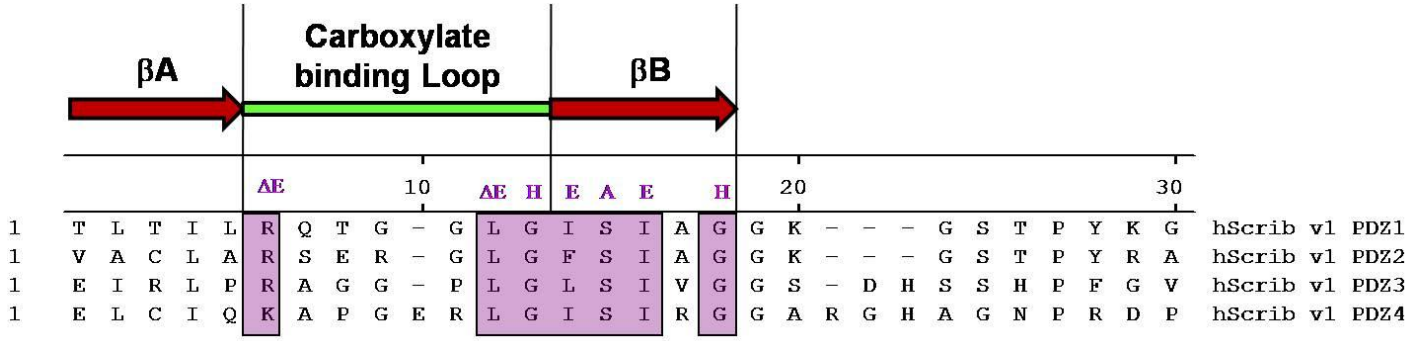
βA
Carboxylate binding Loop
βB
ΔE
10
ΔE H
E A E
H
20
30
1 T L T I L R Q T G – G L G I S I A G G K – – – G S T P Y K G hScrib v1 PDZ1
1 V A C L A R S E R – G L G F S I A G G K – – – G S T P Y R A hScrib v1 PDZ2
1 E I R L P R A G G – P L G L S I V G G S – D H S S H P F G V hScrib v1 PDZ3
1 E L C I Q K A P G E R L G I S I R G G A R G H A G N P R D P hScrib v1 PDZ4

**D**

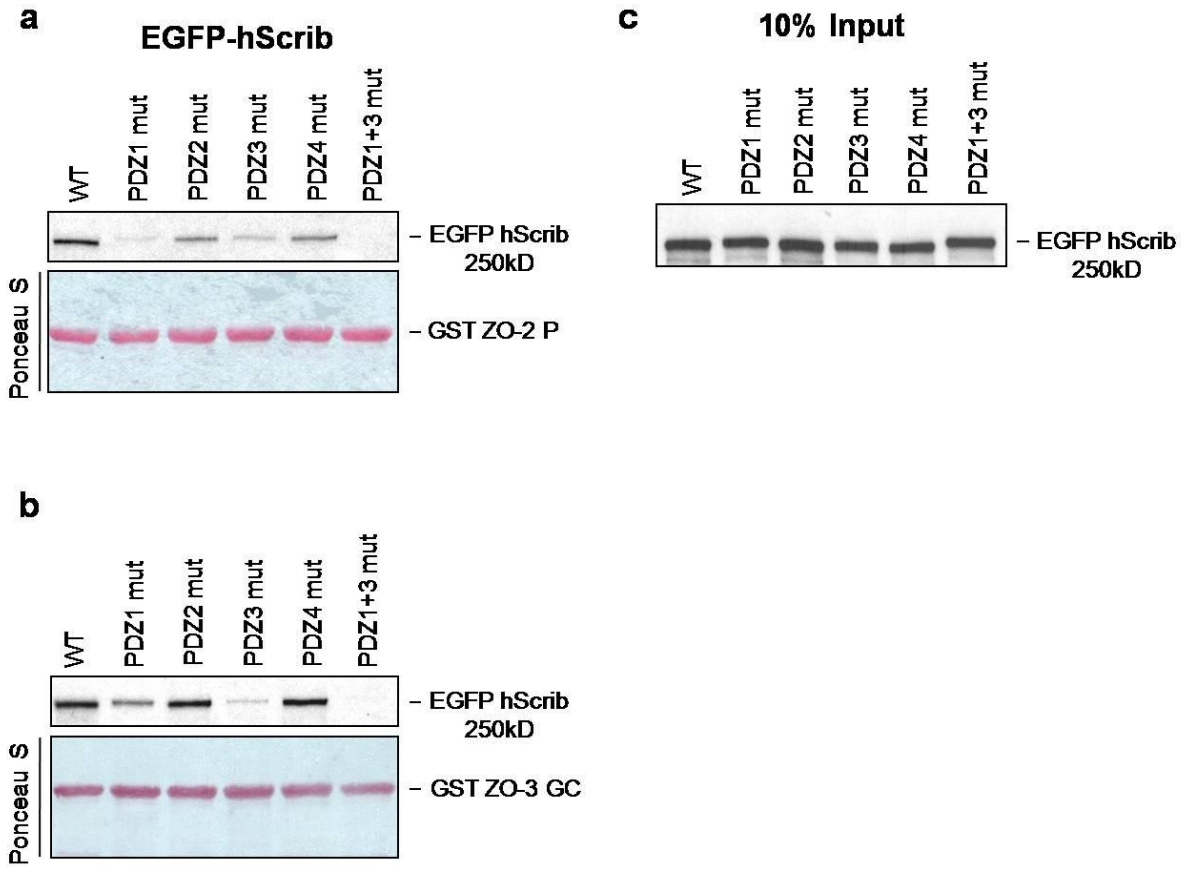


**Figure 2-3. Scrib interacts directly with ZO-2 and ZO-3 via its PDZ domains. (A)** PDZ1 domain associates with ZO-2. Immobilized GST fused to the individual hScrib modules of PDZ1-4 domains or GST alone (negative control) were mixed with either *in vitro* translated (panel a) or COS-1 expressed (panel b) FLAG-ZO-2 WT or PBM; purified and analysed by Western blot. ZO-2 WT but not PBM co-purified with only hScrib PDZ1. Purified GST hScrib fusions were visualized by Ponceau S. **(B)** A similar assay was applied to *in vitro* translated (panel a) or COS-1 expressed (panel b) FLAG-ZO-3 WT of PBM. hScrib PDZ3 exclusively associated with ZO-3 WT but not PBM. Ponceau S visualized the GST hscrib fusions. **(C)** Amino acid sequence alignment of hScrib PDZ domains. The alignment of the βA-carboxylate binding loop-βB amino acid sequence of the four PDZs shows the highly conserved residues crucial for ligand binding (purple box). hScrib PDZ binding mutants were generated by point mutating these residues and substituting them with the residues indicated above the line in purple.**(D)** Full-length EGFP-hScrib WT and PDZ mutants were expressed in COS-1 and harvested lysates applied to immobilized GST ZO-2 P (panel a) or GST ZO-3 GC (panel b). Purified fusion proteins (detected with Ponceau S) and associated hScrib (immunoblot) were detected by Western blot.COS-1 lystes expressing the EGFP-hScrib constructs were monitored as 10% of assay input (panel c).

### 2.1.4 ZO-2 and ZO-3 Co-localize with Scrib in Epithelial Cells

Since ZO-2 and -3 are TJ proteins and Scrib regulates polarity, the association of these proteins and their functional implications were investigated in MDCK cells, a relevant epithelial cell line model. Investigation was carried out on MDCK cells exogenously expressing EGFP-hScrib and cultured as monolayers on permeable polycarbonate filters which allow apical-basal polarization and vertical section observation. Under sparse conditions, cells are not yet polarized and cell-cell contact is being established. Here, hScrib showed extensive filamentous distribution in the cytosol and a diffused cell periphery and lateral membrane localization (Fig. 2-4A and B, panel b). Both ZO-2 (Fig. 2-4A, panel a) and -3 (Fig. 2-4B, panel a) displayed a distinct lateral membrane localization that overlapped well with the apical region of diffused hScrib staining (Fig. 2-4A and B, panel c). In polarized confluent MDCK cells, hScrib filamentous and diffused membrane staining was absent and had instead redistributed distinctly along the length of the lateral membrane (Fig. 2-4A and B, panel e). Furthermore, ZO-2 (Fig. 2-4A, panel d) and ZO-3 (Fig 2-4B, panel d) localization at the lateral membrane had redistributed to a more apicolateral location, only partially overlapping with the lateral membrane staining of hScrib (Fig. 2-4A and B, panel f). In conclusion, in sparse polarizing MDCK cell cultures, ZO-2 and ZO-3 showed obvious co-localization with hScrib at cell-cell contacts. Upon epithelial polarization, both ZO-2 and -3 assumed a more apicolateral localization, likely coinciding with TJ, while hScrib extended along the lateral membrane. Thus this implies that ZO-2/-3 and Scrib interaction might occur in polarizing epithelial cells and subsequently segregate to their

respective apicolateral TJ and basolateral localization upon complete epithelial polarization.

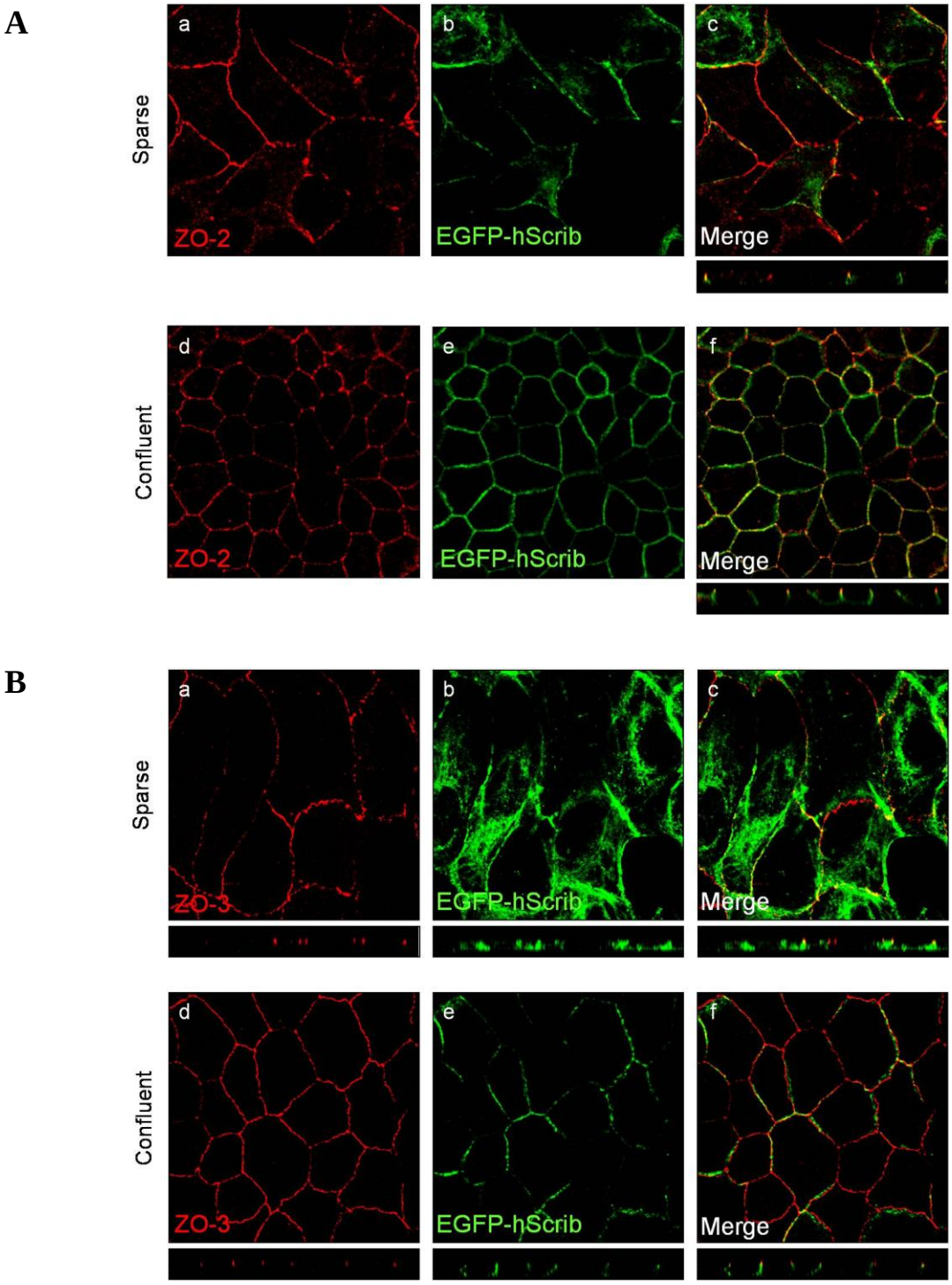


**Figure 2-4. Co-localization of ZO-2 and ZO-3 with Scrib in MDCK epithelial cell monolayer. (A,B)** Exogenous EGFP hScrib (**A** and **B,** panels b and e, green color) was visualized with ZO-2 (**A**, panels a and d, red color) and ZO-3 (**B**, panels a and d, red color) in sparse (**A** and **B**, panels a-c) and confluent (**A** and **B**, panels d-f) cultures using confocal fluorescence microscopy. Vertical Z sections are represented below each panel. Yellow in merged images indicate co-localization. Note the co-localization of ZO-2 and ZO-3 with the diffused lateral membrane distribution of hScrib in sparse non-polarized cultures. In confluent polarized cultures, hScrib is more defined at the lateral membrane, showing little overlap with the now apicolateral ZO-2 and ZO-3.

## 2.2 Discussion

During the biogenesis of epithelial polarization, components of cell-cell junctions co-localize and physically or functionally interact with each other. These include polarity regulating protein complexes Par, Crb and Scrib, and junctional proteins like claudins, ZO proteins and catenins (Assemat *et al.*, 2008). Essential for the proper assembly and polarization of epithelial cells and their junctions, these complex hierarchical and coordinated interactions have yet to be completely elucidated. Here, we show the physical association between the polarity protein Scrib and TJ proteins ZO-2 and ZO-3; and their co-localization in non-polarized epithelial cells. This interaction is direct and is mediated by the PDZ domains of Scrib and the C-terminal motif of ZO-2 and ZO-3.

Using a Y2H screen for ZO-3 C-terminal region binding proteins, cDNA library clones encoding Scrib PDZ domains were identified as interacting partners of ZO-3 and also ZO-2 C-terminus but not ZO-1. The interaction is specific since mutation of the C-terminal PDZ-binding motif of both ZO-2 and ZO-3 results in the abrogation of binding *in vitro* and *in vivo*. This was also corroborated with subcellular localization analysis in COS-1, where Scrib intriguingly appeared on filaments and was recruited to unidentified vesicular-like structures upon binding to either ZO-2 or ZO-3 but not C-terminal mutants. As alluded to previously, it is interesting to note that the binding of Scrib to HTLV-1 Tax in T-cells also re-localizes Scrib to vesicular-like structures (Arpin-Andre and Mesnard, 2007). In addition, further mapping of ZO-2 and ZO-3 binding site on Scrib revealed the specific interaction of both ZO-2 and ZO-3 with PDZ1 and 3 of Scrib but with ZO-2 having a preference for PDZ1 whereas ZO-3 associated stronger with PDZ3.

Investigation in the context relevant MDCK epithelial cell line revealed a co-localization of ZO-2 and ZO-3 with Scrib at the lateral membrane of non-polarized cells unlike the vesicles of non-epithelial COS-1 fibroblast. However, as in COS-1, Scrib localization in non-polarized MDCK appeared similarly filamentous. The lateral membrane overlap of the two interacting proteins diminished with epithelial polarization and the segregation of ZO-2 and ZO-3 to a more apicolateral domain, while Scrib remained basolateral. At the time of this study, the interaction of ZO-2 and Scrib was published by another group (Metais *et al.*, 2005). The data from this was consistent with our *in vivo* binding assays in COS-1 and co-localization in non-polarized but not in polarized MDCK cells. However, mapping of Scrib PDZ domains did not reveal an interaction with PDZ1 unlike our finding, but only with a tandem PDZ3 and 4 region. This discrepancy could be explained by the different experimental approach used as Metais *et al*., 2005 employed a tandem GST PDZ1 and 2 as opposed to our use of individual PDZ domains and full-length Scrib PDZ point mutants. In addition, their study also suggests that LRR-dependent Scrib localization to the plasma membrane was necessary for its interaction with ZO-2, but no function was ascribed to this interaction.

Although experimental investigations to the functional significance of ZO-2/-3 and Scrib interaction have yet to be carried out, this can be speculated based on current knowledge of ZO proteins and Scrib functions. During epithelial polarization, ZO-1 and ZO-2 exhibit a dynamic sequential localization, first appearing at the lateral membrane PA and then segregating to apicolateral TJs (Rajasekaran *et al.*, 1996; Yokoyama *et al.*, 2001; Sheth *et al.*, 2008). Therefore, it is not surprising that we observed both ZO-2 and ZO-3 at the lateral membrane of non-polarized MDCK where they co-localize with Scrib.

Based on our study in COS-1 showing the ZO-2 and ZO-3 binding-dependent recruitment of Scrib into vesicular structures, it is possible that ZO-2 and ZO-3 play a similar role in the recruitment of Scrib to the lateral membrane of epithelial cells. Consistent with this proposal, after LRR-mediated Scrib basolateral membrane localization, enrichment at the basolateral SJ is dependent on its PDZ domains (Zeitler *et al.*, 2004; Wada *et al.*, 2005). Therefore initial LRR-dependent Scrib membrane localization may be enhanced and enriched along the lateral domain by its PDZ-dependent interaction with ZO-2 and ZO-3. The proposed recruitment of Scrib by ZO-2 and ZO-3 is also in line with the finding that ZO-3 possibly recruits another interacting polarity protein, PATJ (Roh *et al.*, 2002a) and that during junctional maturation, ZO protein is present in the spot-like PA before the later recruitment of polarity regulators (Suzuki *et al.*, 2002).

Also consistent with this proposed functional interaction of ZO-2 and ZO-3 with Scrib is the discovery that exogenous expression of the ZO-3 N-terminal PDZ1-3 in MDCK delays AJ and TJ assembly (Wittchen *et al.*, 2000) and also increases cell migration (Wittchen *et al.*, 2003). Based on these phenotypes and the finding that the N-terminal half of ZO-3 can intramolecularly bind its C-terminal SH3 to PDZ-binding motif half (Wittchen *et al.*, 2003), it is possible to envision that ZO-3 N-terminal can act as a dominant negative mutant and compete off Scrib from C-terminal ZO-3 binding. This disrupts proper Scrib basolateral binding and thus impedes its polarity function, and therefore the delay in AJ and TJ assembly. Furthermore, this release of Scrib may allow it to ectopically influence cell migration and thus the reported increase in cell migration.

Although the proposed lateral membrane recruitment of Scrib by ZO-2 and ZO-3, the exclusive expression of ZO-3 in epithelial cells (Inoko *et al.*, 2003) and the apparent

non-redundancy of ZO-3 with ZO-1 and ZO-2 (Umeda *et al.*, 2006) imply a specific importance of ZO-3 to epithelial function, it is surprising that in recent investigations of ZO-3 mouse knock-out models, all epithelial functions including cell polarity and junctional assembly were normal and no significant physiological abnormalities where discovered (Adachi *et al.*, 2006; Xu *et al.*, 2008). This could be due to redundancy in ZO-3 function (e.g. membrane recruitment of Scrib could employ other mechanisms) or the lack of phenotypic analysis of the KO mice under challenging conditions. Nevertheless, it will be of interest to further the investigation of the functional aspects of the interaction of ZO-2 and ZO-3 with Scrib and test the proposed role of these ZO proteins for Scrib membrane recruitment.

During the course of this investigation, the interaction of Scrib with ZO-2 at cell-cell junctions of epithelial cells was reported (Metais *et al.*, 2005). This report corroborated our finding that the interaction of these two proteins is PDZ-dependent but furthermore describes that this association only occurs with LRR-mediated Scrib plasma membrane localization. Consistent with our proposal that ZO-2 or ZO-3 possibly enriches Scrib at the basolateral membrane and therefore functions upstream of Scrib, it was reported that overexpression of Scrib mutants and depletion of Scrib had no effect on ZO-2 subcellular localization.

Although of much potential for further development, it was decided that at this stage and under circumstances of competing interests, the project focus on ZO proteins and Scrib was to be shifted to the study of the novel Scrib filamentous localization.

# Chapter 3: Vimentin Regulates Scribble Activity By Protecting It From Proteasomal Degradation

The observation of Scrib distribution on filamentous structures (see above) led us to investigate the nature of this localization and its functional significance. The prospect of a potential Scrib interaction with the cytoskeletal network, although surprising, is not at odds with the current knowledge of the Scrib polarity complex function. As discussed, Lgl interacts with non-muscle myosin-II and negatively regulates the assembly of actomyosin cytoskeleton during basolateral definition. Furthermore, Dlg1 together with APC mediate microtubule polarization by anchoring the growing plus ends to the leading edge membrane of migrating cells. Moreover, the ability of Scrib to act as a scaffold protein positions it as a likely candidate for cytoskeletal network association.

In this next study, we have identified the specific and direct interaction of Scrib with the intermediate filament (IF) network, in particular vimentin and keratin filaments.

## 3.1 The Intermediate Filament Cytoskeletal Network

Intermediate filaments (IFs), together with actin microfilaments and microtubules make up the three cytoskeletal systems found in metazoan cells. Although all three regulate the structural organization of the cell and physically interact with each other (Jefferson *et al.,* 2004), IFs have basic biochemical and functional differences compared with the other two systems. Unlike the universal expression and function of eukaryotic actin and microtubule cytoskeletal systems, IFs are expressed only in higher metazoans and thus are fundamentally not essential for basic cellular functions (Erber *et al.*, 1998). However, they are nevertheless functionally important as evidenced by IF-related

diseases such as skin fragility (Omary *et al.*, 2004). Biochemically, IFs have very different structural characteristics compared with the other cytoskeletal networks. IFs derive their name from the observation that assembled IFs have diameters of approximately 10 nm, which is intermediate to that of the other two filaments. Unlike the globular actin and microtubule proteins (Holmes *et al.*, 1990; Nogales *et al.*, 1998), IFs are made up of filamentous proteins which are non-enzymatic and do not have nucleotide-binding and hydrolyzing activity. Furthermore, assembled IFs are non-polar and thus are not known to act as tracks for motor proteins (Herrmann and Aebi, 2004; Strelkov *et al.*, 2004).

### 3.1.1 Intermediate Filament Protein Structure

IFs belong to a large and diverse protein family that is encoded by at least 65 genes in humans. This classification is based on the conserved sequence of the α-helical domain typical of all IF proteins. Members of this protein family are expressed abundantly with a broad differential representation in both embryonic and adult tissues. This reflects the diversity of the individual members and allows each IF network to be customized to specific cell type functions. Moreover, such unique expression acts as an identification in distinguishing between each cell type (Herrmann *et al.*, 2003). Despite their diversity, all IF proteins have a common secondary structure, which consists of the conserved 310-320 aa central α-helical "rod" domain flanked by divergent non-α-helical N- and C-terminal domains termed "head" and "tail" respectively. While the rod domain is highly conserved within the family, the terminal domains vary in aa length and sequence, especially between subclasses of IFs. This diversity likely contributes to the

different functions of IF members (Herrmann *et al.*, 2007). Both the head and tail domains are predicted to form poorly structured and flexible regions. The rod domain consists of typical α-helical protein heptad repeats (*abcdefg*), where *a* and *d* are hydrophobic and *b,c,e,f,g* are typically charged. These form four α-helical segments 1A, 1B (Coil 1) and 2A, 2B (Coil 2) interrupted by short linkers L1, L12 and L2 which act as flexible hinges. α-helical segment 2B has a highly conserved four aa residue insertion called "stutter" that disrupts the continuity of the heptad-repeat pattern (Herrmann and Aebi, 2004; Parry *et al.*, 2007). On the basis of aa sequence, assembly properties and expression patterns, IF proteins can be divided into five classes. Type-I and -II are the acidic (pI 4.9-5.7) and basic (pI 6.1-7.8) keratins which are expressed in epithelial cells. Type-III IFs include the mesenchymal cell vimentin; desmin and synemin of muscle cells; Glial fibrillary acid protein (GFAP) of Glial cells and neuronal cell peripherin. Neuronal cell derived neurofilament (NF) proteins and α-internexin; neuroepithelial nestin and muscle cell syncolin make up type-IV IFs and type-V comprise the ubiquitous nuclear lamins. IF types-I to -IV are localized in the cytoplasm whereas type-V forms filaments attach to the inner nuclear membrane (Strelkov *et al.*, 2003) (Fig. 3-1).

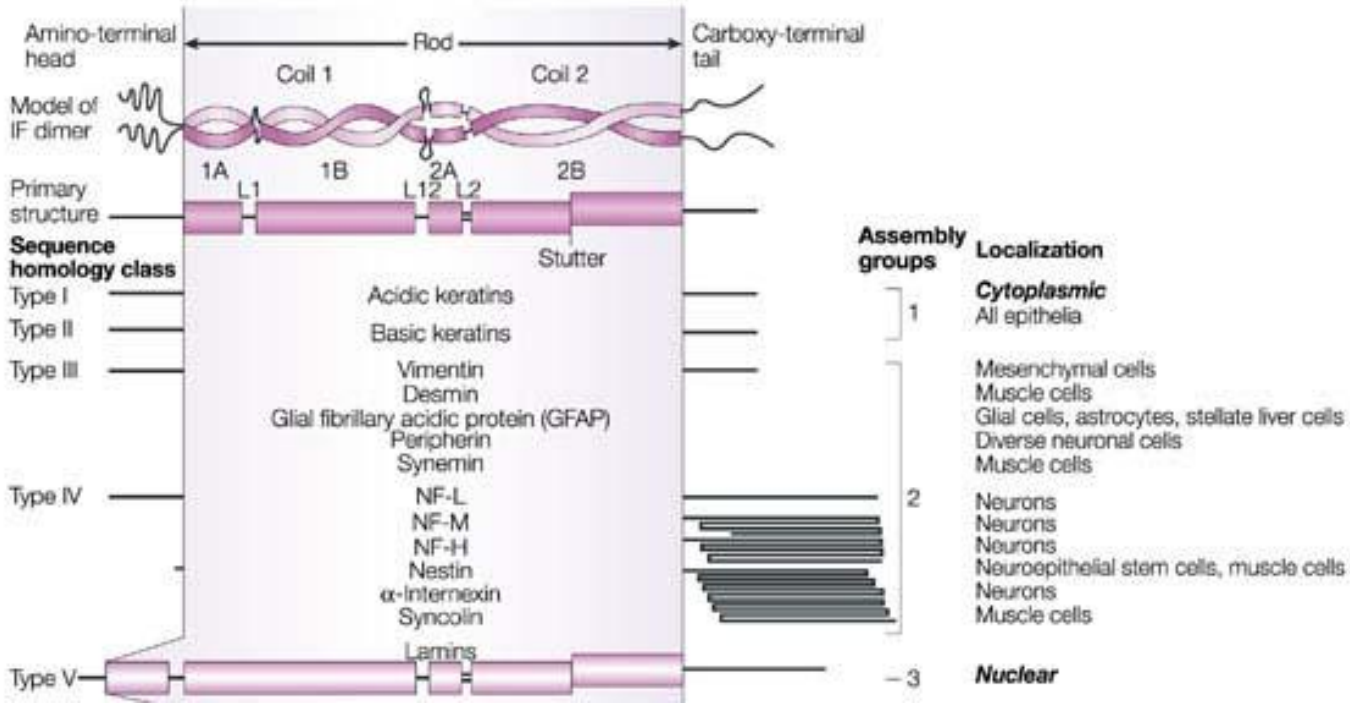


**Figure 3-1. IF molecular structure, classification, assembly groups and tissue and subcellular expression.** The conserved secondary structure of IFs consists of divergent non-α-helical N- and C-terminal domains termed "head" and "tail" respectively that flank a central conserved α-helical "rod" domain. The primary structure of heptad repeats form α-helical segments1A, 1B (Coil 1) and 2A, 2B (Coil 2) interrupted by short linker regions L1, L12 and L2 and a four residue "stutter". The IFs are classified into five sequence homology classes on the basis of aa sequence, assembly properties and expression patterns. These are further grouped into three assembly groups based on the combination of IF homology classes that form hetero or homodimerized parallel coiled-coil dimers. (Reprinted from Nature Reviews Molecular Cell Biology, 5, 601-613, Chang, L., and Goldman, R.D., Intermediate filaments mediate cytoskeletal crosstalk. (2004), with permission from Nature Publishing Group.)

### 3.1.2 Intermediate Filament Assembly and Dynamics

IF proteins assemble into filaments in a step-wise manner. The rod domain initiates the formation of parallel coiled-coil dimers in exact alignment and these are the basic building blocks of IF. Keratin proteins are categorized as assembly group-1 and form obligate heterodimers, with each partner from type-I and -II. Assembly group-2 consists of type-III and –IV IF proteins that form homodimers but can also co-polymerize to form mixed polymers. Type-V lamins belong to assembly group-3 and polymerize only with its own members (Chang and Goldman, 2004). The rods of the dimers in turn associate laterally in an anti-parallel, staggered and over-lapping manner to form tetramers. This anti-parallel arrangement is the reason for the non-polarity of IFs. The further lateral aggregations of tetramers form full-width unit-length filaments (ULFs). These serve as nuclei for IF formation and associate longitudinally to form loosely packed immature polymerized filaments. Upon further elongation, the filaments reorganize internally and radially compact to finally form mature 10 nm IFs (Chang and Goldman, 2004; Herrmann *et al.*, 2007) (Fig. 3-2). The core of IFs is formed by rod domains with the head and tail termini exposed on the filament surface. The N-terminal head domain is required for IF assembly whereas the C-terminal tail is involved in lateral interactions and organization. Furthermore, the surface display of both head and tail domains allow them to associate with other filaments and cellular proteins. Consistent with this, the non-helical domains are known to be post-translationally modified and thus reflect tissue specific functions of IF and a role in signal transduction (Chang and Goldman, 2004; Godsel *et al.*, 2008).

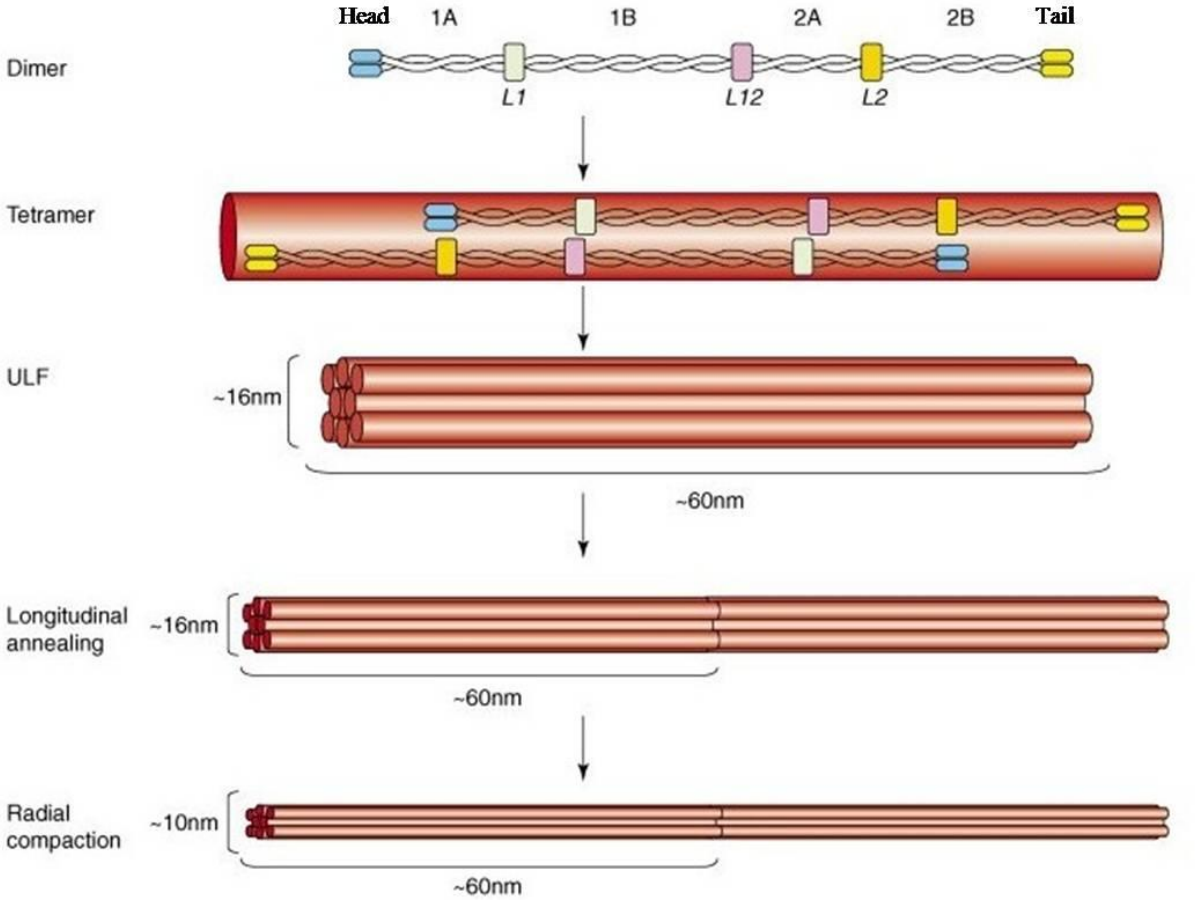


**Figure 3-2. IF protein assembly.** Parallel IF dimerization is mediated by the formation of coiled-coils by the four α-helical segments, 1A, 1B, 2A and 2B of the rod domain. These coiled-coils are interrupted by the non-coiled linkers, L1, L12 and L2. At the next level of assembly, dimers associate laterally in an anti-parallel and staggered fashion to form tetramers. These tetramers further associate laterally and assemble into a ULF, which then goes through longitudinal annealing to form a loosely arranged immature filament. This filament is then compacted radially and results in a 10 nm radius, mature filament. (Reprinted from Trends in Cell Biology, 18, 28-37, Godsel, L.M., Hobbs, R.P., and Green, K.J., Intermediate filament assembly: dynamics to disease. (2008), with permission from Elsevier Ltd.)

Traditionally, IF networks like vimentin and keratin have been seen as static cytoskeletal systems surrounding the nucleus and extending to the cell periphery where they anchor to cell-cell or cell-substratum adhesion complexes, conferring mechanical integrity to cells and tissues (Goldman *et al.*, 1996). However, studies have shown that IF networks are highly dynamic and exhibit rapid turnover. This dynamic nature is regulated by kinases and phosphatases that control the organization, distribution and turnover of IFs according to the cellular context (Ku and Omary, 2000; Izawa and Inagaki, 2006).

IF proteins can be incorporated quickly along the length of existing filaments in a non-polar manner (Vikstrom *et al.*, 1992). Also, these proteins exist in various structural forms which are highly motile. These structures can appear as non-filamentous particles, short filaments called "squiggles" and long polymerized filaments. The three forms represent various stages of IF assembly. The IF particles can fuse to form larger particles and subsequently into squiggles. Following this, squiggles can incorporate into existing mature filaments or join end to end forming longer filaments before incorporation (Prahlad *et al.*, 1998; Yoon *et al.*, 1998). Although in general, cytoplasmic IFs assemble in such a fashion, there are subtle difference between the various IF types. In spreading fibroblasts, while vimentin IFs are found throughout the cytoplasm, filamentous vimentin concentrates more to the perinuclear region whereas particles and squiggles are abundant at the cell periphery. This probably reflects the need for extensive network rearrangements at the leading edge (Ho *et al.*, 1998; Martys *et al.*, 1999). IF reorganization requires the rapid movements of vimentin particles and squiggles and this motility is mediated by plus-end directed kinesin and minus-end directed dynein motor proteins running on microtubule tracks. (Prahlad *et al.*, 1998; Helfand *et al.*, 2002).

Epithelial keratin IFs display different dynamics to vimentin. Keratin particles and squiggles originate from actin-rich cortex and focal adhesions and their movement relies on actin microfilaments, although mediation by myosin motor protein is not known (Windoffer *et al.*, 2004; Windoffer *et al.*, 2006). In agreement with these differences, during the assembly of IF networks in newly divided cells, particles and squiggles form long vimentin filaments that originate from centrosomal regions and extend towards the cell periphery whereas keratin filaments first form a cortical network at the cell cortex which subsequently spreads towards the nucleus (Rosevear *et al.*, 1990; Windoffer and Leube, 2001).

### 3.1.3 Intermediate Filament Function

Because of the fibrous nature of IFs and their relative insolubility (Herrmann and Aebi, 2004), traditionally, IFs are often thought of as rigid structures that provide mechanical stability to cells and tissues. For example, keratin IFs anchor to the cadherin-based cell-cell junction desmosome and the integrin-associated cell-basement membrane junction hemidesmosome and in conjunction with actin and microtubule networks, provide structural resilience to epithelial cells (Borradori and Sonnenberg, 1999; Green and Gaudry, 2000). Similarly, vimentin IFs associate with integrin-based focal adhesions of mesenchymal cells and give mechanical support (Gonzales *et al.*, 2001). Furthermore, various IF deficiencies in tissues subjected to mechanical stress lead to fragility phenotypes linked to loss of cellular integrity and structure (Omary *et al.*, 2004). However, in recent years, this paradigm has been challenged. Investigations have revealed novel non-mechanical IF functions in the regulation of cell adhesion, migration,

polarization, proliferation, growth and apoptosis (Ivaska *et al.*, 2007; Magin *et al.*, 2007; Marceau *et al.*, 2007; Oriolo *et al.*, 2007). Although the underlying mechanisms relating IFs to these cellular processes are as yet poorly understood, the various roles of IFs in cell signaling and organelle and protein targeting may offer some insight and will be briefly discussed; with an emphasis on vimentin and keratin (Toivola *et al.*, 2005; Chou *et al.*, 2007; Kim and Coulombe, 2007).

Vimentin interaction and regulation of various cell-matrix adhesion complexes and membrane trafficking proteins may impinge on the cellular processes like cell adhesion and migration. In endothelial cells, vimentin associates with dynamic focal adhesion-like structures known as vimentin-associated matrix adhesions (VAMs). These adhesions consist of vimentin and actin filaments connected to integrins via adaptor molecules like plectin and vinculin respectively. Here, vimentin plays a crucial role in positively regulating the stability of this structure and maintaining its adhesive function (Gonzales *et al.*, 2001; Tsuruta and Jones, 2003). This regulation could be related to the role of protein kinase C (PKC)-phosphorylated vimentin in recycling of integrin-containing endocytic vesicles to the plasma membrane and promotion of cell migration (Ivaska *et al.*, 2005). In a further relation to vesicle recycling, vimentin also directly interacts with adaptor protein AP-3 and together regulate sorting of vesicles between endosomal-lysosomal compartments (Styers *et al.*, 2004). Furthermore, another mechanism in which IFs may influence cell migration is in the vesicular membrane fusion to the leading edge of migrating cells. In fibroblasts, vimentin sequesters SNAP23 in the cytoplasm and acts as a reservoir from which SNAP23 is mobilized and recruited to form t-SNARE complexes at the plasma membrane where it mediates exocytic

membrane fusion (Faigle *et al.*, 2000). With reference to the vimentin-dependent movement of proteins and vesicles, it is of interest to note that in injured neurons, vimentin squiggles can bind, protect and transport active phosphorylated MAPK via dynein mediated retrograde movement along microtubule tracks from the lesion site to the cell body (Perlson *et al.*, 2005). This mode of transport could provide a novel mechanism for movement of IF-associated proteins.

The mechanism of sequestration or redistribution of interacting partners is not unique to vimentin. Keratins are known to sequester associates and regulate various signal transduction processes. Serum-dependent keratin 17 (K17) relocalization of adaptor protein 14-3-3 is essential for promoting keratinocyte cell growth. This redistribution of 14-3-3 from the nucleus to cytoplasm allows it to positively regulate Akt/mTOR (mammalian target of rapamycin) signaling pathways important in protein synthesis and cell growth (Kim *et al.*, 2006). 14-3-3 also binds other IFs like vimentin and GFAP. The significance of these interactions are not yet clear but could have pleiotropic roles based on the ability of 14-3-3 to influence processes like apoptosis and cell cycle progression (Bridges and Moorhead, 2005; Kim and Coulombe, 2007). Protein sequestration by keratins also has an influence on apoptosis. K18 modulates tumor necrosis factor (TNF)-induced apoptosis by sequestering the TNF receptor type 1 (TNFR1)-associated death domain (TRADD). On TNF activation of TNFR1, TRADD dissociates from K18 and perpetuates the apoptotic signal in concert with TNFR1 (Inada *et al.*, 2001).

Keratins have also been implicated in epithelial cell polarization. The roles of IFs in vesicular trafficking discussed previously could possibly have implication in epithelial

polarity. Another mechanism investigated is that of keratin as a scaffold for compartmentalizing proteins to various membrane domains. In polarized simple epithelial cells, the microtubule minus end is positioned at the apical submembrane region where it mediates apical exocytosis and secretion (Bacallao *et al.*, 1989). This microtubule polarization is preceded by the apical localization of keratin bundles which act as scaffolds that localize the microtubule organizing centres (MTOCs) to the apical membrane and thus polarized the microtubules (Salas, 1999). This localizing function of keratins is important since its absence leads to mispolarization of apical targeted proteins (Ameen *et al.*, 2001).

Taken together, these studies indicate that IFs, in particular vimentin and keratin, play important roles in cell adhesion, migration and epithelial polarity, overlapping well with the known functions of Scrib. The interaction of Scrib and IF thus presents an interesting development in the understanding of the polarity functions and underlying mechanism of these two proteins. In the present study, we characterize the association of Scrib with the intermediate filament cytsokeleton. Silencing of either Scrib or vimentin results in similar phenotypes, consistent with a functional link between the two proteins. Furthermore, we provide evidence that vimentin stabilizes Scrib by protecting it from proteasomal degradation. Our results thus reveal a novel role for vimentin in the regulation of Scrib protein levels and function.

## 3.2 Results

### 3.2.1 Scrib and Intermediate Filaments Co-localize in MDCK Cells

Epitope tagged human (EGFP-hScrib) or mouse (HA-mScrib) Scrib were observed in a filamentous network when expressed in Madin-Darby canine kidney (MDCK) epithelial (Fig. 3-3) or in monkey kidney fibroblast COS-1 (Fig. 3-4A, panel g) cells. In MDCK cells, these filaments were particularly prominent in sparse cell cultures during cell spreading and the establishment of cell-cell contact (Fig. 3-3, panel a). EGFP-hScrib containing filaments emanated from a perinuclear region and extended towards the cell periphery. Once the cells had formed a confluent monolayer, Scrib displayed its well-established predominant plasma membrane localization (Fig. 3-3, panel b). This redistribution from a more filamentous to a mostly plasma membrane localization was also observed for endogenous Scrib in MDCK cells (Fig. 3-3, panels c and d). In contrast to overexpressed Scrib, however, the endogenous protein did not decorate the full-length of the filaments, but aligned as punctuated labeling on what appeared to be filaments in the cell periphery (Fig. 3-3, panel c). This discrepancy in Scrib subcellular localization could be due to the difference in expression levels between the overexpressing exogenous Scrib and that of the basal level expression of endogenous Scrib.

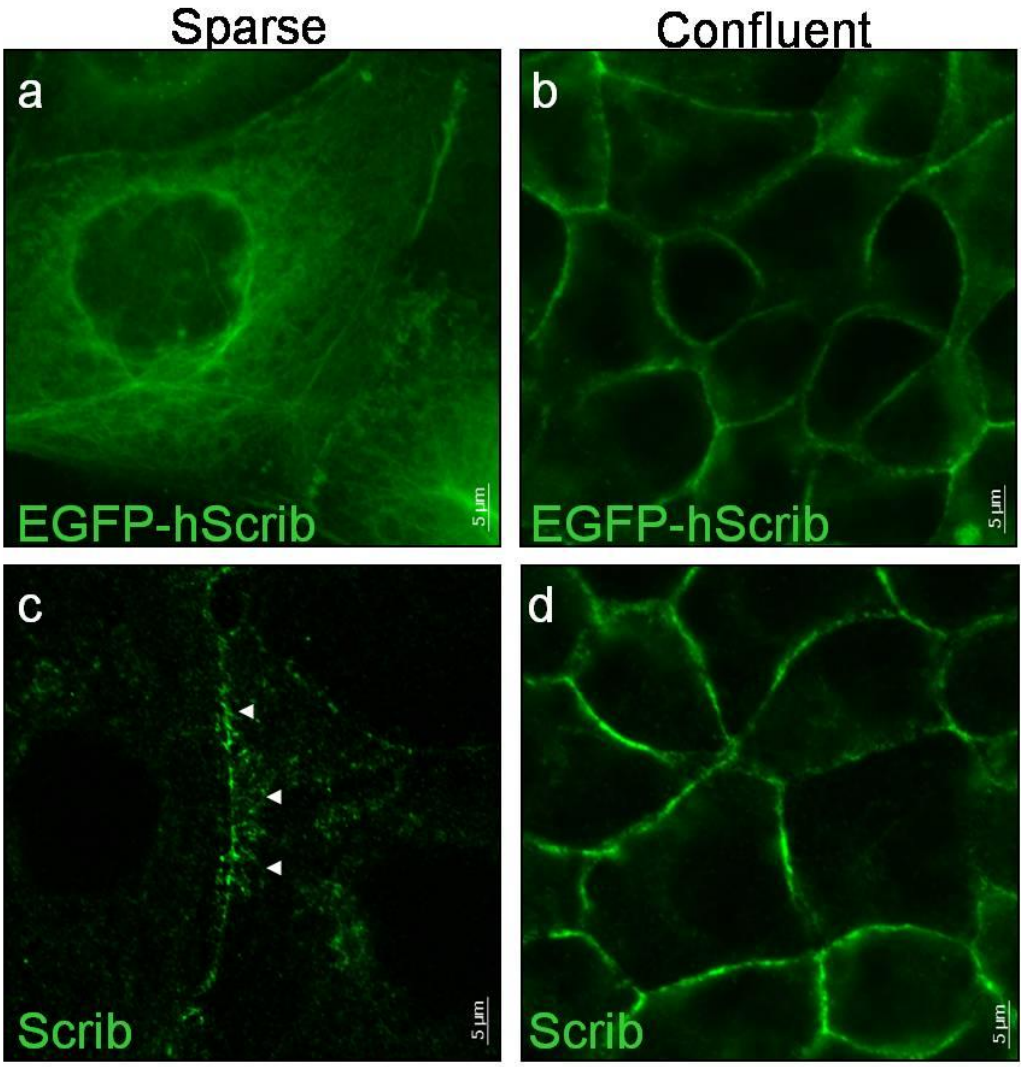


**Figure 3-3. Filamentous localization of Scrib.** Exogenously expressed EGFP-hScrib (panels a and b) or endogenous Scrib (panels c and d) were visualized by fluorescence microscopy in sparse (panels a and c) or confluent (panels b and d) MDCK cell cultures. In sparse cultures, EGFP-Scrib extensively localizes to filaments, whereas filamentous localization of endogenous Scrib is most pronounced in the cell periphery (arrowheads), with both the exogenous and endogenous protein apparently relocalizing to the plasma membrane in confluent cultures.

To ascertain the nature of these filamentous structures, colocalization studies with proteins of the major cellular cytoskeletal networks were performed in MDCK cells. EGFP-hScrib filaments extensively overlapped with vimentin and keratin 18 of intermediate filaments (IF) (Fig. 3-4A, panels a-f). Also HA-tagged mouse Scrib expressed in COS-1 cells aligned with vimentin, showing that colocalization with intermediate filaments was not restricted to a single cell line and was independent of the particular tag (Fig. 3-4A, panels g-i). Furthermore, staining for endogenous Scrib in MDCK cells coincided with vimentin-positive fibrils at the cell periphery of sparse cultures (Fig. 3-4B), but this was less prominent in confluent cells (Fig. 3-4C). No significant colocalization was observed with either the microtubule (Fig. 3-4D, panels a-c) or the actin (Fig. 3-4E, panels a-c) networks. Treatment of cells with nocodazole or cytochalasin D disrupted the microtubule (Fig. 3-4D, panels d-f) or actin (Fig. 3-4E, panels d-f) cytoskeleton, neither affecting the filamentous appearance of EGFP-hScrib (Fig. 3-4D and E, panels d-f) nor its colocalization with vimentin (Fig. 3-4D and E, panels g-i). This thus confirms the absence of Scrib from either actin microfilaments or microtubules.

The colocalization of Scrib with IF was further corroborated in MDCK monolayers cultured on permeable polycarbonate filters (Fig. 3-4F and G). Under sparse culture conditions when cell-cell contact was being established, EGFP-hScrib showed extensive colocalization with vimentin (Fig.3-4F, panels a-c) and keratin 18 (K18) (Fig. 3-4F, panels d-f) based IFs and the lateral membrane. In confluent MDCK cell monolayers, EGFP-hScrib localized along the length of the lateral plasma membrane and the IFs had acquired an apical localization (Fig. 3-4G, panels a-f), apparently lining the

apical pole of the lateral plasma membrane and only showing partial overlap with hScrib at the apical pole of the lateral membrane (Fig. 3-4G, panels c and f).

In conclusion, in COS-1 or sparse MDCK cell cultures, Scrib shows extensive colocalization with vimentin and keratin based IF. In MDCK cells, Scrib redistributes to the lateral plasma membrane during the establishment and maturation of cell-cell adhesion.

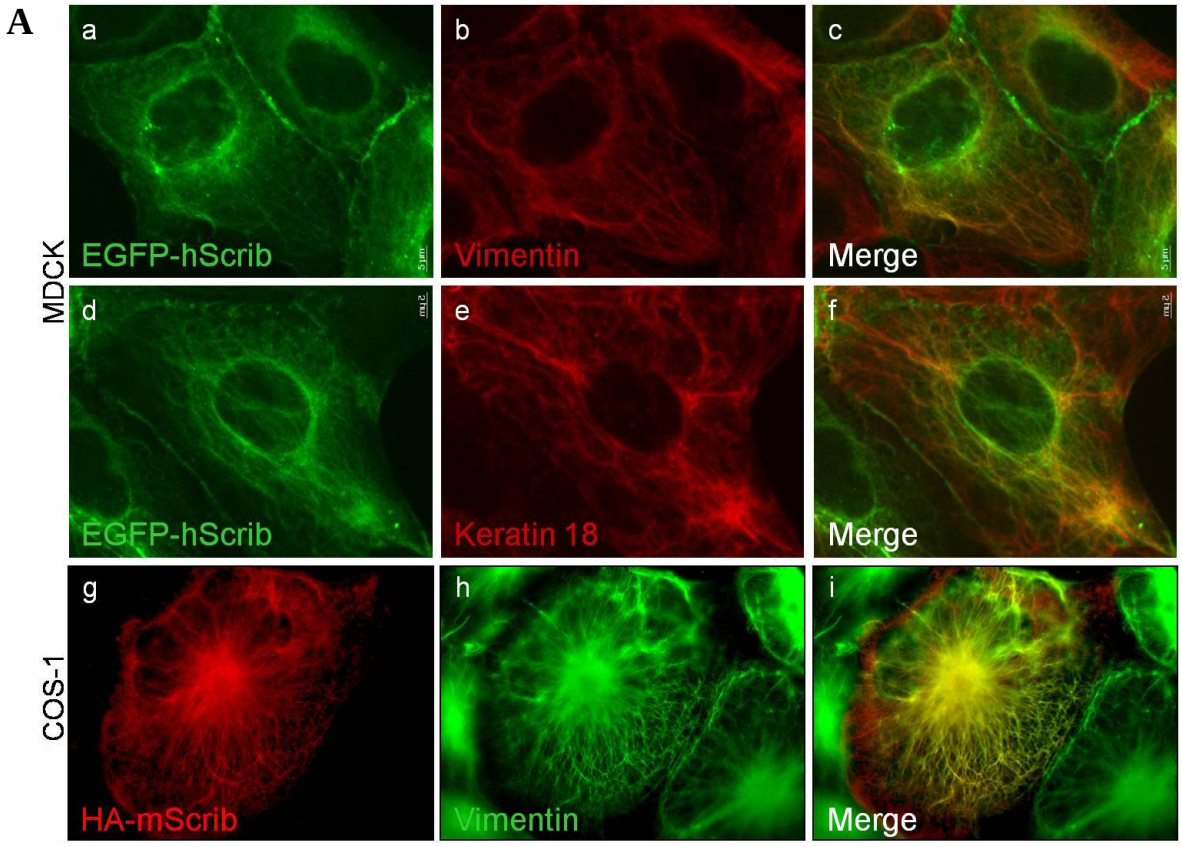


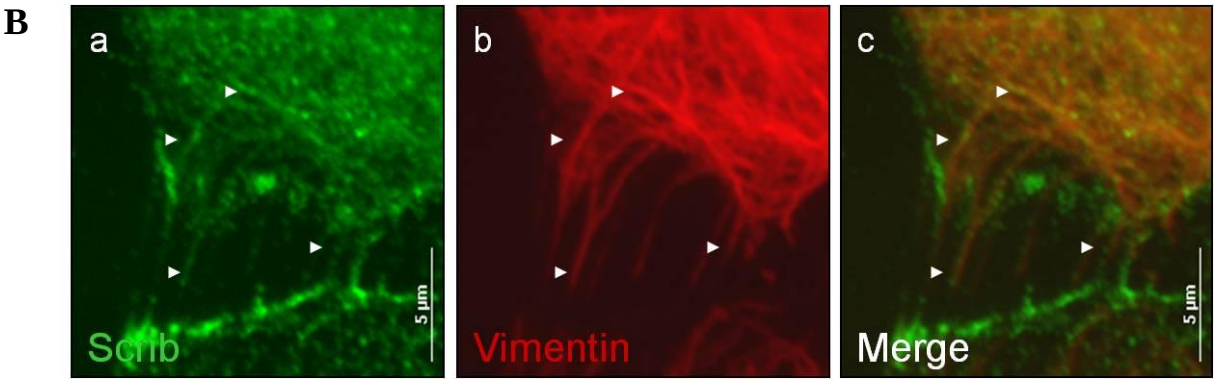

**C**

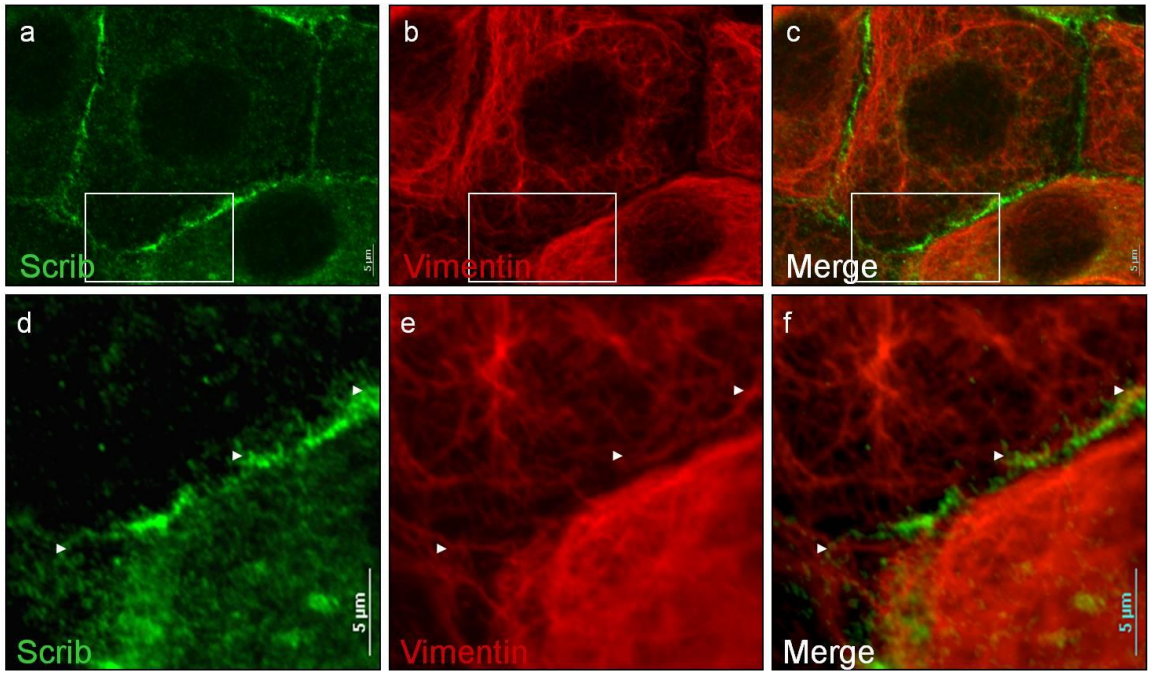
a
b
c
Scrib
Vimentin
Merge
d
e
f
Scrib
Vimentin
Merge
5 µm

**D**

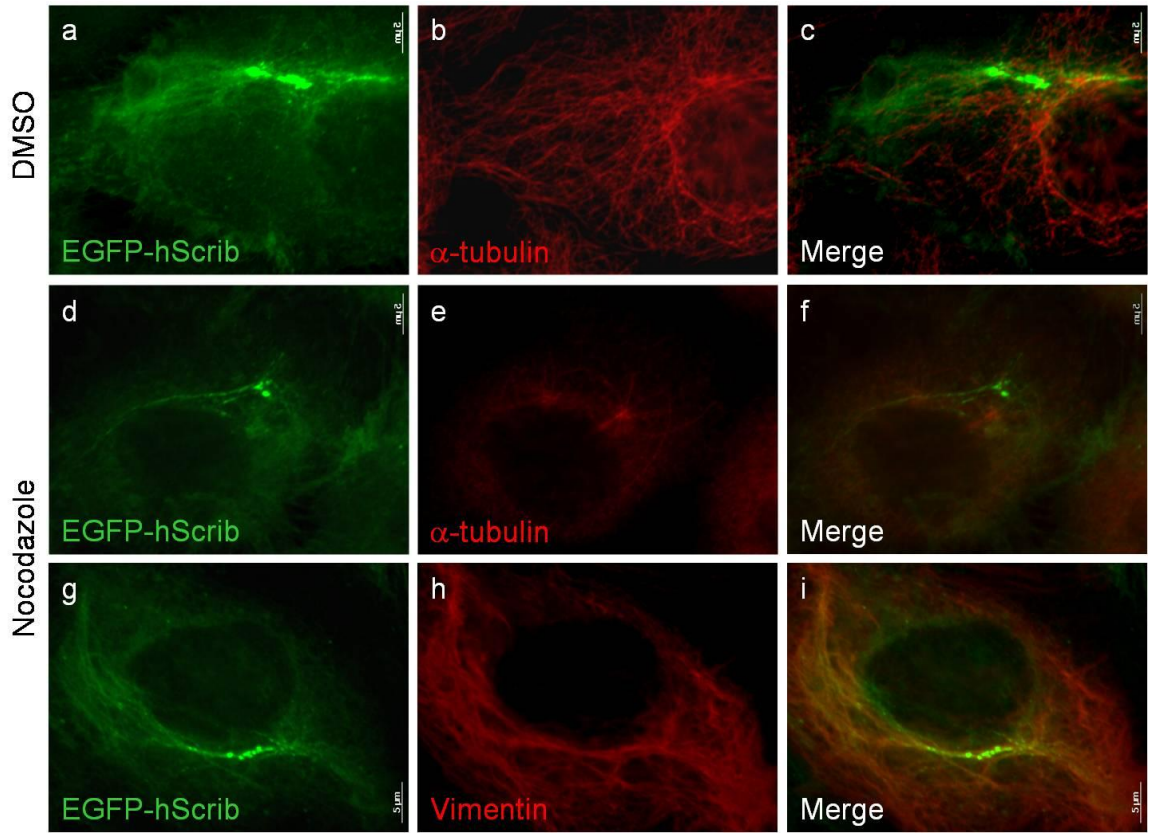
DMSO
Nocodazole
a
b
c
EGFP-hScrib
α-tubulin
Merge
d
e
f
EGFP-hScrib
α-tubulin
Merge
g
h
i
EGFP-hScrib
Vimentin
Merge

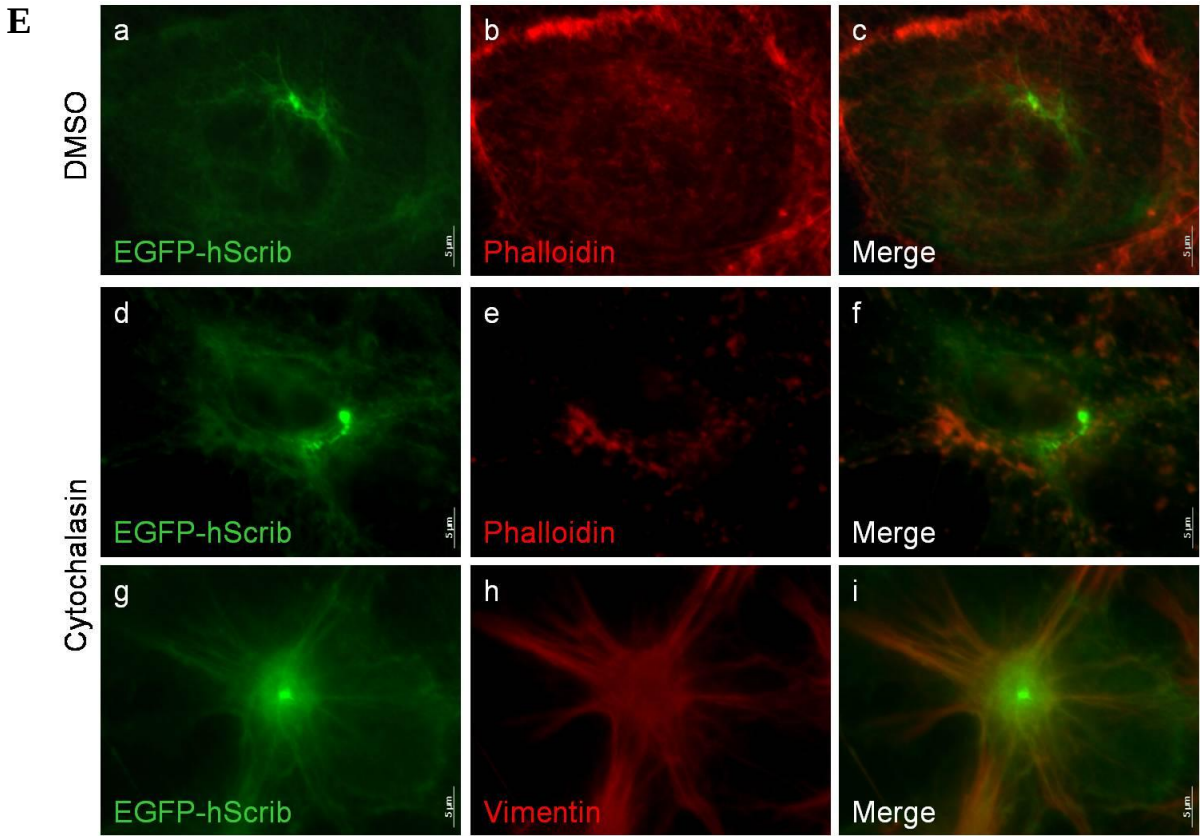


**Figure 3-4. Scrib localizes to intermediate filaments**. (**A**) Epitope tagged Scrib colocalizes with vimentin and keratin 18. EGFP-hScrib (panels a and d, green color) and vimentin (panel b, red color) or keratin 18 (panel e, red color) were visualized in sparse MDCK cells expressing EGFP-hScrib. HA-mScrib (panel g, red color) and vimentin (panel h, green color) were also visualized in COS-1 cells. Yellow in the merged images (panels c, f and i) indicates colocalization of Scrib with the intermediate filament. (**B**, **C**) Localization of endogenous Scrib to vimentin intermediate filaments. Scrib (**B** and **C** panel a, green color) and vimentin (**B** and **C**, panel b, red color) were immunostained in sparse (**B**) or higher density (**C**) MDCK cell cultures. Yellow in the merged images (**B** and **C**, panel c) indicates colocalization. In sparse cultures, endogenous Scrib can be detected on peripheral vimentin filaments (arrowheads). Upon establishment of cell-cell contact, Scrib is concentrated at contact sites and present on vimentin filaments in the cell periphery (see arrowheads in magnification of insets in **C**, panels d-f). (**D**, **E**) EGFP-hScrib does not colocalize with the actin or microtubule network in MDCK cells. EGFP-hScrib (**D** and **E**, panels a, d, g) was visualized together with microtubules (stained with anti-α-tubulin, **D**, panels b, e) or vimentin (panel h), or actin (stained with phalloidin, **E**, panels b and e) or vimentin (panel h). Cells were treated with DMSO solvent (**D** and **E**, panels a-c) or Nocodazole (10ug/ml for 1hr) (**D**, panels d-i) and Cytochalasin D (10ug/ml for 30min) (**E**, panels d-i).

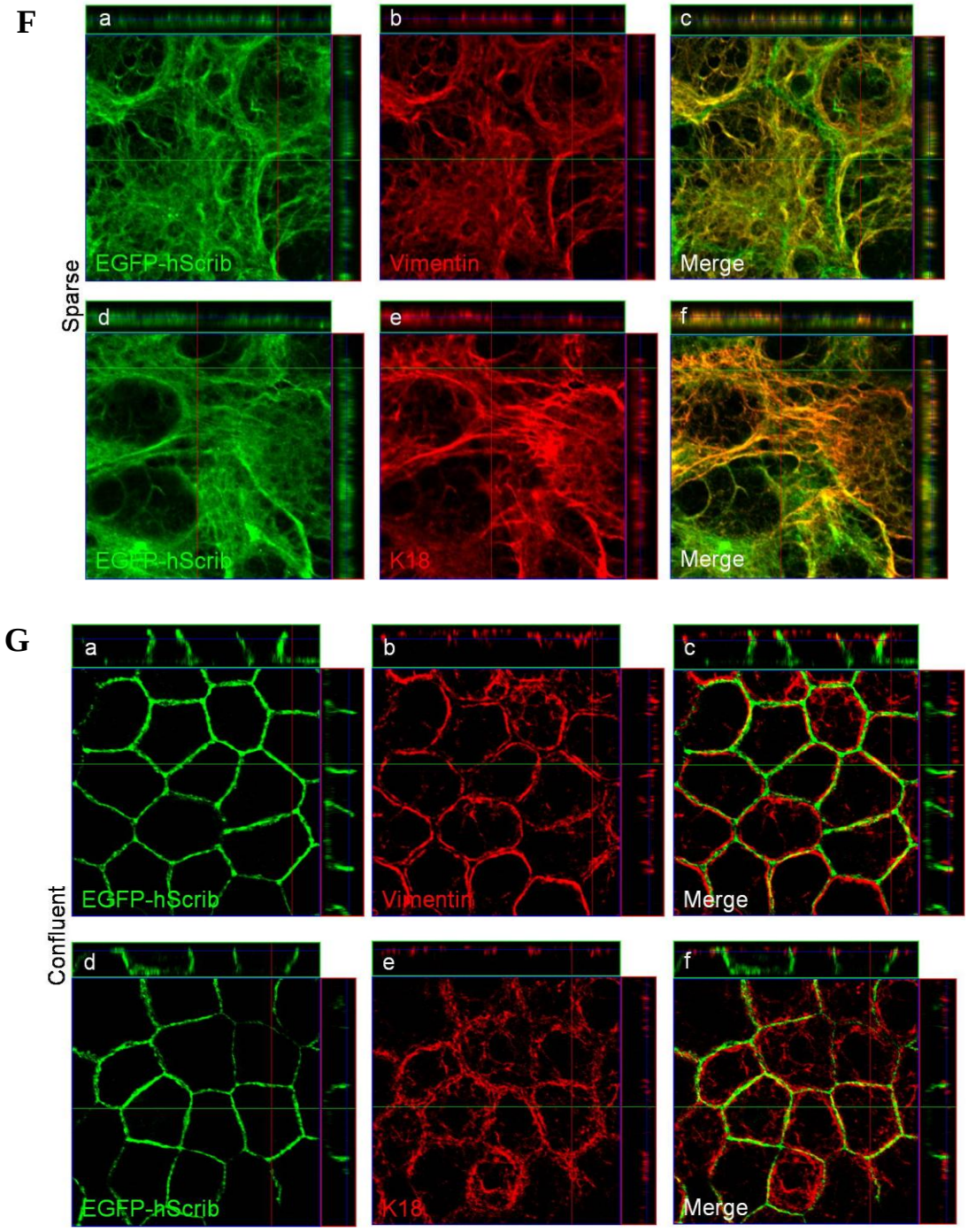


(**F**,**G**) Relocalization of EGFP-hScrib, vimentin and keratins during formation of polarized MDCK cell monolayers grown on permeable supports. EGFP-hScrib (**F** and **G**, panels a and d, green color) and vimentin (**F** and **G**, panel b, red color) or keratin 18 (**F** and **G**, panel e, red color) were visualized by confocal fluorescence microscopy in sparse (**F**) or polarized (**G**) MDCK cell cultures. Blue lines indicate the location of the horizontal confocal section, red and green lines indicate the site of vertical confocal *z*-axis side views along the apical-basal axis of the monolayer. Yellow in the merged images indicate colocalization (**F** and **G**, panels c, f). Note the extensive colocalization of EGFP-hScrib with vimentin and keratins in non-polarized cells. In polarized cells, vimentin and keratin 18 accumulate at the apical pole, whereas EGFP-hScrib is present on the lateral membrane and only shows minimal overlap with intermediate filaments at the apical end of the lateral membrane.

### 3.2.2 Scrib Directly Associates with Intermediate Filaments

Next, we biochemically corroborated the colocalization of Scrib with intermediate filaments using MDCK, MCF10A, HeLa and COS-1 cells which all express endogenous Scrib (Fig. 3-5A, panel a). Endogenous vimentin was immunoprecipitated from cell lysates and probed for the coprecipitation of endogenous Scrib. As shown in Fig. 3-5A, panel b, Scrib specifically coprecipitated with vimentin in the cell lines tested. Furthermore, overexpressed EGFP-hScrib (Fig. 3-5A, panel c) or endogenous Scrib (Fig. 3-5A, panel d) coimmunoprecipitated with endogenous vimentin from both sparse and confluent MDCK cell cultures.

To determine if the association of Scrib with IF reflects a direct binding to vimentin, we carried out cosedimentation assays between purified non-polymerized or *in vitro* polymerized hamster vimentin and *in vitro* translated N-terminally HA-tagged mScrib (Fig. 3-5B). While purified non-polymerized vimentin remained in the supernatant after ultracentifugation, *in vitro* polymerized vimentin sedimented to the pellet (Fig. 3-5B, panel a). *In vitro* translated mScrib was recovered in the pellet, but only in the presence of polymerized vimentin (Fig. 3-5B, panel b). Furthermore, both polymerized (Fig. 3-5B, panel c) and non-polymerized (Fig. 3-5B, panel d) vimentin coimmunoprecipitated with *in vitro* translated HA-Scrib. These experiments thus confirm the association between Scrib and vimentin observed *in vivo* and show that the interaction is direct and, at least *in vitro*, occurs with both non-polymerized vimentin and vimentin filaments.

A

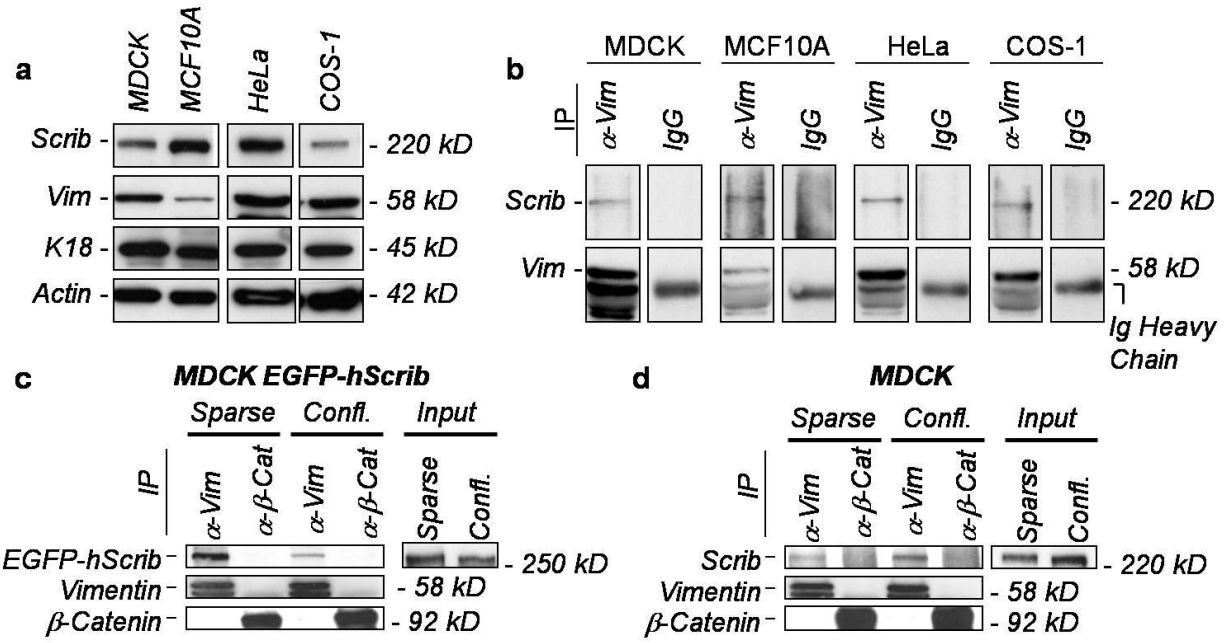
a
MDCK
MCF10A
HeLa
COS-1
Scrib -
Vim -
K18 -
Actin -
- 220 kD
- 58 kD
- 45 kD
- 42 kD
b
MDCK
MCF10A
HeLa
COS-1
IP
α-Vim
IgG
Scrib -
Vim -
- 220 kD
- 58 kD
Ig Heavy Chain
c
MDCK EGFP-hScrib
Sparse
Confl.
Input
IP
α-Vim
α-β-Cat
Sparse
Confl.
EGFP-hScrib -
Vimentin -
β-Catenin -
- 250 kD
- 58 kD
- 92 kD
d
MDCK
Sparse
Confl.
Input
IP
α-Vim
α-β-Cat
Sparse
Confl.
Scrib -
Vimentin -
β-Catenin -
- 220 kD
- 58 kD
- 92 kD

**B**

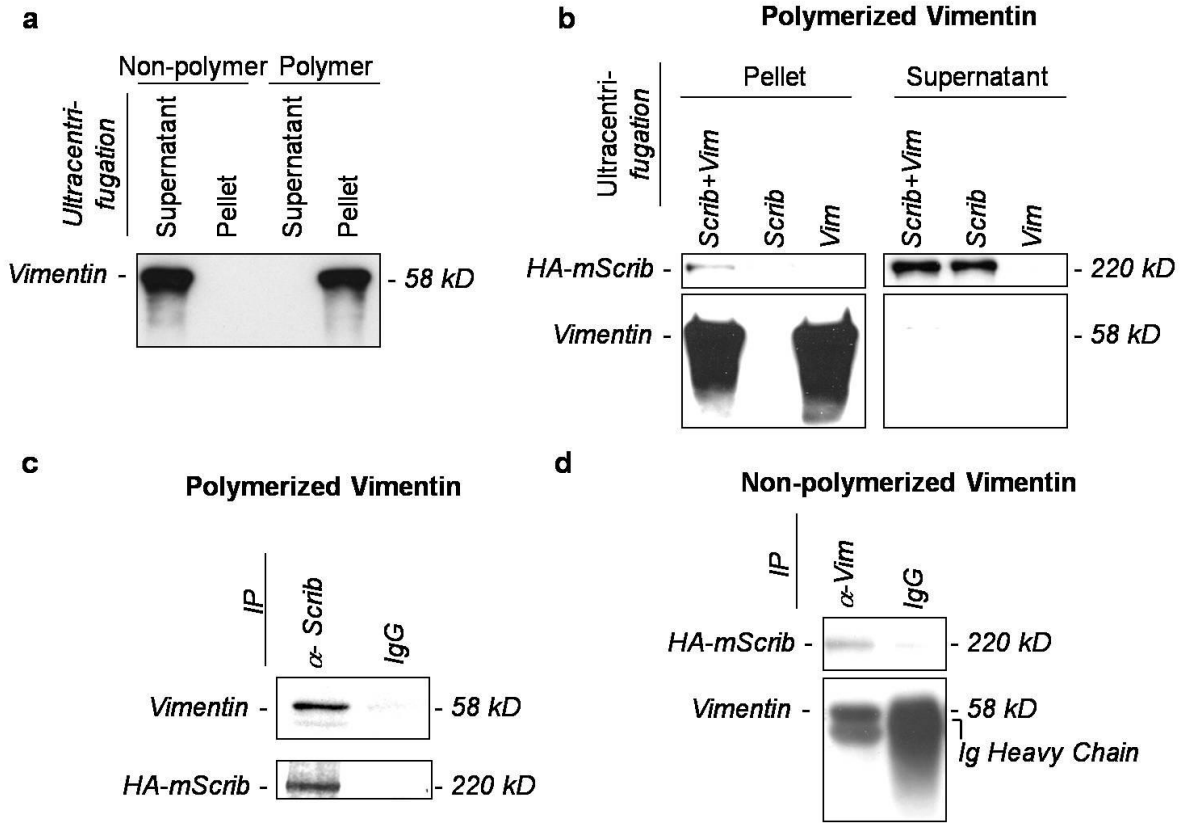


**Figure 3-5. Scrib associates with intermediate filaments via its PDZ domains**. (**A**) Coimmunopercipitation of Scrib with vimentin. Endogenous Scrib, vimentin and keratin 18 were detected by Western blot in various cell lines (panel a) and Scrib was coimmunoprecipitated with vimentin (panel b). Vimentin was immunoprecipitated from lysates of sparse or confluent (Confl.) MDCK cells expressing (panel c) or not expressing (panel d) EGFP-hScrib. Associated exogenous (panel c) or endogenous (panel d) Scrib was detected by Western blot. Precipitation with an antibody to β-catenin served as a negative control. An aliquot of the cell lysate (5%) was directly analyzed by Western blot to monitor Scrib expression levels (Input). (**B**) Scrib associates directly with both non-polymerized or polymerized vimentin *in vitro*. Vimentin assembly was monitored through fractionation by ultracentifugation. Fractions were subjected to Western blot and vimentin visualized as non-polymerized (Non-Polymer) or polymerized (Polymer) forms in the supernatant or pellet respectively (panel a). *In vitro* translated HA-mScrib cosedimented with vimentin only when applied to polymerized vimentin but not alone (panel b). HA-mScrib also associated with both polymerized (panel c) and non-polymerized (panel d) vimentin in coimmunoprecipitation assays. Note that even in the presence of a large excess of normal IgG (panel d), little if any Scrib is found in the precipitate.

### 3.2.3 Scrib Associates with Intermediate Filaments via Its PDZ Domain-Containing Region

To map the domain in Scrib responsible for the interaction with intermediate filaments, two N-terminally EGFP-tagged hScrib constructs encompassing either of the two major domains, namely the LRR (leucine-rich repeats) and the PDZ (PSD-95/DLG/ZO1) regions, were generated (Fig 3-5C) and tested for their association with intermediate filaments. Confirming the data above (Fig. 3-5A, panel c), vimentin, and also keratin 18, coimmunoprecipitated with EGFP-hScrib (Fig. 3-5D, panels a and b). Intermediate filaments predominantly bound to hScrib PDZ, with only a comparatively weak interaction with hScrib LRR observed. As a positive control, ZO-2 bound both hScrib WT (full-length hScrib) and hScrib PDZ, consistent with a previous report (Metais *et al.*, 2005). As a negative control, EGFP did not associate with the intermediate filament proteins (Fig. 3-5D, panel a and b). Furthermore, *in vitro* translated HA-mScrib PDZ, but not the HA-mScrib LRR, coimmunoprecipitated with purified *in vitro* polymerized (Fig.3-5D, panel c) or non-polymerized (Fig. 3-5D, panel d) vimentin. This data thus implicates the regions containing the four PDZ domains in mediating the association of Scrib with IFs.

**C**

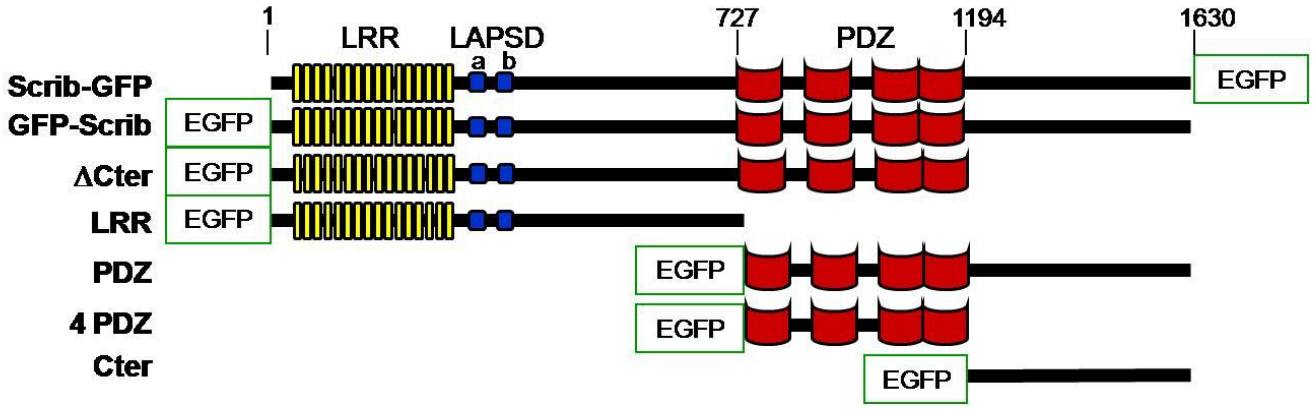
1
LRR
LAPSD
a b
727
PDZ
1194
1630
Scrib-GFP
GFP-Scrib
ΔCter
LRR
PDZ
4 PDZ
Cter
EGFP

**D**

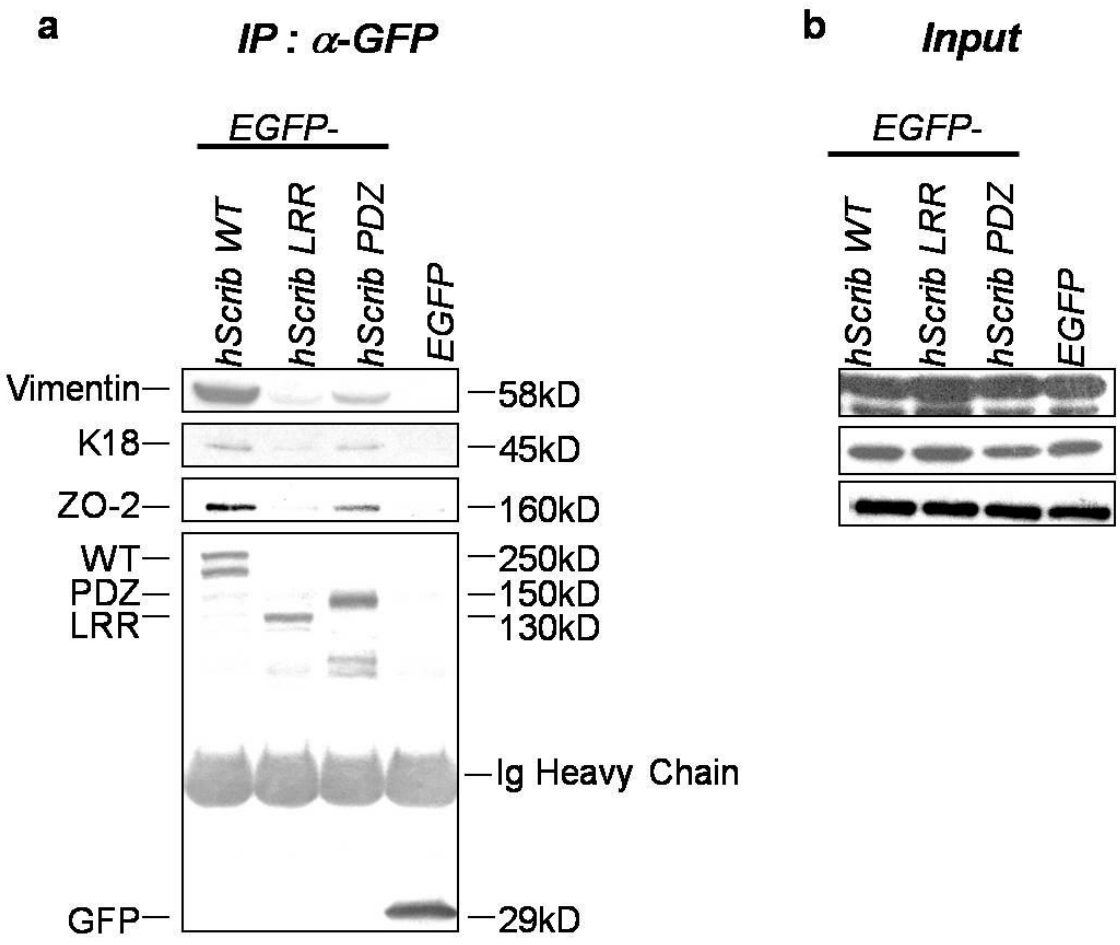
a
IP : α-GFP
b
Input
EGFP-
hScrib WT
hScrib LRR
hScrib PDZ
EGFP
Vimentin
K18
ZO-2
WT
PDZ
LRR
GFP
58kD
45kD
160kD
250kD
150kD
130kD
Ig Heavy Chain
29kD

**D**

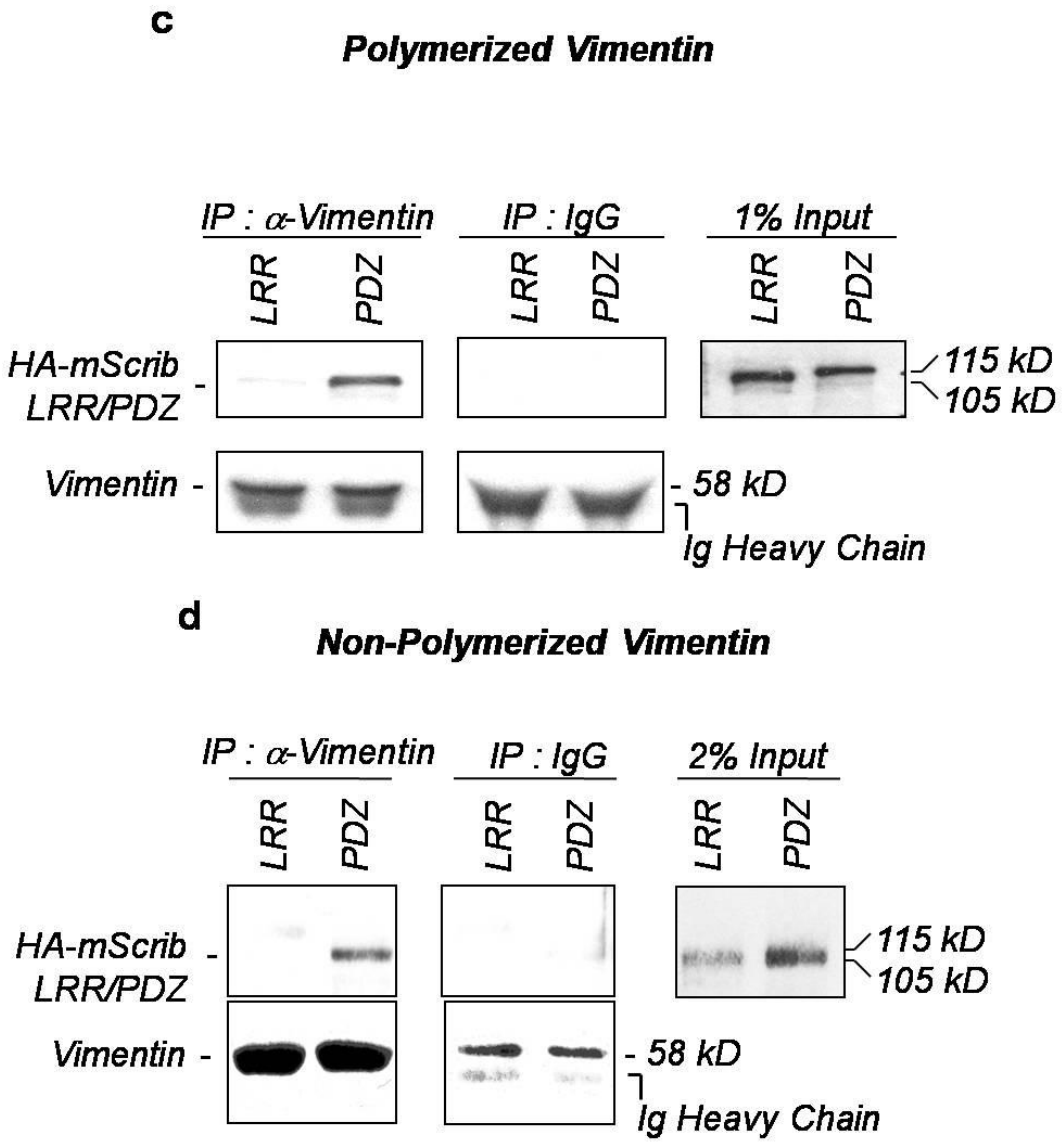


(**C**) Schematic diagram of EGFP-hScrib deletion mutants. Full-length human Scrib was either tagged at the N- (GFP-Scrib) or C- (Scrib-GFP) terminus with EGFP. ΔCter lacks the region C-terminal to the PDZ domains, which is contained in the Cter construct. LRR and PDZ encode the N-terminal LRR-LAPSD or the C-terminal 4 PDZ domains, respectively. 4PDZ contains the PDZ domains only. Amino acids demarcating the beginning or end of constructs generated are represented by numbers above each line. (**D**) Scrib associates with intermediate filaments via the region containing the 4 PDZ domains. EGFP-hScrib WT, LRR and PDZ were immunoprecipitated from sparse MDCK cells and associated vimentin and keratin 18 as detected by Western blot analysis (panel a). The detection of ZO-2 served as a positive control for the interaction with hScrib WT or PDZ and as a negative control for the interaction with LRR (Metais *et al.*, 2005). An aliquot (5%) of the cell lysate was directly subjected to Western blot analysis to monitor the expression levels of vimentin, keratin 18 and ZO-2 (Input) (panel b). Scrib directly binds to vimentin via its PDZ domains. Purified, *in vitro* polymerized (panel c) or non-polymerized (panel d) vimentin and *in vitro* translated HA-mScrib LRR or HA-mScrib PDZ were combined and incubated. Vimentin was then immunoprecipitated and vimentin or HA-Scrib detected by Western blot. Normal IgG served as a negative control.

The interaction of the Scrib-PDZ domain with vimentin was corroborated by expressing the different EGFP-hScrib deletion constructs (Fig. 3-5E, panel a) in sparse (Fig. 3-5E, panels b-o) MDCK cells and analyzing their localization. Similarly to the EGFP-hScrib, a C-terminally tagged protein (hScrib-EGFP) was present on filaments (Fig. 3-5E, panel c), excluding the possibility that filamentous localization was due to the location of the tag or to truncated Scrib molecules arising from either premature translational arrest or C-terminal degradation. Consistent with the binding data, hScrib-PDZ (Fig. 3-5E, panels d-f) but not hScrib-LRR (Fig. 3-5E, panels g-i) displayed a filamentous localization. Deletion of the region C-terminal to the PDZ domains (hScrib ΔCter) did not affect filamentous localization (Fig. 3-5E, panels j-l). Furthermore, the 4 PDZ domains themselves were sufficient for colocalization with vimentin (Fig. 3-5E, panels m-o), whereas the C-terminal fragment downstream of the PDZ domains (hScrib-Cter) was absent from filaments (data not shown).

To determine if a particular PDZ domain is responsible for the interaction with intermediate filaments, each of the 4 PDZ domains was expressed as a GST-fusion protein and tested in binding assays. PDZ3 efficiently interacted with both vimentin and keratin 18 (Fig. 3-5F). Less efficient associations were also observed for PDZ1 and PDZ2, whereas no binding to vimentin or keratin 18 could be detected for PDZ4.

Taken together, Scrib directly binds via its PDZ domains to the intermediate filament components vimentin and keratin 18.

**E**

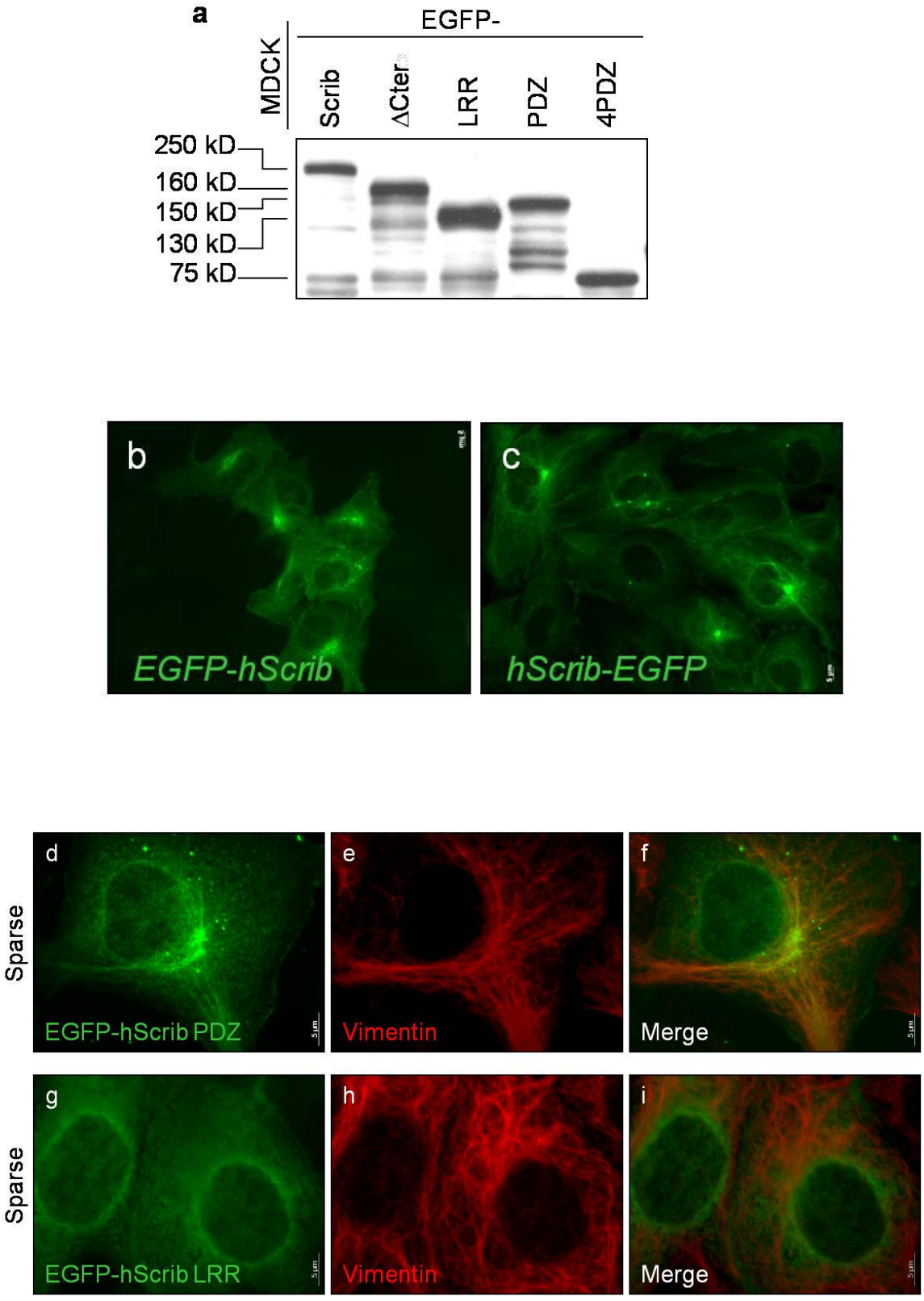
a
EGFP-
MDCK
Scrib
ΔCter
LRR
PDZ
4PDZ
250 kD
160 kD
150 kD
130 kD
75 kD
b
EGFP-hScrib
c
hScrib-EGFP
d
EGFP-hScrib PDZ
e
Vimentin
f
Merge
Sparse
g
EGFP-hScrib LRR
h
Vimentin
i
Merge
Sparse

**E**

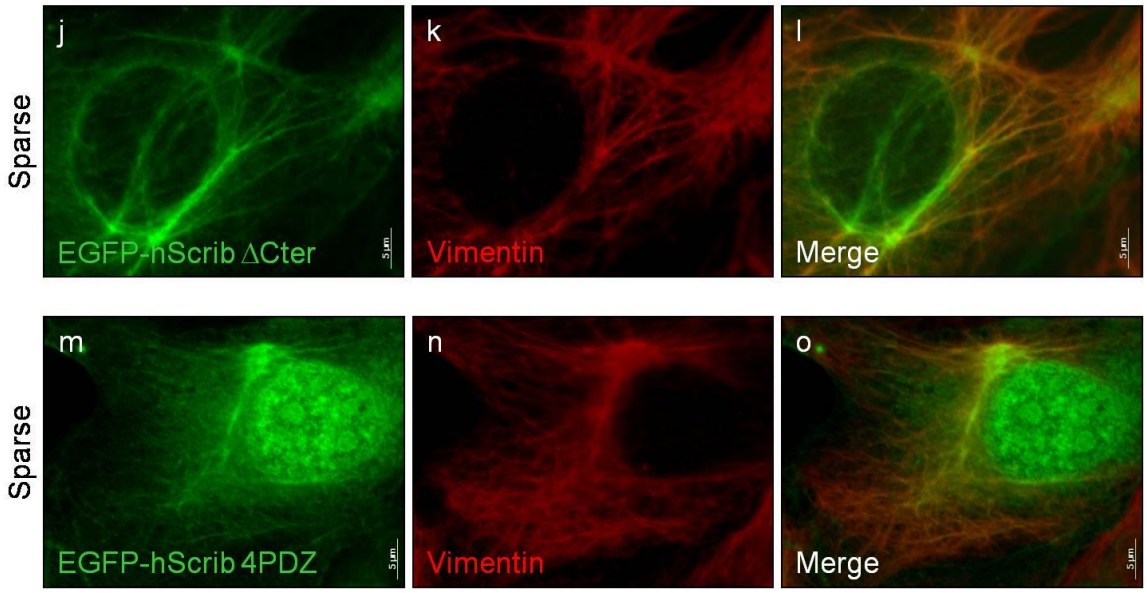


**F**

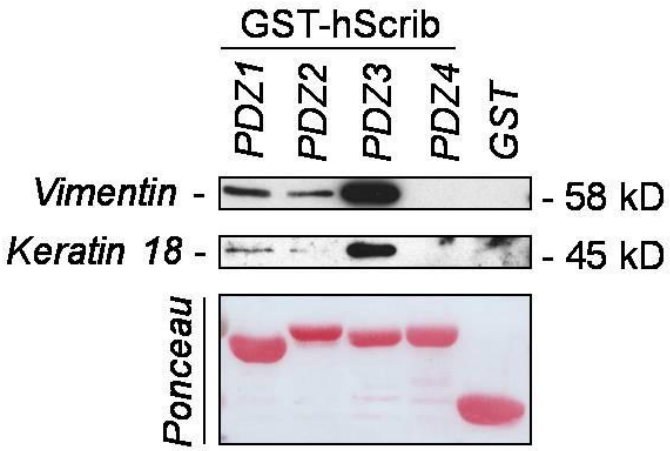


(**E**) Scrib PDZ localizes to vimentin filaments in sparse MDCK cells. The different Scrib constructs tagged with EGFP were expressed in MDCK cells and visualized by Western blot analysis (panel a) or fluorescence microscopy (panels b-o). Note that both N- and C-terminally tagged Scrib (panels b and c) and only constructs containing the PDZ domains (panels d-f, j-l and m-o) show extensive filamentous localization.**(F)** Immobilized GST fusion proteins carrying the isolated PDZ1, PDZ2, PDZ3 or PDZ4 domain of hScrib were incubated with MDCK cell lysate. Bound proteins were subjected to Western blot analysis to detect vimentin or keratin 18. The amount of the different GST fusion proteins was monitored by staining with Ponceau S.

### 3.2.4 Silencing of either Scrib or Vimentin Leads to Similar Effects on Cell Motility and Morphology

To explore the functional relationship of the interaction between Scrib and vimentin, their protein levels were reduced in MDCK cells using pools of four small interfering RNAs (siRNA) targeting specifically either canine Scrib or vimentin. Immunofluorescence (Fig. 3-6A) and Western blot (Fig. 3-6B) analysis confirmed the gradual decrease of Scrib and/or vimentin protein levels following treatment with the respective siRNAs. We then analyzed the effect of the siRNAs on several cellular processes that have been linked to Scrib, including cell morphology, migration and polarity. All subsequent assays were carried out on the 4th day following addition of the siRNA, unless indicated otherwise.

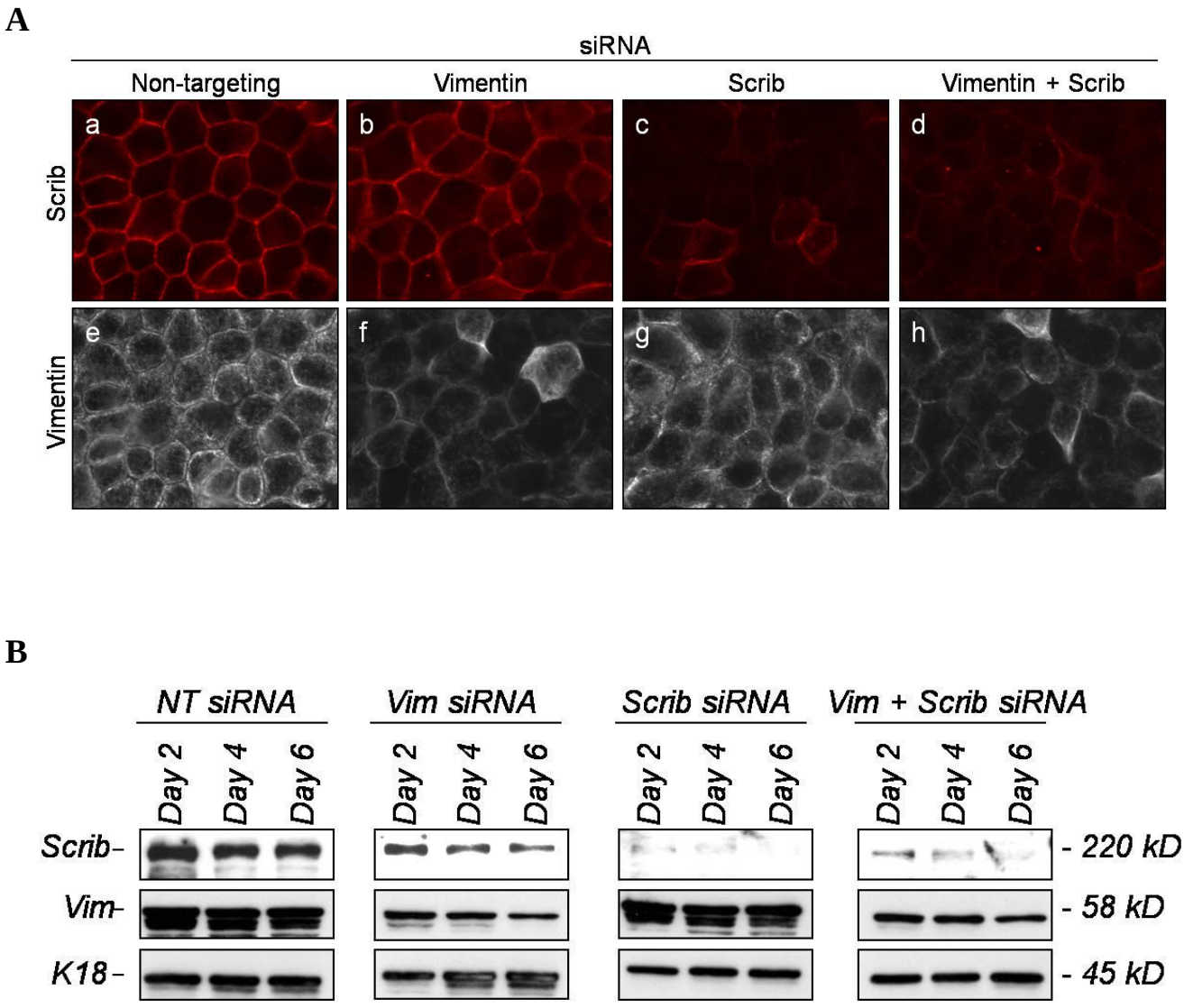


**Figure 3-6. siRNA mediated depletion of endogenous vimentin and Scrib in MDCK cells.** (**A**) Silencing of Scrib and vimentin monitored by imunofluorescence microscopy. Scrib (panels a-d, red color) and vimentin (panels e-h, white color) were visualized in MDCK cells treated for 3 days with a non-targeting siRNA (panels a and e) or siRNAs to vimentin (panels b and f), Scrib (panels c and g) or both, Scrib and vimentin (panels d and h). (**B**) Silencing of Scrib and vimentin monitored by Western blot analysis. Scrib and vimentin protein levels in lysates of cells treated with siRNA over a 6 day period were monitored by Western blot on days 2, 4 and 6. Keratin 18 was detected to monitor for equal cell lysate loading.

Directed migration of cells in which Scrib and/or vimentin expression had been silenced was studied using wound-healing assays. Depletion of either vimentin or Scrib alone or in combination resulted in an aberrant cell morphology and orientation at the migration front (Fig. 3-7A). Whereas control cells migrated as an organized sheet with their long axis perpendicular to the migration front, silencing of Scrib and/or vimentin lead to a randomized cell orientation and a disorganized appearance of the cell sheet at the wound edge. At the leading edge, cells normally polarize their Golgi complex towards the direction of migration (Kupfer *et al.*, 1982) and this polarization is affected upon depletion of Scrib (Osmani *et al.*, 2006; Dow *et al.*, 2007). Consistent with these findings, Scrib knock-down cells failed to polarize their Golgi complex in our assay (Fig. 3-7B, panels a-f). Interestingly, a randomized Golgi complex orientation was also observed in vimentin siRNA treated cells, either alone or in combination with Scrib siRNA.

In conclusion, cell morphology and Golgi complex polarization were similarly affected in migrating MDCK cells upon silencing of either Scrib, vimentin or both.

**A**

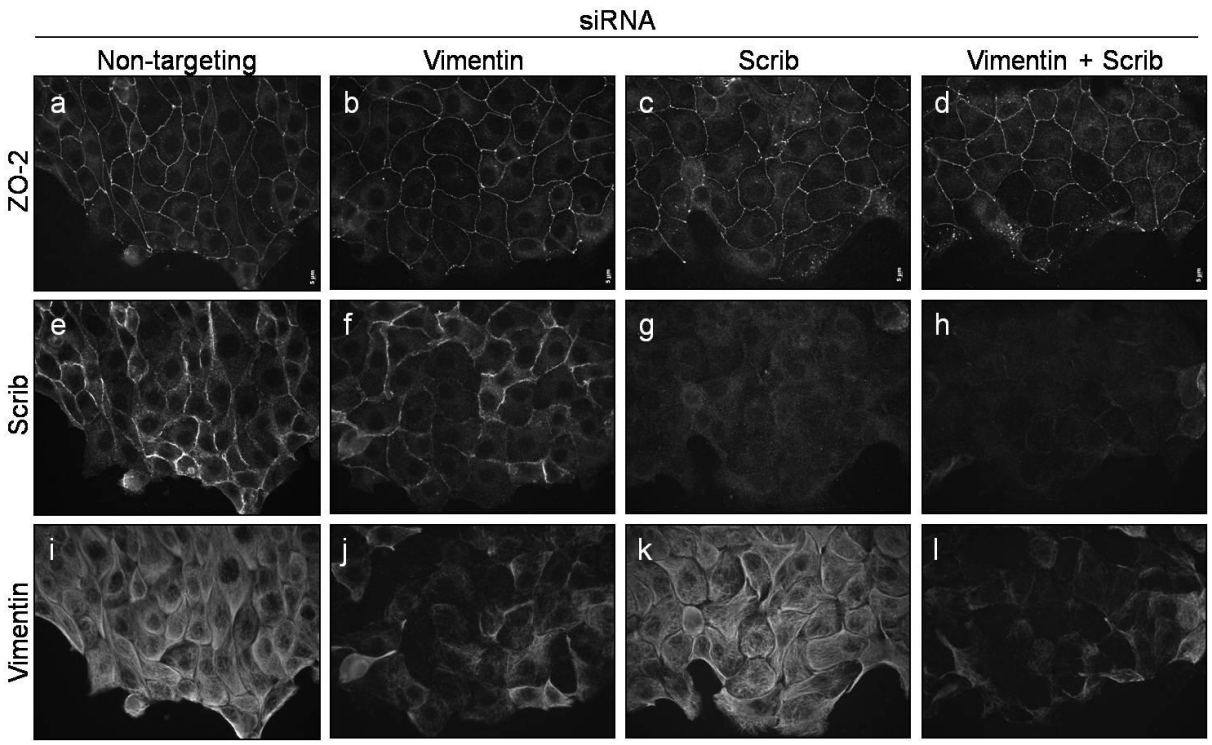


**Figure 3-7. Silencing of Scrib or vimentin expression in MDCK cells leads to defects in cell morphology and Golgi complex orientation during directed cell migration**. (**A**) Aberrant morphology. Monolayers of cells treated with non-targeting (panels a, e and i), vimentin (panels b, f, j), Scrib (panels c, g, k) or Scrib and vimentin (panels d, h, l) siRNA were wounded and stained with an antibody to ZO-2 (panels a-d) to visualize the cell outline. Scrib (panels e-h) and vimentin (panels i-l) were stained to monitor the effectiveness of the siRNA treatment. Note how in control cells the long axis of the cells is directed towards the wound edge (bottom of the images), whereas it is random in cells treated with the specific siRNAs.

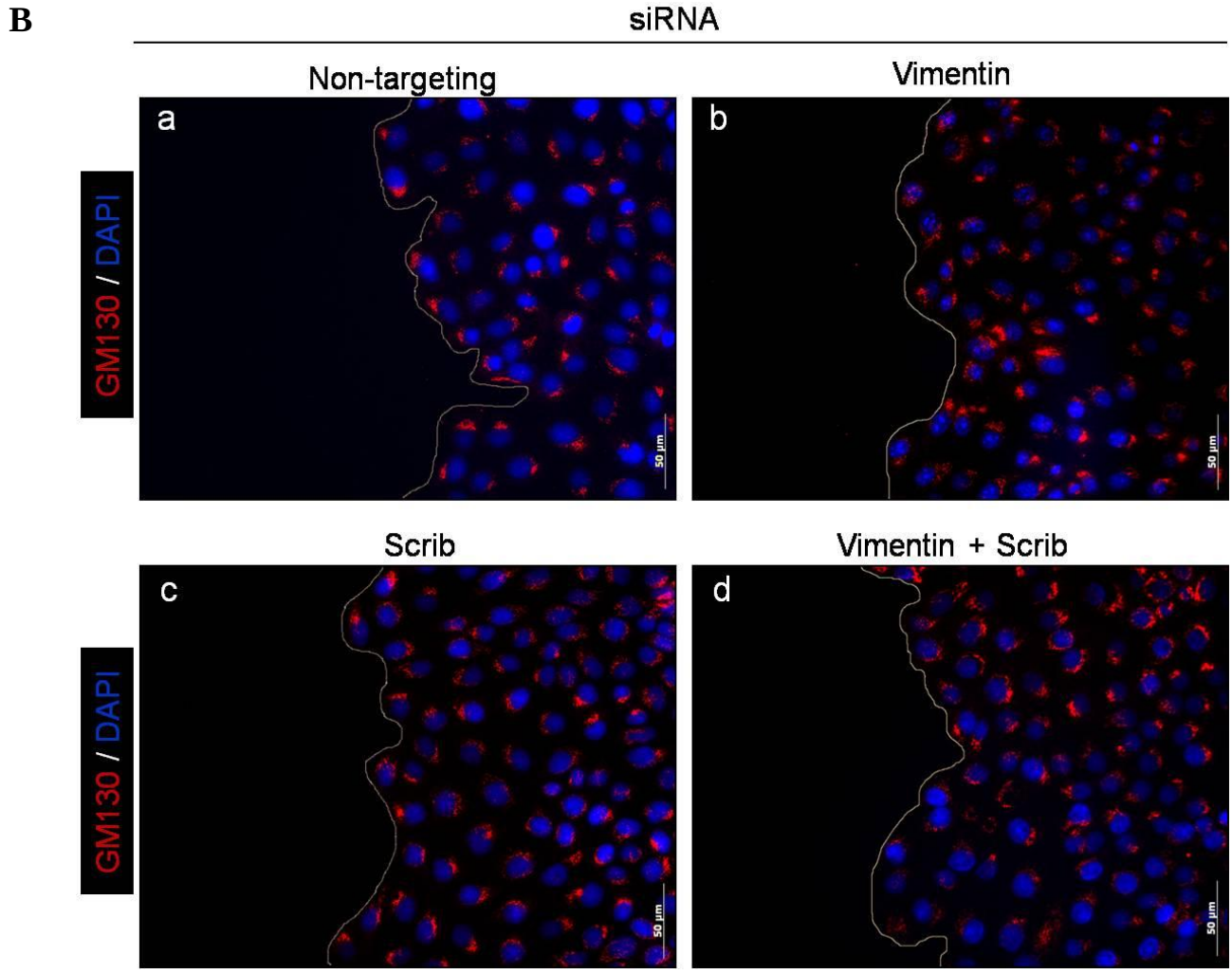
B
siRNA
Non-targeting
Vimentin
Scrib
Vimentin + Scrib
a
b
c
d
GM130 / DAPI
GM130 / DAPI
50 µm

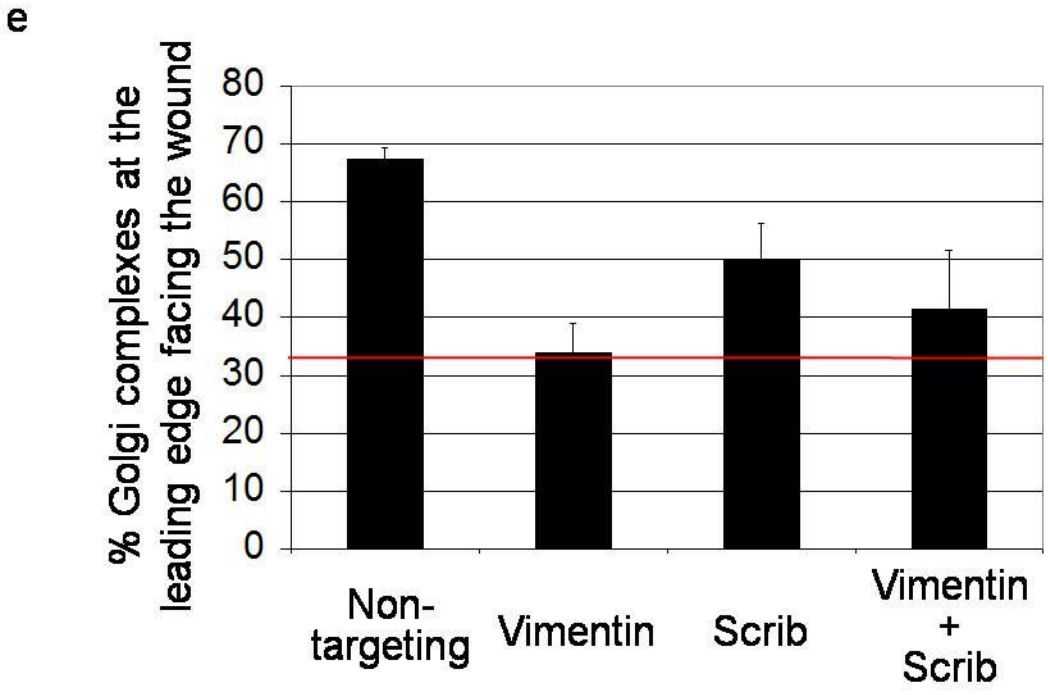
e
% Golgi complexes at the leading edge facing the wound
80
70
60
50
40
30
20
10
0
Non-targeting
Vimentin
Scrib
Vimentin + Scrib

**B**

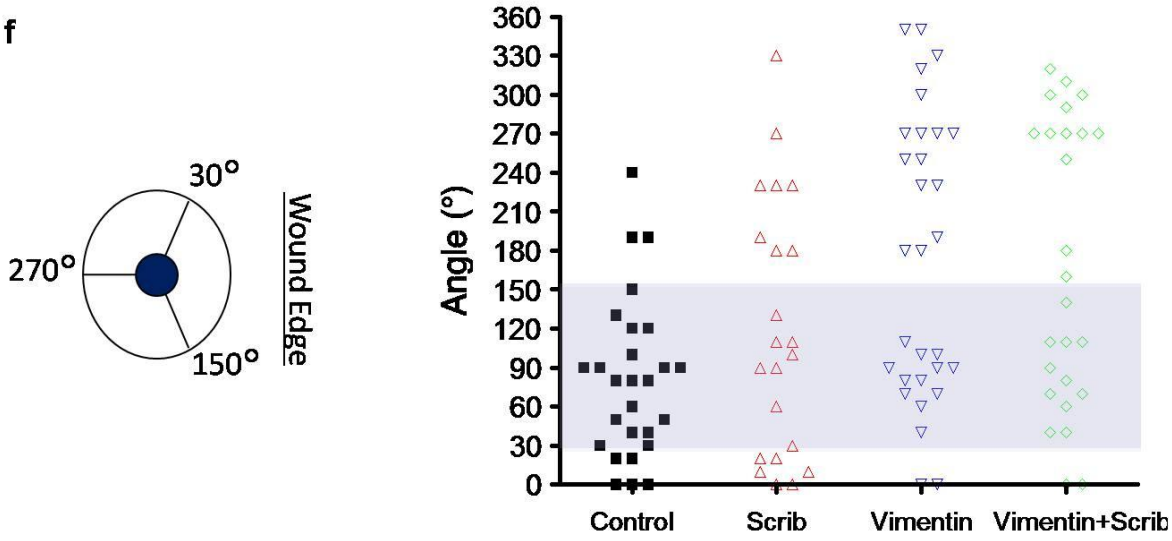


(**B**) Monolayers of cells treated with non-targeting (panel a), vimentin (panel b), Scrib (panel c) or Scrib and vimentin (panel d) siRNA were wounded and stained with an antibody to the cis-Golgi complex marker GM130 (red) and DAPI (blue) to label nuclei. The wound edge is demarcated with a white line. Panel e. Golgi complex orientation relative to the nucleus and the migration front was quantified as described in Materials and Methods. Shown is the fraction of leading edge cells with correctly polarized Golgi complexes that position in front of the nucleus, facing the wound. Results represent the means of 3 independent experiments, in which at least 400 cells where scored for each condition. Error bars represent SD of the mean. A red line indicates basal levels for a random orientation of 33%. Panel f. Schematic representation of Golgi complex orientation. The position of Golgi complex relative to the nucleus (blue) and wound edge was determined for ~30 individual cells for each siRNA treatment and plotted. The shaded sector from 30°-150° faces the wound edge and is bisected perpendicular to this edge. Note how the positioning of the Golgi complex of most control siRNA-treated cells falls within this sector, whereas that of cells where vimentin, Scrib or both had been silenced is randomized.

### 3.2.5 Silencing of Scrib and Vimentin Affects Wound Closure Rates Due to Randomized Cell Migration

In light of the cellular abnormalities observed in migrating Scrib and vimentin knock-down cells, we analyzed in more detail migration parameters, such as rate of wound closure, migration speed and tortuosity. While wounds in control cell monolayers closed over a 16 hr period, cells treated with Scrib and/or vimentin siRNA showed significantly slower wound closure rates (Fig. 3-8A), although this was less pronounced for cells treated with vimentin siRNA alone. To explore the parameters responsible for this reduced wound closure rate, we monitored velocity and tortuosity of cell movement at the wound edge using time-lapse microscopy and cell tracking. In contrast to control cells, which migrated unidirectionally towards the wound as a cohesive sheet, knock-down cells displayed a random and uncoordinated movement (Movies 1-4). No significant differences in velocity of migration could be established for the different knock-down cells (data not shown). We therefore analyzed the straightness of migration, which can be quantitatively assessed in terms of tortuosity, with a straight track having a value of 1 and a more tortuous or twisted route a value >1. Control cells migrated with a mean tortuosity of 1.1, whereas cells treated with siRNAs to Scrib, vimentin or both, recorded tortuosities of 2.1, 1.5 and 2.2, respectively (Fig. 3-8B). The differences in tortuosity thus correlate well with the reduced wound closure rates for cells depleted of Scrib and Scrib-vimentin, and the less pronounced effect in cells treated with vimentin siRNA only (see above).

Taken together, these data thus demonstrate similar requirements for Scrib and vimentin in directed migration of MDCK cells.

**A**

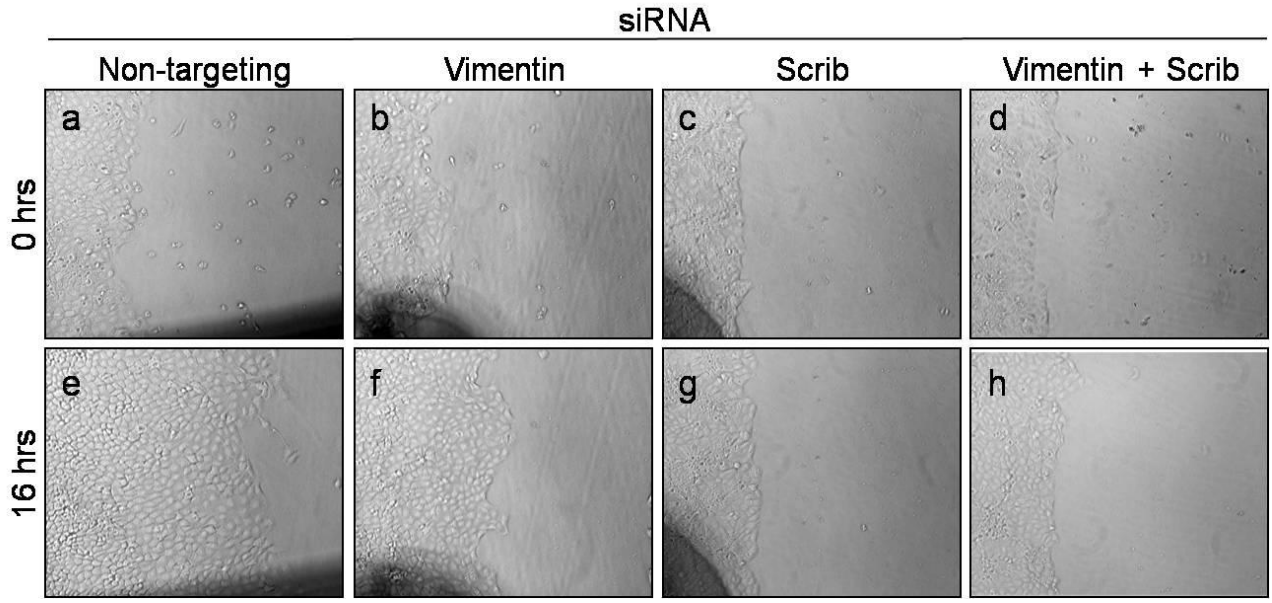


**Figure 3-8. Slower wound closure rates due to a less directional migration of MDCK cells treated with Scrib or vimentin siRNA.** (**A**) Wound closure. Monolayers of cells treated with non-targeting (panels a and e), vimentin (panels b and f), Scrib (panels c and g) or Scrib and vimentin (panels d and h) siRNA were wounded and allowed to migrate for 16 hrs. Images were taken after wounding (0 hrs, panels a-d) or 16 hrs of migration (panels e-h). The black marks at the bottom of the panels allow alignment of the wounds. Panels shown are representative of at least 3 independent experiments.

**B**

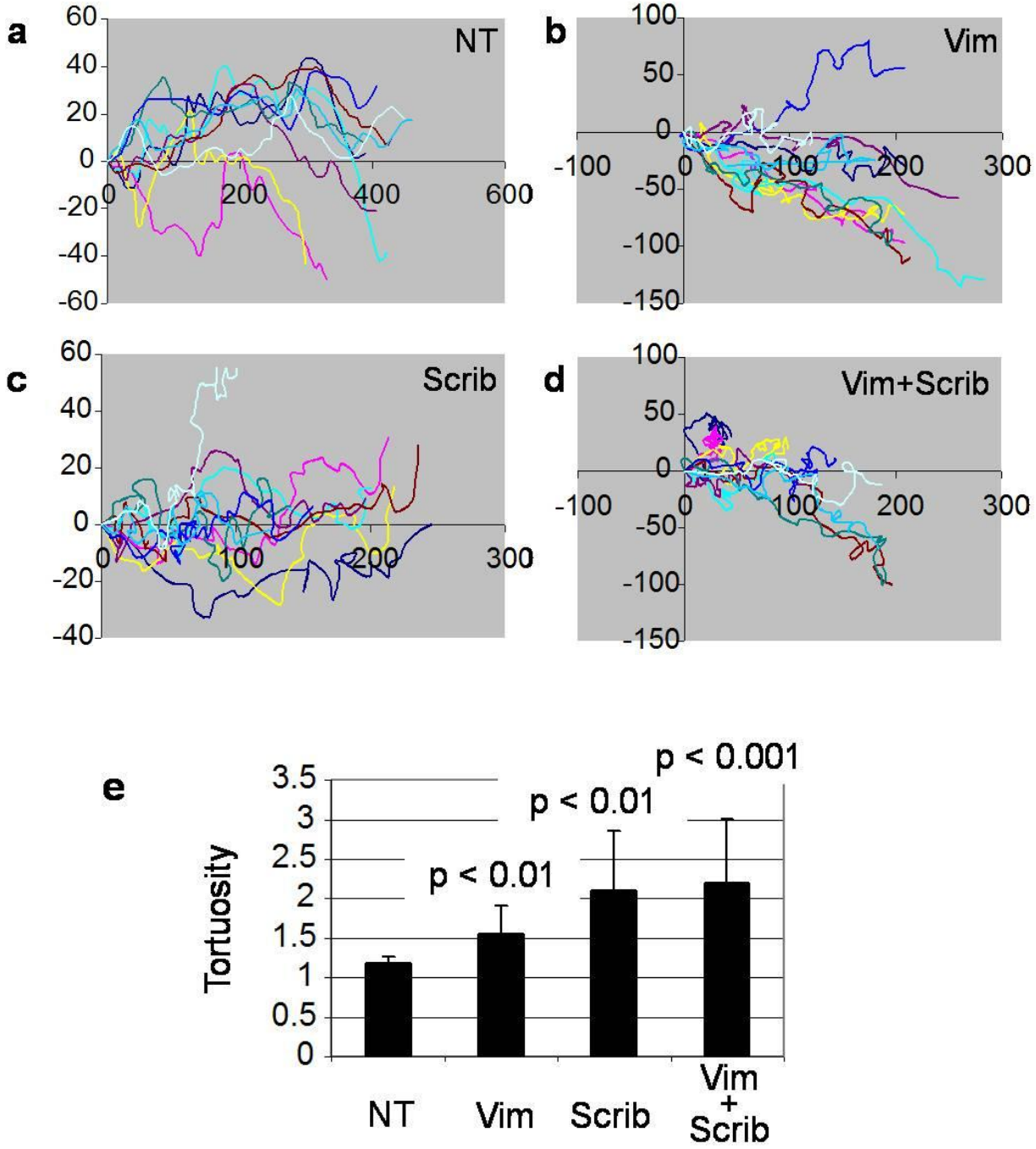


(**B**) Quantification of cell migration directionality using live cell tracking. The X-Y graphs represent migration coordinates of 10 different cells at the wound edge treated with non-trageting (panel a), vimentin (panel b), Scrib (panel c) or vimentin and Scrib (panel d) siRNA, tracked over time 4 days after siRNA transfection. Start points for the different cells were adjusted to (0,0) coordinates. Results are representative of at least 3 independent experiments. Panel e. Tortuosity was scored for at least 30 individual cells for each siRNA treatment (n=3; $p$<0.01-0.001, Student's $t$-test). A value of 1 indicates linear movement. Error bars represent SD of the mean.

### 3.2.6 Scribble and Vimentin Are Required For Efficient Cell Aggregation

Altered cell morphology and directed migration of Scrib and vimentin knock-down cells suggested defects in cell-cell adhesion. This possibility was explored using a hanging drop cell aggregation assay (Redfield *et al.*, 1997; Kim *et al.*, 2000a). Control cells suspended in a hanging drop for 24 hrs formed dense cell aggregates (Fig. 3-9A). In contrast, cells treated with Scrib or vimentin siRNA, or both, only showed sparse aggregates. If aggregates from the hanging drop were transferred onto cover slips, control cells adhered to the substratum, spread and after 24 hrs formed cobblestone-like cell islands typical for MDCK cells (Fig. 3-9B). Knock-down cells on the other hand failed to remain tightly organized following attachment to the cover slip and spreading.

Thus, Scrib and vimentin are required for normal cell-cell adhesion and reduced levels in these proteins could explain the loss of directed migration of knock-down cell monolayers.

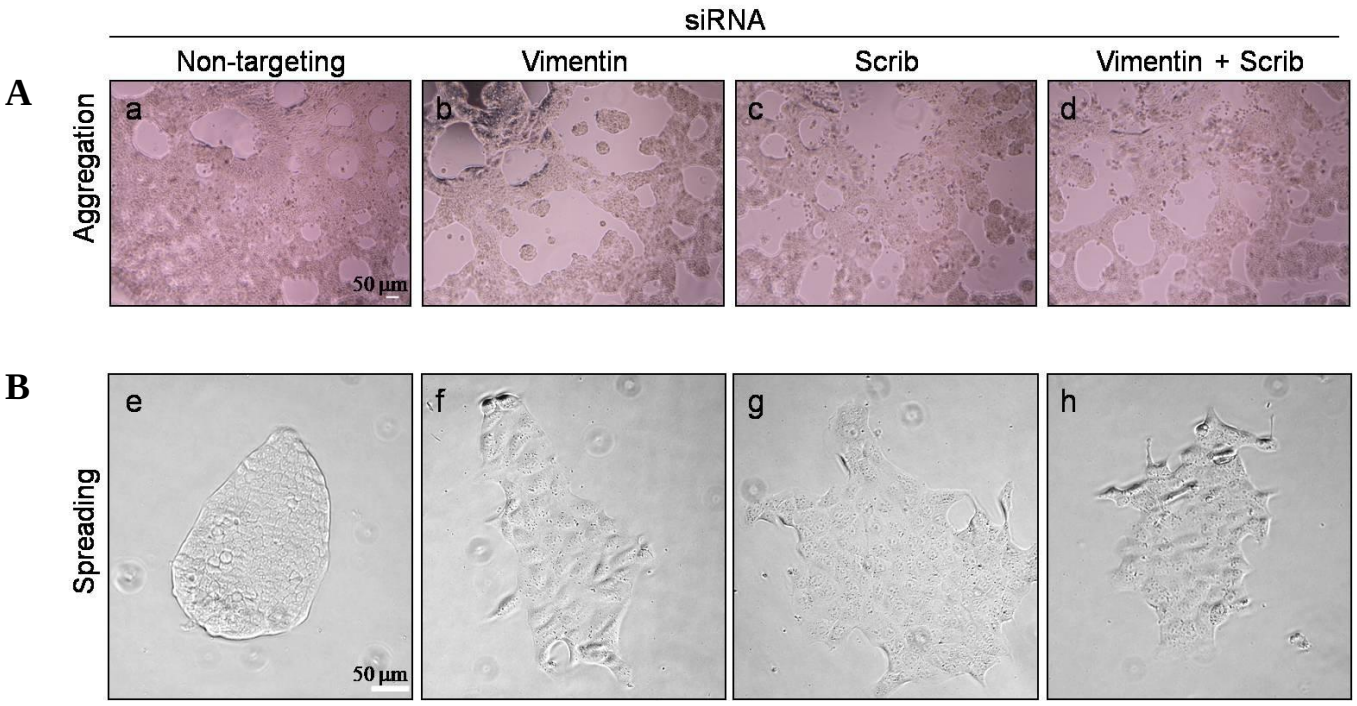


**Figure 3-9. Silencing of Scrib and vimentin expression affects cell-cell aggregation and spreading.** (**A**) Cell aggregation. MDCK cells treated with non-targeting (panel a and e), vimentin (panels b and f), Scrib (panels c and g) or Scrib and vimentin (panels d and h) siRNA were allowed to aggregate in a hanging drop and photographed (panels a-d). (**B**) Cell spreading. Cell aggregates were transferred from the hanging drop onto cover slips and allowed to adhere and spread (panels e-h). Note how cells treated with specific siRNAs form less compact aggregates (panels b-d) and show enhanced spreading (panels f-h) when compared to control cells (panels a and e, respectively). Assays were carried out 4 days after siRNA transfection.

### 3.2.7 Vimentin Stabilizes Scrib by Protecting It from Proteasomal Degradation

The phenotypic convergence of silencing Scrib and vimentin inferred a functional relationship for the interaction of the two proteins. To gain an insight into possible mechanisms underlying this function, we examined possible effects of Scrib or vimentin depletion on vimentin or Scrib protein levels, respectively. Silencing of Scrib did not alter vimentin or keratin 18 expression levels (Fig. 3-6B) or intermediate filament organization (data not shown). Interestingly, however, endogenous Scrib levels were significantly reduced following knock-down of vimentin in both sparse and confluent MDCK cell cultures (Fig. 3-6B and Fig. 3-10A). Quantification of 3 independent experiments showed a correlation between the extent of vimentin silencing and the degree of endogenous Scrib protein decrease (Fig. 3-10B). Silencing of keratin 18 also resulted in reduced Scrib protein levels, and similar effects were observed in other cell lines (Fig. 3-10C). Interestingly, Erbin, a protein related to Scrib (Borg *et al.*, 2000; Santoni *et al.*, 2002), was upregulated in vimentin siRNA treated cells, suggesting a possible compensatory mechanism (Fig. 3-10D).

**A**

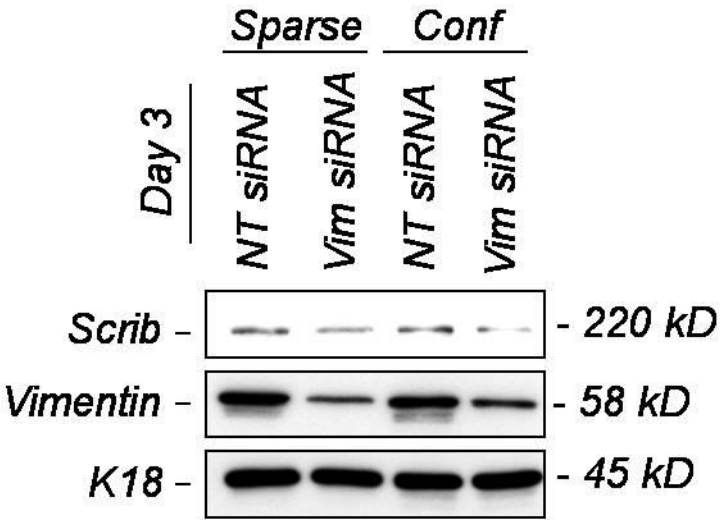


**B**

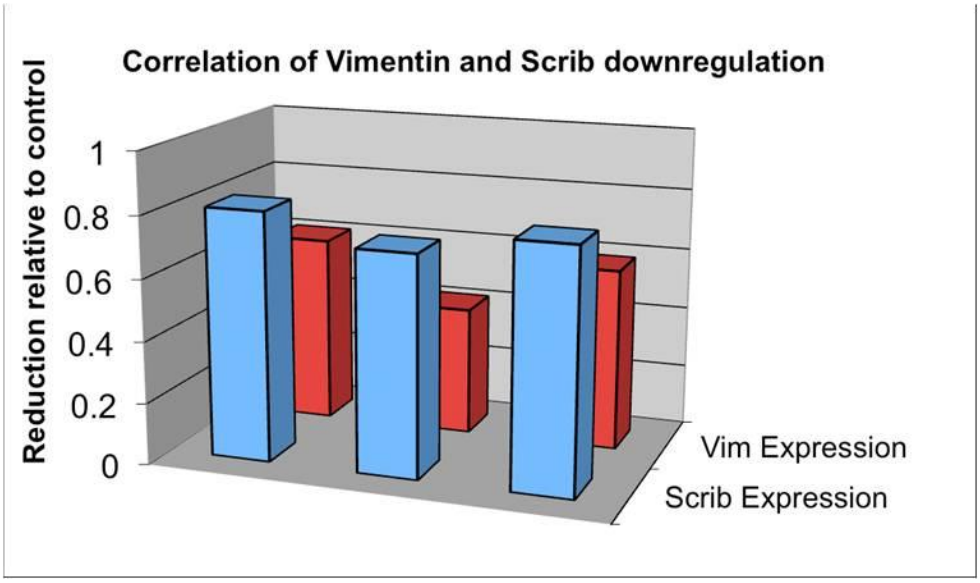


**Figure 3-10. Proteasome-dependent degradation of Scrib is inhibited by its interaction with vimentin.** (**A**) Vimentin expression in MDCK cells was silenced using siRNA over 3 days. Cells were subsequently re-seeded to sparse and confluent cultures and Scrib protein levels were monitored by Western blot analysis on Day 4. K18 was detected to check for equal cell lysate loading. (**B**) Quantitative representation of Scrib downregulation relative to levels of vimentin silencing in MDCK cells.

**C**

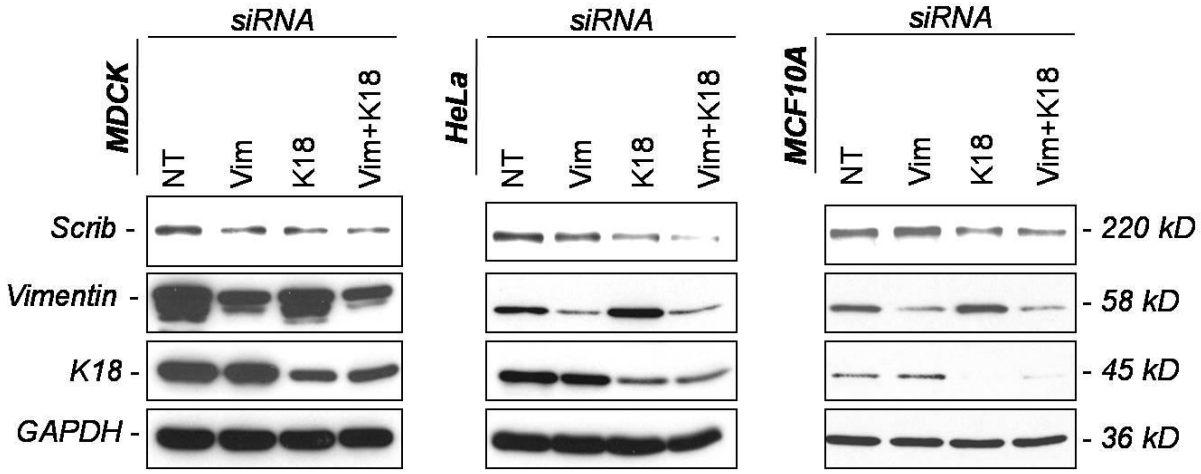


**D**

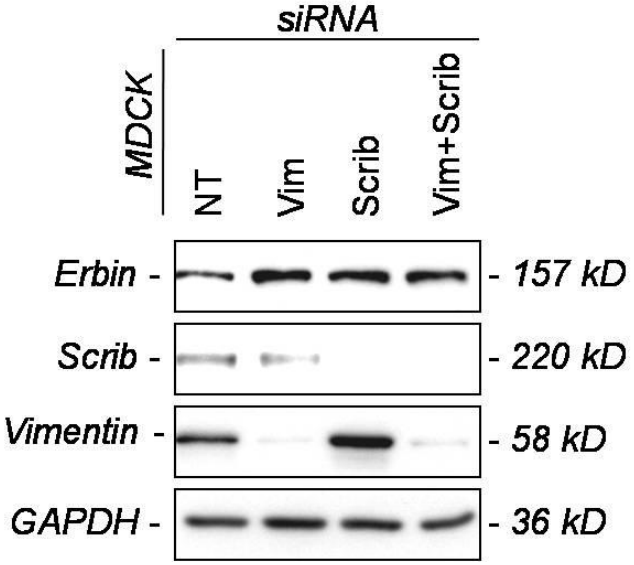


(**C**) Scrib turnover in vimentin and/or keratin 18 depleted cells. MDCK, HeLa and MCF10A cells were treated with siRNA for 4 days and Scrib and IF expression were analyzed by Western blot. GAPDH served as a control for equal lysate input. (**D**) MDCK expression of vimentin, Scrib or both was silenced and protein levels of Erbin, Scrib and vimentin were monitored by Western blot analysis. Note the silencing of vimentin or Scrib leads to an upregulation of Erbin, possibly as a compensatory mechanism. GAPDH was detected to check for equal cell lysate loading.

A similar but more dramatic effect was observed for cells overexpressing Scrib. Both EGFP-hScrib and EGFP-hScrib PDZ, but not EGFP-hScrib LRR which does not associate with vimentin, were significantly reduced in vimentin siRNA treated MDCK cells as evidenced by Western blot (Fig. 3-10E) or immunofluorescence microscopy (Fig. 3-10F). Conversely, overexpression in MDCK cells of vimentin, keratin 8 (K8) or keratin 18 (K18) resulted in a significant increase in endogenous Scrib protein levels (Fig. 3-10G).

**E**

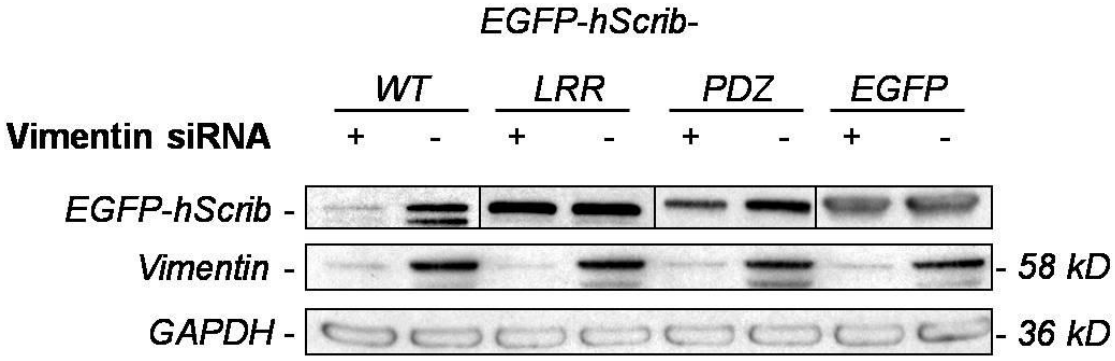


**F**

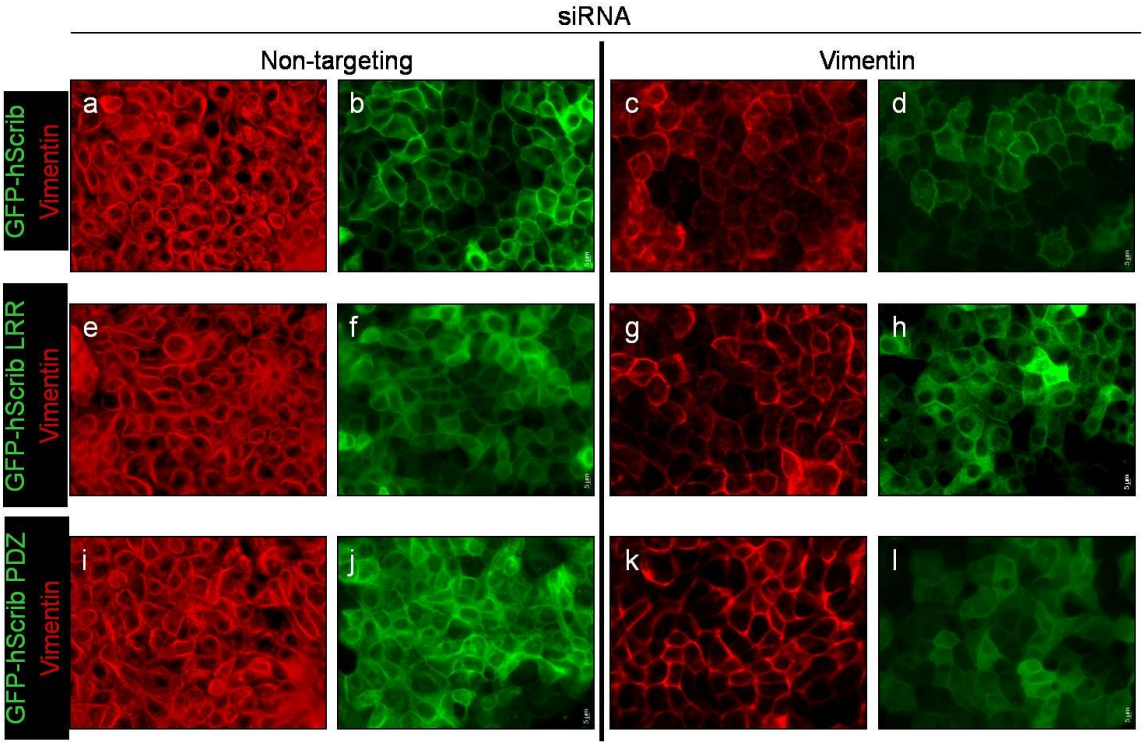

**G**

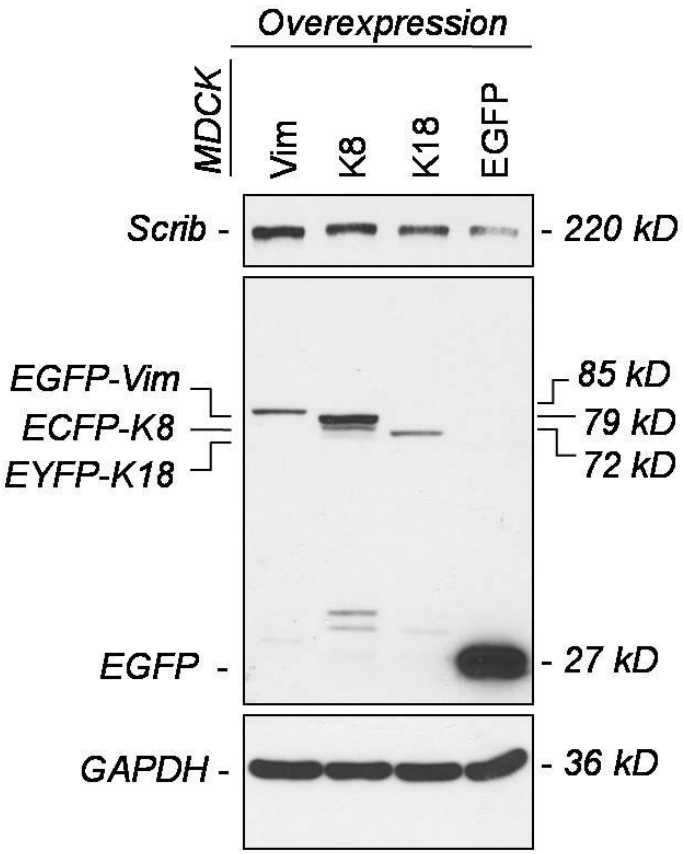


(**E**) MDCK cells expressing EGFP-hScrib WT (~250 kDa), LRR (~130 kDa), PDZ (~150 kDa) or, as a control, EGFP alone were treated with vimentin (+) or non-targeting (-) siRNA. hScrib expression was analyzed by Western blot using antibodies to GFP. GAPDH served as a control for equal lysate input. (**F**) MDCK cells expressing EGFP-hScrib WT (panels a-d), LRR (panels e-h) or PDZ (panels i-l) were treated with non-targeting (panels a, b, e, f, i and j) or vimentin (panels c, d, g, h, k and l) siRNA and Scrib (panels b, f, j, d, h and l, green color) and vimentin (panels a, e, i, c, g and k, red color) expression was visualized by fluorescence microscopy. (**G**) MDCK cells exogenously expressing EGFP-vimentin, ECFP-K8, EYFP-K18 or EGFP alone were analyzed by Western blot for expression of Scrib. GAPDH served as a control for equal lysate input.

Scrib has been reported to undergo E6AP ubiquitin ligase and proteasome-mediated degradation in high-risk HPV infected epithelial cells (Nakagawa and Huibregtse, 2000; Massimi *et al.*, 2007). We therefore tested if proteasomal degradation accounted for the reduction of Scrib protein levels in vimentin knock-down cells. Indeed, in vimentin knock-down cells treated with a proteasome inhibitor, EGFP-hScrib protein remained at similar levels as in control siRNA treated cells (Fig. 3-10H and I). Furthermore, although less pronounced, endogenous Scrib protein levels were also reduced in vimentin deficient MDCK cells and this decrease was blocked in the presence of the proteasome inhibitor (Fig. 3-10J). To further corroborate the role of proteasomal degradation of Scrib in vimentin knock-down cells, we immunoprecipitated hScrib-EGFP from control or vimentin knock-down MDCK cells and analyzed whether it was ubiquitinated. Indeed, ubiquitinated Scrib was readily detected in vimentin siRNA treated cells (Fig. 3-10K). Furthermore, in the presence of proteasome inhibitor, ubiquitination of Scrib was also observed in control cells and this was enhanced for vimentin siRNA treated cells.

Taken together, these data therefore reveal a role for vimentin in stabilizing Scrib protein by protecting it from proteasomal degradation.

**H**

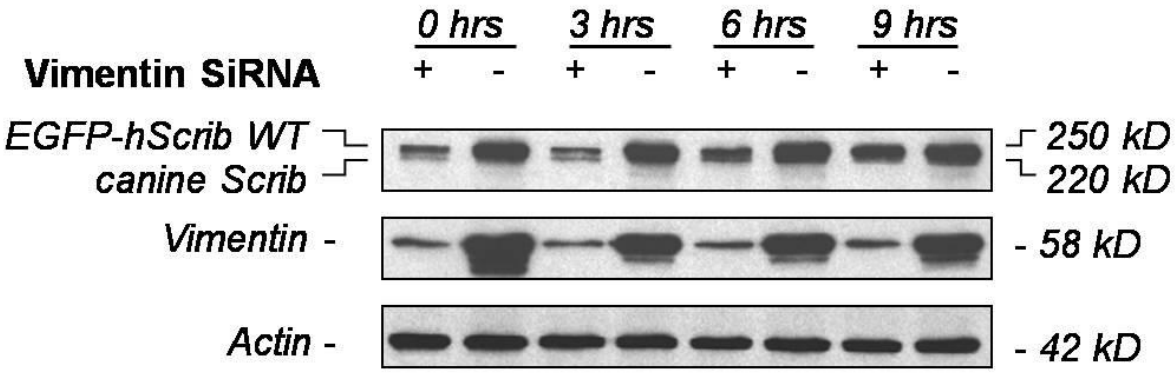
0 hrs
3 hrs
6 hrs
9 hrs
Vimentin SiRNA
+ - + - + - + -
EGFP-hScrib WT
canine Scrib
250 kD
220 kD
Vimentin -
- 58 kD
Actin -
- 42 kD

**I**

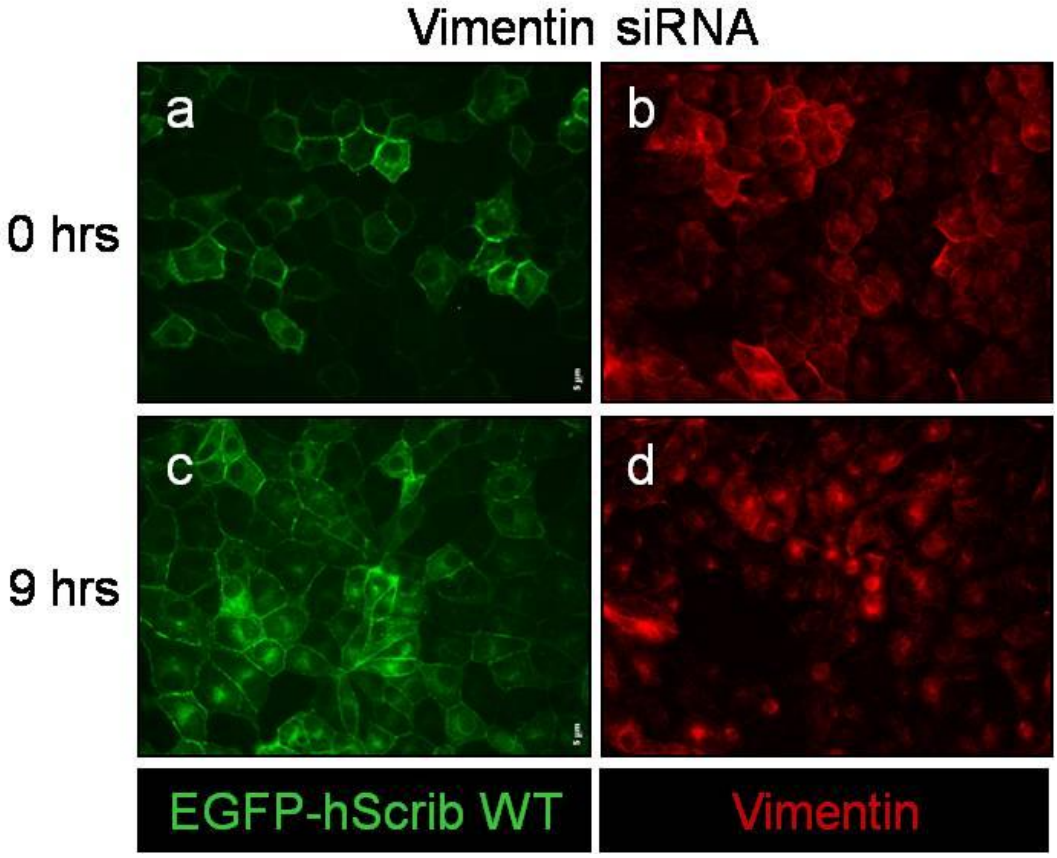
Vimentin siRNA
a
b
0 hrs
c
d
9 hrs
EGFP-hScrib WT
Vimentin

**J**

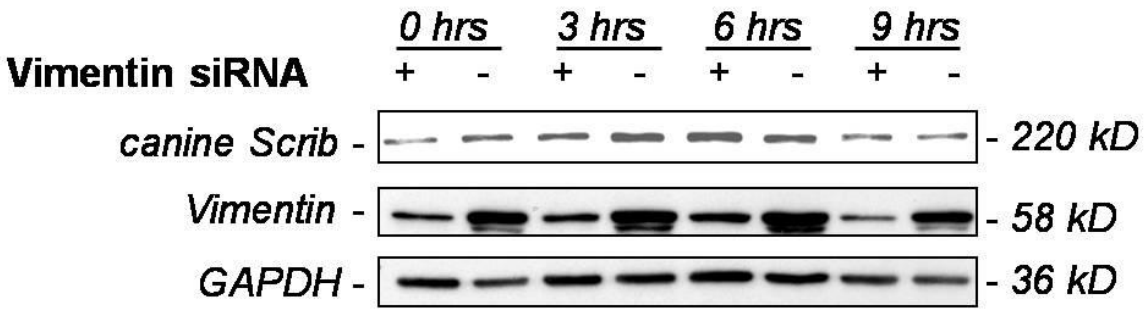


(**H**, **I** and **J**) Effect of a proteasome inhibitor on Scrib turnover. (**H**) Western blot. MDCK cells expressing EGFP-hScrib WT, were treated with vimentin (+) or non-targeting (-) siRNA in the presence of a proteasome inhibitor for 0, 3, 6 or 9 hrs. Scrib and vimentin expression levels were then analyzed by Western blot. Note how in vimentin depleted cells, EGFP-hScrib (250 kDa) as well as endogenous Scrib (220 kDa) degradation is blocked by the proteasome inhibitor (see also **J**, below). Actin served as a control for equal lysate input. (**I**) Immunofluorescence microscopy. MDCK cells expressing EGFP-hScrib WT were treated with vimentin siRNA and a proteasome inhibitor for 0 hrs (panels a and b) or 9 hrs (panels c and d) and Scrib (panels a and c, green color) and vimentin (panels b and d, red color) expression was visualized by fluorescence microscopy. (**J**) Western blot of endogenous Scrib. MDCK cells were treated with vimentin (+) or non-targeting (-) siRNA in the presence of a proteasome inhibitor for 0, 3, 6 or 9 hrs. Endogenous levels of canine Scrib and vimentin were then analyzed by Western blot. GAPDH served as a control for equal lysate input.

**K**

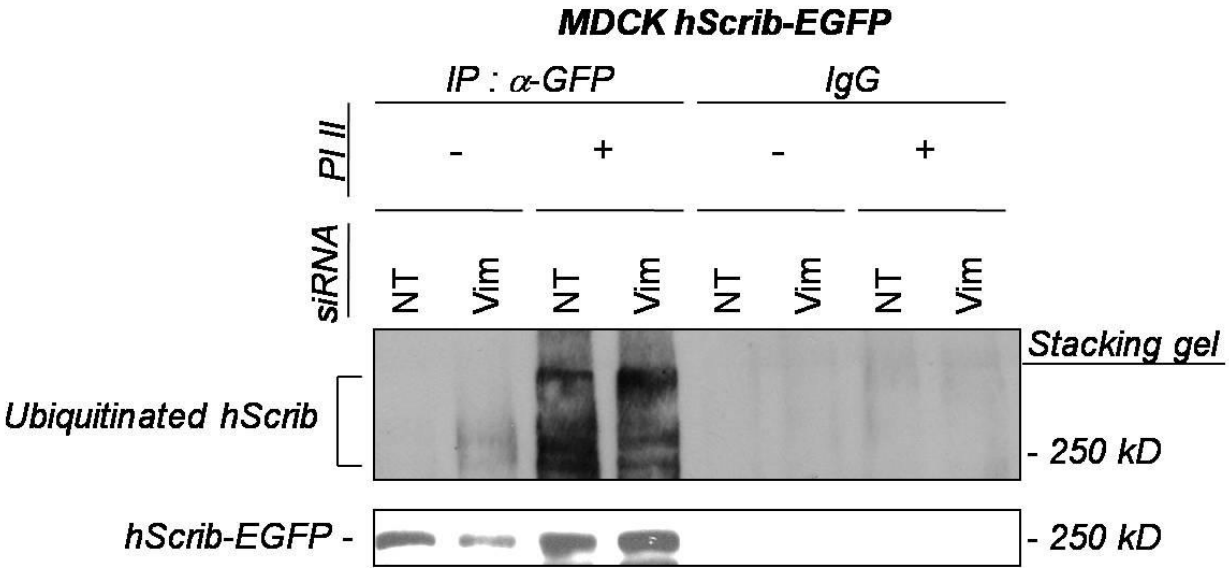


**(K)** hScrib-EGFP of non-targeting or vimentin SiRNA treated cells in the 9 hr presence (+) or absence (-) of proteasome inhibitor was immunoprecipitated and ubiquitinated hScrib detected by Western blot. Normal IgG served as a negative control.

## 3.3 Discussion

Since its discovery as a tumor suppressor in *Drosophila*, Scrib has been attributed to play roles in an array of polarity-related processes in morphologically and functionally different cells such as epithelial, neuronal and T-cells. Recently, the function of mammalian Scrib has been implicated in cell-cell adhesion and polarized migration in various cell types. Similarly, IFs like vimentin and keratins are known to play non-mechanical roles in protein trafficking and signaling, which in turn influences cellular processes like cell adhesion and polarization. Here we report the identification and functional characterization of a Scrib and IF interaction. We show that Scrib can colocalize with IFs and bind the IF components vimentin and keratin 18. Silencing of Scrib, vimentin, or both, affects different cellular functions associated with epithelial polarization, including anterior-posterior cell polarization, wound-healing, directed migration and formation of cell aggregates. In the absence of vimentin, Scrib is subjected to increased proteasomal degradation, implicating that the interaction with the IF cytoskeleton is important to stabilize Scrib proteins levels required for directed migration and cell-cell adhesion. Although we provide evidence based on colocalization and coprecipitation experiments to support an interaction between Scrib and keratin 18, the biochemical and functional details of its association with keratin IFs will require additional work. The following discussion will thus focus on the role of vimentin in Scrib function.

In MDCK cells, the filamentous localization of exogenous EGFP-hScrib is most prominent in sparse cell cultures, where Scrib shows an extensive filamentous localization. However, this is also observed, albeit to a lesser extent, in confluent cultures

when Scrib predominantly localizes to the plasma membrane. The filamentous labeling of Scrib partially colocalizes with vimentin and keratin 18 staining of IFs, but not with the actin or microtubule cytoskeleton. In addition to the filamentous labeling, Scrib and vimentin often accumulate in a perinuclear region of the cell from where IFs appear to emanate. The nature of this perinuclear structure is not known. Since Scrib undergoes proteasomal degradation ((Nakagawa and Huibregtse, 2000; Massimi *et al.*, 2007) and this paper), this structure could represent the aggresome, which forms when the degradative capacity of the proteasome is exceeded and is associated with the MTOC and encaged by vimentin (Johnston *et al.*, 1998). Although less pronounced, endogenous Scrib can also be detected on IFs, where it is found as punctate structures that line up along vimentin or keratin 18 positive filaments, in particular in proximity to the cell periphery. Interestingly, during establishment of cell-cell contacts and apical-basal cell polarization, exogenous EGFP-hScrib redistributes from a predominant filamentous to a mainly plasma membrane localization. This redistribution is observed both in cells grown on glass coverslips and polarized monolayers grown on permeable supports. On coverslips, hScrib is often concentrated in the vicinity of the plasma membrane, where there is partial overlap with IFs. In fully polarized MDCK cell monolayers, Scrib is found along the length of the lateral membrane, whereas vimentin, as with keratins, accumulates on the apical-most end of the lateral membrane (Oriolo *et al.*, 2007), where it shows minimal overlap with hScrib. The mechanism by which hScrib redistributes during establishment of cell-cell contact is not known, but live cell video microscopy provided no evidence for motility of EGFP-hScrib along IFs (data not shown).

Both exogenously expressed and endogenous Scrib binds to vimentin, both in sparse and confluent MDCK cell cultures. An association of Scrib with vimentin is also observed in several other cell lines, including MCF10A, HeLa and COS-1. Since *in vitro* translated Scrib specifically binds purified vimentin, the interaction is likely direct. Scrib was found to associate with both non-polymerized and polymerized vimentin. However, it is unclear if Scrib interacts with vimentin monomers, since non-polymerized purified vimentin generally contains low molecular oligomers (Herrmann and Aebi, 2004). The N-terminal part of Scrib containing the LRR domain shows little if any binding to vimentin or K18. In contrast, the C-terminal region containing the four PDZ domains binds vimentin and K18, albeit less efficiently than full-length Scrib. A similar behaviour was observed for ZO-2, which, like vimentin, binds to the PDZ domains of Scrib (Metais *et al.*, 2005) and may reflect a role for the N-terminus on the conformation or accessibility of the PDZ domains. In accordance with the binding data, only constructs containing the PDZ domains showed filamentous localization. Analysis of individual PDZ domains revealed an efficient binding of vimentin to PDZ3, less efficient associations with PDZ1 and PDZ2, and no detectable interaction with PDZ4, consistent with an interaction with the PDZ domains themselves as opposed to intervening sequences. Since vimentin does not encode a typical C-terminal PDZ-binding motif, the association is likely mediated by an internal loop in vimentin. Such a mode of interaction is not uncommon and has been established for several PDZ-domain proteins, including ZO-1 (Harris and Lim, 2001; Utepbergenov *et al.*, 2006). Moreover, TBEV NS5 has been reported to bind PDZ4 of Scrib via an internal binding site (Werme *et al.*, 2008).

Several lines of evidence support the notion that the interaction with IFs stabilizes Scrib by protecting it from proteasomal degradation. First, silencing of vimentin or keratin 18 expression leads to reduced Scrib protein levels. Second, the extent of the decrease in Scrib protein levels correlates with the extent of vimentin knock-down. This stabilizing function of vimentin is observed both in sparse and confluent MDCK cells, as well as in other cell lines. Third, only Scrib constructs that contain the PDZ domains are affected if vimentin is depleted, showing that the interaction with vimentin is important for protection from degradation. Fourth, Scrib protein levels remain high in vimentin siRNA treated cells in the presence of a proteasome inhibitor. Fifth, Scrib proteins levels are increased in cells overexpressing vimentin or keratin 18. Finally, in vimentin siRNA treated cells, ubiquitinated Scrib can be detected and its levels are increased in control and vimentin siRNA treated cells in the presence of proteasome inhibitor. Importantly, both overexpressed as well as endogenous Scrib show an enhanced turnover if vimentin expression is silenced. In MDCK, HeLa and MCF10A cells, the simultaneous silencing of vimentin and keratin 18 lead to a larger reduction in Scrib levels, consistent with a contribution of both types of IFs in stabilizing Scrib.

If endogenous Scrib protein levels are reduced in cells treated with vimentin siRNA, these cells present a similar phenotype as observed in Scrib knock-down cells. Indeed, several well-established effects linked to reduced Scrib protein levels were phenocopied in cells where vimentin was silenced. The role of Scrib in anterior-posterior cell polarization during migration has been extensively characterized. In wound healing assays, MDCK cells migrate as a sheet to close the wound. Cells at the leading edge polarize their MTOC and Golgi apparatus in the plane of migration (Kupfer *et al.*, 1982).

As previously reported (Osmani *et al.*, 2006; Dow *et al.*, 2007), Scrib knock-down abolished the reorientation of the Golgi complex, and this was also observed in cells treated with vimentin siRNA. Furthermore, wound closure was slower in both Scrib and vimentin knock-down cells. Live imaging and computation of tortuosity indexes showed a more randomized migration for both knock-down cells. Loss of directionality likely accounts for the slower wound closure since velocity of migration was not significantly affected (data not shown). The slower closure of wounded Scrib knock-down cell monolayers in our study contrasts with an earlier report also using MDCK cells (Qin *et al.*, 2005), but is consistent with the delayed migration of MCF10A cells upon Scrib silencing and the delayed wound closure in mice lacking Scrib (Dow *et al.*, 2007). In agreement with (Qin *et al.*, 2005), we observed a defect in cell-cell aggregation of Scrib knock-down cells and this was also the case for cells exposed to vimentin siRNA. The concomitant silencing of both Scrib and vimentin showed no synergistic effect on polarization, directionality of migration or aggregation, consistent with the notion that the effect of suppressing vimentin expression reflects to a significant extent the concomitant reduction in Scrib protein levels below a critical threshold.

The phenotypic convergence of Scrib and vimentin silencing in MDCK is not surprising considering the effect of vimentin on Scrib protein stability. This relationship with Scrib is also reflected in the similar function of vimentin in cell migration and adhesion that have been reported previously. This function is particularly exemplified in the event of epithelial-mesenchymal transition (EMT). EMT is the process in which polarized immotile epithelial cells are converted to motile mesenchymal cells and is crucial in metazoan embryonic development. For example during gastrulation, under

controlled EMT, primitive epithelial cells lose their distinct apical-basal polarity and cell-cell adhesive properties and acquire non-epithelial mesenchymal properties by the change of expression, localization and activity of various proteins related to epithelial or mesenchymal cell characteristics. This allows single cells to break free from the epithelium, invade the ECM, migrate and subsequently populate areas in the embryo and develop into the germ layers. These motile and invasive properties are recapitulated in metastatic carcinomas and not surprisingly, the loss of regulated control of EMT can have pathological effects and has been associated with tumor progression (Thiery and Sleeman, 2006). During EMT, with the gain of mesenchymal characteristics, increased cell motility is correlated with the upregulation of vimentin expression (Lee *et al.*, 2006). This correlation has been aptly demonstrated in migrating epithelial MCF10A cells where vimentin was transiently and exclusively expressed in actively migrating cells at the wound edge where it positively regulates migration (Gilles *et al.*, 1999). Furthermore fibroblasts of vimentin null mice exhibited defective wound healing due to reduced cell migration (Eckes *et al.*, 1998; Eckes *et al.*, 2000) and in a pathological context, expression of vimentin promoted cell migration and invasion in breast, colon and prostate carcinomas (McInroy and Maatta, 2007; Zhao *et al.*, 2008). The function of vimentin in cell migration and adhesion has also been reported in the transendothelial adhesion and extravasation of leukocytes. Here, the reorganization and polarization of vimentin in both the receiving endothelial sheets and migrating lymphocytes positively regulate the protein levels and defined surface expression of CAMs and integrins on the respective cell types. Incidentally, vimentin is polarized in the uropod of lymphocytes similarly to Scrib in T-cells (Ludford-Menting *et al.*, 2005; Nieminen *et al.*, 2006).

In conclusion, we show that Scrib associates with intermediate filaments and that this association stabilizes Scrib by sequestering it from proteasomal degradation. Although this presents an intriguing finding in Scrib and vimentin function, the concept of protein sequestration or stabilization by IFs is by no means unique and has been observed in several studies as discussed earlier. Vimentin sequesters SNAP23 and creates a mobilizable reservoir of SNAP23 for t-SNARE function (Faigle *et al.*, 2000). Other proteins like 14-3-3 and TRADD are also sequestered by either vimentin and/or keratins and regulate cellular processes like cell growth and apoptosis (Kim and Coulombe, 2007). Furthermore, activated MAPK is protected from phosphatases and transported by vimentin during nerve injury (Perlson *et al.*, 2005). Likewise, Scrib is also known to be sequestered by Tax protein of HTLV-1 in T-cells (Arpin-Andre and Mesnard, 2007). Indeed IF interaction with polarized proteins and their recruitment or stabilization during the polarization of epithelial cells has been recently documented. The apical brush boarder polarization of scaffold protein ezrin in intestinal epithelial cells is dependent on its transient interaction with keratins. Dormant ezrin is recruited in a keratin-dependent manner to the subapical membrane of non-polarized undifferentiated cells where they can be activated. Upon activation, ezrin is released from keratin and subsequently localizes to the actin-based apical membrane scaffold of polarized differentiated cells (Wald *et al.*, 2005). Most recently, keratin IFs have also been reported to interact with the polarity regulatory protein Albatross. The mutually-dependent apicolateral localization and interaction of Albatross and Par3 allows them to function in lateral membrane junctional complex formation. The depletion of these two polarity regulators results in the loss of TJ, AJ and DS, apical mislocalization of E-cadherin and desmoglein, disorganization of

the cortical actin ring and the disruption of cell-cell adhesion. Key to the function of Albatross is its association with keratins. As with Scrib, these IFs stabilize the protein levels of Albatross and also mediate its localization to the lateral domain (Sugimoto *et al.*, 2008).

Based on our findings and that of other investigations, we propose a model that explains our observations. The interaction and stabilizing effect of vimentin on Scrib occurs when there is remodeling of the plasma membrane. This can be demonstrated during cellular processes like EMT, migration and cell-cell contact maturation where junctional and polarity proteins are in dynamic flux (Matsuda *et al.*, 2004; Drees *et al.*, 2005; Thiery and Sleeman, 2006). Furthermore, junctional proteins are also known to engage in dynamic remodeling even in confluent steady state epithelial monolayers (Shen *et al.*, 2008). This flux creates both a soluble cytoplasmic and an insoluble membrane pool of Scrib. It is the soluble Scrib pool that has been reported to be degraded in HPV E6-containing epithelial cells via the proteasome, while the insoluble pool remained largely protected (Massimi *et al.*, 2004). We hypothesize that part of this soluble Scrib pool can interact with the IF networks, thus behaving like an insoluble membrane pool and therefore protected from proteasome-mediated degradation targeted by a cellular protein acting much like HPV E6. Although no such regulatory protein has been discovered, this might be part of the machinery involved in the natural homeostatic turnover of Scrib. Accordingly, disrupting IFs may lead to an increased pool of free Scrib, which is subject to proteasomal degradation and thus decreasing Scrib protein levels. Conversely, the overexpression of IF creates supernumerary IF networks that can enlarge the protected Scrib reservoir and thus manifests as increased Scrib protein levels.

This enlargement of IF protected proteins has been observed in keratin-ezrin and keratin-Albatross interactions (Wald *et al.*, 2005; Sugimoto *et al.*, 2008). The protected Scrib may represent a reservoir which can be mobilized to carry out its functions much like with the vimentin-SNAP23 interaction (Faigle *et al.*, 2000). This hypothesis would be consistent with the observation that silencing of vimentin affects the known functions of Scrib in cell polarization, directed migration and cell-cell adhesion.

# Chapter 4: Concluding Remarks

Apical-basal, planar and anterior-posterior polarity represent the three forms of epithelial cell polarization and are essential for the proper progress of cellular processes like junctional assembly and directed cell migration. The cell polarity regulator Scrib plays crucial roles in these processes (Dow and Humbert, 2007).

Although Scrib function in apical-basal epithelial cell polarization has been well documented, its placement in the precise sequence of hierarchical events leading to this polarization and junctional assembly is poorly elucidated. The discovery of Scrib interaction with TJ proteins ZO-2 and ZO-3 present a further understanding of this hierarchical assembly of polarity-related proteins. The possible role of these ZO proteins in the recruitment of Scrib to the lateral membrane in non-polarized epithelial cells emphasizes the importance of controlled spatio-temporal activity of polarity regulators in cell polarization.

The discovery of vimentin IF interaction with and stabilization of Scrib introduces a novel angle to the regulation of Scrib polarity function. The notion of IFs as static cellular mechanical supports has been replaced in recent years with a paradigm where IFs also play non-mechanical functions in cellular processes including epithelial polarization, cell adhesion and migration (Kim and Coulombe, 2007). The phenotypic convergence of Scrib and vimentin depletion suggests a relationship of vimentin and Scrib in a single regulatory pathway in these processes, with vimentin acting upstream of Scrib by protecting it from degradation and in effect, sustaining the amount of Scrib to a critical threshold in order to actuate its functions. This presents a better understanding of the

Scrib mechanistic pathway and gives an insight to the little known upstream events that regulate Scrib function.

Although we have detected an interaction and co-localization of Scrib with both vimentin and keratin in MDCK cell cultures, the functional significance of these associations might not be reflected fully since normally, keratin and vimentin are exclusively expressed in epithelial and mesenchymal cells respectively. It is only in cultured immortalized epithelial cell lines that both IFs are co-expressed as distinct filamentous networks (Virtanen *et al.*, 1981). It therefore will be interesting to investigate Scrib-IF interactions in a more relevant physiological model which displays cell-specific expression of either vimentin or keratins only. With the focus on Scrib-vimentin interaction, we are furthering our study of this association and its functional aspects in mesenchymal cells such as endothelial and T-cells. The T-cell model will be especially relevant since both Scrib and vimentin have been attributed functions in T-cell polarity and migration (Ludford-Menting *et al.*, 2005; Nieminen *et al.*, 2006).

# Chapter 5: Materials and Methods

## 5.1 Plasmid Constructs

### 5.1.1 ZO Constructs

All ZO constructs were generated by PCR amplification using their respective full-length ZO cDNA constructs as a template. Full-length human ZO-1 (NCBI Accession NM_003257) in pLNCX was previously described (Reichert *et al.*, 2000) and full-length canine ZO-2 (NCBI Accession NM_001003204) and ZO-3 (NCBI Accession NM_001003202) cloned into pBluescript II SK (+) were kindly provided by Manuela Reichert. ZO-1 GA (amino acids 644-895), ZO-2 GA (amino acids 714-946), ZO-2 P (amino acids 947-1174), ZO-3 SGC (amino acids 468-898), ZO-3 SH3 (amino acids 468-606) and ZO-3 GC (amino acids 607-898) were inserted into pGBKT7 (Clontech Laboratories, Inc). ZO-1 P (amino acids 896-1748), ZO-2 P (amino acids 947-1174) and ZO-3 GC (amino acids 607-898) were cloned into pGEX-6p-1 (GE Healthcare). Full-length ZO-2 and ZO-3 were subcloned into N-terminal FLAG tagged pCDNA3 vector (Invitrogen).

### 5.1.2 Scrib Constructs

Full-length cDNA encoding human Scribble, hScrib WT (NCBI Accession NM_015356) cloned into N-terminal tagged pEGFP-C1 (BD Biosciences Clontech) was described earlier (Dow *et al.*, 2003). hScrib PDZ binding mutants were generated using overlapping primer pairs to amplify hScrib WT with substitutions at PDZ1 (R733E, L738E, G739H, I740E, S741A, I742E and G744H ), PDZ2 (R867E, L872E, G873H, F874E, S875A, I876E and G878H ), PDZ3 (R1009E, L1014E, G1015H, L1016E,

S1017A, I1018E and G1020H ) and PDZ4 (K1105E, L1111E, G1112H, I1113E, S1114A, I1115E and G1117H ) and cloned into pEGFP-C1. hScrib deletion constructs Δ Cter (amino acids 1-1194), LRR (amino acids 1-727), PDZ (amino acids 728-1630), 4PDZ (amino acids 728-1194) and Cter (amino acids 1195-1630) were also PCR amplified from hScrib WT template and inserted into pEGFP-C1. hScrib WT was also subcloned into C-terminal tagged pEGFP-N1. The mouse Scribble, mScrib WT construct was created by subcloning the cDNA clone mKIAA0147 (NCBI Accession AK122211), which encodes full-length mouse Scribble, into N-terminal HA tagged pCDNA3 vector (Invitrogen). Using mScrib WT as a template, mScrib LRR (amino acids 1-713) and PDZ (amino acids 714-1638) were PCR amplified and cloned into HA-pCDNA3. hScrib PDZ1, PDZ2, PDZ3 and PDZ4 cloned into pGEX-6p-2 (GE Healthcare) were gifts from Sachdev S. Sidhu (Department of Protein Engineering, Genentech, Inc, California, USA).

### 5.1.3 Intermediate Filament Constructs

EGFP-tagged rat vimentin and ECFP- and EYFP-tagged human keratin 8 and 18 cDNAs were generously provided by Ronald Liem (Department of Pathology and Cell Biology, Columbia University College of Physicians and Surgeons, New York, USA) and Rudolf Leube (Department of Anatomy, Johannes Gutenberg University, Mainz, Germany), respectively.

## 5.2 siRNA

Custom SMARTpool PLUS of four siRNAs directed against canine Scribble (Cat. Q-120233-00) based on EnsEMBL transcript ENSCAFT00000002152, vimentin (Cat. Q-120187-00) based on NCBI Accession XM_535175 and keratin 18 (Cat. Q-120323-00) based on NCBI Accession XM_534794, XM_854026 and XM_854071 were designed by and purchased from Thermo Fisher Scientific, Dharmacon RNAi Technologies. ON-TARGETplus SMARTpool of four SiRNAs directed against human vimentin (Cat. L-003551-00) based on NCBI Accession NM_003380 and keratin 18 (Cat. L-010604-00) based on NCBI Accession NM_199187 were also purchased from Dharmacon as was the si*Control* non-targetting SiRNA #1.

## 5.3 Yeast Two-Hybrid Screen

A yeast two-hybrid screen for novel ZO-3 interaction partners was performed using the MATCHMAKER GAL4 Two-Hybrid System 3 and a pretransformed 17 day mouse embryo MATCHMAKER cDNA Library (Clontech Laboratories, Inc) according to the manufacturer's instructions. Briefly, the pGBKT7 construct containing the N-terminal GAL4 DNA-binding domain (DNA-BD) fused bait protein ZO-3 SGC was transformed into the tryptophan $(Trp)^{-}$ auxotrophic yeast strain AH109. pGBKT7 harbours the *TRP1* selectable marker and the transformants were selected in synthetic dropout (SD) medium without Trp (SD/-Trp). The cDNA library had been cloned into the GAL4 activation domain (AD) containing vector pACT2 as an N-terminal fusion. This construct contains the *LEU2* selectable marker and had been pretransformed into the leucine $(Leu)^{-}$ auxotrophic yeast strain Y187, selected and enriched by the manufacturer.

The transformed compatible mating strains AH109 (MATa) and Y187 (MATα) were mixed to allow mating in 2X YPDA (yeast extract, peptone, dextrose, adenine) optimal growth medium. The diploid cells formed from mating contain reporter genes inherited from the AH109 yeast report strain. These are *HIS3*, *ADE2* and *MEL1*and are respectively under the transcriptional regulation of three heterologous GAL4-responsive upstream activating sequences (UAS) and TATA box promoter elements. Interacting hybrid protein-induced *HIS3* and *ADE3* expression allows auxotrophic yeast strains to grow in histidine (His) and adenine (Ade) minus medium respectively. *MEL1* expresses the secreted enzyme α-galactosidase which breaks down X-α-Gal in a blue/white colorimetric assay. Note that both AH109 and Y187 are $Trp^{-}$, $Leu^{-}$, $His^{-}$, $Ade^{-}$ auxotrophs. The mated yeast strains were first selected for positive ZO-3 SGC bait and library protein interaction in low stringency SD/-His/-Trp/-Leu medium and clones were subsequently transferred to high stringency SD/-Ade/-His/-Trp/-Leu medium with supplemented X-α-Gal. Blue positive colonies were picked and grown in SD/-Leu medium to select for the pACT2 plasmid encoding the ZO-3 SGC interacting library protein. The purified plasmid was later sequenced and a basic local alignment search tool (BLAST) was used to identify the protein. The identified library pACT2 plasmids were co-transformed with PGBKT7 bait plasmids into AH109 and selected on SD/-Trp/-Leu medium. Positive interaction was monitored by X-α-Gal colorimetric assay.

## 5.4 Cell Culture and Transfection

MDCK strain II (Canine non-tumorigenic kidney epithelial) and COS-1 (Monkey transformed kidney fibroblast) cells were cultured in DMEM (Glucose 1000 mg/l) supplemented with 10% fetal bovine serum (HyClone), 100 U/ml Penicillin, 100 μg/ml Streptomycin, 2 mM L-Glutamine and 2 mM Sodium Pyruvate (Invitrogen) and maintained at 37˚C in 5% $CO_2$. HeLa (Human cervical adenocarcinoma) and 293T (Human transformed kidney epithelial) cells were cultured like-wise but in DMEM (Glucose 4500 mg/l) instead. MCF-10A (Human non-tumorigenic mammary gland epithelial) cells were cultured in DMEM/F12 (Invitrogen) supplemented with 5% horse serum (Invitrogen), 10 μg/ml human Insulin (Sigma Aldrich), 20 ng/ml Epidermal Growth Factor (Upstate), 100 ng/ml Cholera toxin (Calbiochem), 0.5 μg/ml Hydrocortisone (Calbiochem), 100 U/ml Penicillin, 100 μg/ml Streptomycin, 2 mM L-Glutamine and 2 mM Sodium Pyruvate (Invitrogen) and maintained at 37˚C in 5% $CO_2$. All plasmid constructs were transfected using LipofectAMINE and PLUS reagent (Invitrogen) according to the manufacturer's instructions. MDCK cell-lines stably expressing pEGFP hScrib constructs were selectively maintained in 0.5 mg/ml G418 Sulfate (Calbiochem), pooled and enriched using the Fluorescence Activated Cell Sorter FACSVantage SE (Becton Dickinson). SiRNAs were transiently transfected using DharmaFECT 1 according to the manufacturer's protocol

## 5.5 Antibodies and Reagents

Primary polyclonal antibodies used in this study were rabbit anti-Scrib H-300, goat anti-Scrib C-20, rabbit anti-ZO-2 H110 and rabbit anti-ubiquitin FL-76 (Santa Cruz Biotechnology, Inc.), rabbit anti-Erbin and goat anti-GFP (Abcam), rabbit anti-ZO-3 (Chemicon International) and rabbit anti-actin (Sigma Aldrich). Monoclonal antibodies were mouse anti-GM130 clone 35 and anti-β-catenin clone 14 (BD Transduction Laboratories), mouse anti-vimentin clone V9, anti-alpha tubulin clone GTU-88 and anti-FLAG M2 (Sigma Aldrich), rat anti-HA clone 3F10 (Roche Diagnostics), mouse anti-GAPDH clone 6C5 (Chemicon International), mouse anti-keratin 18 clone C-04 (Abcam) and mouse anti-keratin 18 clone LDK18, which was a gift from Birgit E. Lane (Institute of Medical Biology, Singapore). Control antibodies used in immunoprecipitations were normal mouse and goat IgG (Santa Cruz Biotechnology, Inc.) Secondary antibodies used for immunofluorescence were donkey anti-mouse, anti-goat and anti-rabbit IgG Alexa Fluor 488 and 594 (Invitrogen) and donkey anti-mouse IgG AMCA (Jackson ImmunoResearch Laboratories, Inc.). For Western blots, HRP-coupled goat antibodies to mouse, rabbit (Bio-Rad) or rat IgG (Pierce), or HRP-coupled donkey antibodies to goat IgG (Jackson ImmunoResearch Laboratories, Inc.) were used. Actin was labeled with BODIPY 558/568 phalloidin and nuclei were stained with DAPI (Invitrogen). Cytochalasin D (10 μg/ml) and Nocodazole (10 μg/ml) (Sigma Aldrich) were used to disrupt actin and microtubule filaments, respectively.

## 5.6 GST Fusion Protein Expression and Purification

GST-fusion constructs were transformed into expression host BL21-Gold(DE3) (Stratagene) and clones were cultured to an OD600nm of 0.5-0.7. Expression was then induced with 0.1-0.5 mM IPTG (Promega) at 37°C for 3 hrs and the culture subsequently harvested. Harvested bacterial pellet was resuspended and sonicated in sonication buffer (50 mM Tris, pH 7.5, 150 mM NaCl, 1 mM EDTA, 1 mM DTT and supplemented with complete EDTA-free protease inhibitor cocktail (Roche Diagnostics)). Clarified cell lysates were obtained by centrifugation, applied to Glutathione Sepharose 4B (GE Healthcare) and washed three times with PBS. The bound GST fusion proteins were then eluted with elution buffer (100 mM Tris pH 8, 120 mM NaCl and 20 mM reduced glutathione (Sigma Aldrich). The eluate was recovered and purified by dialysis in PBS using a Slide-A-Lyzer (Pierce). The dialyzed GST fusion proteins were then analyzed quantitatively by Bradford assay and qualitatively by SDS PAGE and Coomassie brilliant blue staining.

Purified GST-hScrib PDZ1, 2, 3 and 4 recombinant proteins were provided by Sachdev S. Sidhu (Department of Protein Engineering, Genentech, Inc, California, USA).

## 5.7 Cell Lysate Preparation

Cell lysates were prepared in RIPA lysis buffer (50 mM Tris, pH 7.4, 150 mM NaCl, 1% Triton X-100, 0.5% Sodium deoxycholate, 0.1% SDS, and supplemented with complete EDTA-free protease inhibitor cocktail (Roche Diagnostics)). Soluble fractions were obtained by centrifugation at 13,200 rpm for 20 min.

## 5.8 Binding Assays

### 5.8.1 GST Pull-Down Assay

GST pull-down assays were performed using purified GST fusion proteins. These were incubated with proteins *in vitro* translated using the TNT T7 Quick Coupled Transcription/Translation system (Promega) or soluble lysates fractions for 16 hrs at 4ºC in binding buffer (25 mM Tris, pH 7.4, 50 mM NaCl, 20 mM $MgCl_2$, 0.1% Triton X-100, 1 mM DTT and supplemented with complete EDTA-free protease inhibitor cocktail (Roche Diagnostics)). GST-fusion proteins were pulled down using Glutathione Sepharose 4B (GE Healthcare), washed four times with washing buffer (25 mM Tris, pH 7.4, 150 mM NaCl, 20 mM $MgCl_2$, 0.1% Triton X-100, 1 mM DTT) and analyzed by Western blot as mentioned next.

### 5.8.2 *In vitro* Vimentin Binding Assay

In the *in vitro* vimentin binding assays, HA-mScrib pcDNA3 constructs were *in vitro* translated using TNT T7 Quick Coupled Transcription/Translation and Transcend Non-Radioactive Translation Detection Systems (Promega). Polymerized vimentin was obtained using the Vimentin Filament Biochem Kit (Cytoskeleton), where lyophilized recombinant Syrian hamster vimentin protein was reconstituted in polymerization buffer (5 mM PIPES, pH 7, 1 mM DTT, 150 mM NaCl) and processed according to the manufacturer's instructions. Non-polymerized vimentin was obtained by reconstitution of the vimentin protein in subunit buffer (5 mM Tris, pH 7.4, 5 mM NaCl, 1% Triton X-100, 0.5% Sodium deoxycholate, 0.1% SDS). Reconstituted vimentin was subjected to

ultracentrifugation at 100,000xg for 30 min. Supernatant and pellet fractions were recovered and analyzed by Western blot to monitor vimentin assembly.

In cosedimentation assays, polymerized vimentin was incubated with HA-mScrib gene products in polymerization buffer at 4 ºC for 16 hrs, subjected to ultracentrifugation at 100,000xg for 30 min and the supernatant and pellet fractions analyzed by Western blot. For *in vitro* immunoprecipitation assays, HA-mScrib gene products were incubated with the reconstituted non-polymerized or polymerized vimentin at 35 ºC for 2 hrs in subunit buffer or RIPA buffer respectively. This was then precleared, immunoprecipitated and subjected to Western blot analysis as mentioned next.

### 5.8.3 Co-immunoprecipitation Assay

In immunoprecipitation assays, appropriate antibodies were applied to precleared lysates for 16 hrs at 4ºC and immunoprecipitated with Protein G Sepharose 4 Fast Flow (GE Healthcare) for 2 hrs at 4ºC. Immunoprecipitates were washed with lysis buffer four times and analyzed by Western blot as mentioned below.

## 5.9 SDS-PAGE and Western Blot Analysis

Cell lysates, purified GST-fusion and *in vitro* translated proteins were analyzed by fractionation by denaturing SDS-PAGE (Bio-Rad). Fractionated proteins were either visualized on-gel using Coomassie brilliant blue staining or Western transferred (Bio-Rad) onto nitrocellulose membrane Hybond-C Extra (GE Healthcare). Protein visualization on-membrane was achieved by staining with Ponceau S (Bio-Rad), autoradiography or immuno-detection. For immunodetection, blots were blocked with

5% skimmed milk in 0.1% Tween-20 in PBS and incubated with appropriate primary and secondary antibodies in 1% skimmed milk in 0.1% Tween-20 in PBS. Membranes were visualized by chemiluminescence (Super Signal West Pico, Pierce or ECL Detection Reagents, GE Healthcare)

## 5.10 Immunofluorescence Labeling

Poly-D-lysine (Sigma Aldrich) coated glass coverslips or 0.4 μm permeable polycarbonate filters (Costar) were used as a platform for cell growth. Cells were fixed with either cold methanol at -20ºC for 2.5 min or 3.7% paraformaldehyde at ambient temperature for 30 min. PFA fixed cells were quenched with 50 mM ammonium chloride and permeabilized with 0.2% Triton X-100 in PBS. Cells were then blocked in 1% BSA in 0.1% Triton X-100 in PBS. Primary antibodies were then applied and subsequently labeled with appropriate fluorescent dye conjugated secondary antibodies. Images were acquired using either a LSM 510 META laser scanning confocal microscope or an Axio Imager.D1 upright microscope coupled to a AxioCam HR or a MRm digital camera, respectively (Carl Zeiss, Inc.).

## 5.11 Wound Healing Assay

MDCK cells were grown to confluence in previously described culture conditions. Wounds were created with a P1000 micropipette tip and allowed to recover for 16 hrs before analysis. Subsequently, wounded monolayers were either fixed and analyzed by immunofluorescence, or tracked over time using time-lapse video microscopy. Fixed cells were analyzed for their morphology and Golgi complex

orientation. The Golgi complex position relative to the nucleus and wound was scored in cells of the leading edge according to Kupfer *et al.,* 1982. Briefly, Golgi complex orientation relative to the nucleus and the migration front was quantified by dividing the cell into three 120° sectors with the nucleus at the centre. One sector faces the wound edge and is bisected perpendicular to this edge. Correct orientation was scored when at least 50% of the Golgi complex fell within this sector. Based on this assay, a score of 33% denotes a random orientation. For live cell tracking, wound closure was either tracked statically using an Eclipse TE2000-S (Nikon) inverted microscope or continually by time-lapse video microscopy using an Axiovert 200M (Carl Zeiss, Inc.) inverted microscope in a controlled humidified chamber at 37˚C in 5% $CO_2$. Images were captured digitally with a Nikon DS-5Mc or a Carl Zeiss AxioCam HRc respectively. Time-lapse images were analyzed using the AxioVision software (Carl Zeiss, Inc.).

## 5.12 Cell Aggregation Assay

Assay conditions were previously described (Redfield *et al.*, 1997; Kim *et al.*, 2000a). Briefly, trypsinized MDCK cells were resuspended at 1.2 x $10^6$ cells/ml in culture medium and 20 μl (2.4 x $10^4$ cells) drops were placed onto the inner surface of a 10 cm tissue culture dish lid. The lid was then placed onto the dish containing 10 ml of PBS in the bottom to prevent evaporation of the drops. After subsequent incubation, drops were directly analyzed for cell aggregation by inverting the lid and viewing under an Eclipse TE2000-S inverted microscope. Alternatively, cell drops were replated onto poly-D-lysine coated glass coverslips, allowed to adhere and later studied for cell spreading.

## 5.13 Proteasome Inhibitor Assay

MDCK cells treated with appropriate SiRNAs for three days were incubated at 37˚C in 5% $CO_2$ with 10 μM Proteasome Inhibitor II (Z-Leu-Leu-Phe-aldehyde) (A.G. Scientific Inc.) in culture medium from 0 to 9 hrs. Subsequently, cells were lysed or fixed and analyzed by Western transfer or immunofluorescence microscopy respectively as previously described.

# References


Adachi, M., Inoko, A., Hata, M., Furuse, K., Umeda, K., Itoh, M., and Tsukita, S. (2006). Normal establishment of epithelial tight junctions in mice and cultured cells lacking expression of ZO-3, a tight-junction MAGUK protein. Mol Cell Biol *26*, 9003-9015.

Albertson, R., Chabu, C., Sheehan, A., and Doe, C.Q. (2004). Scribble protein domain mapping reveals a multistep localization mechanism and domains necessary for establishing cortical polarity. J Cell Sci *117*, 6061-6070.

Albertson, R., and Doe, C.Q. (2003). Dlg, Scrib and Lgl regulate neuroblast cell size and mitotic spindle asymmetry. Nat Cell Biol *5*, 166-170.

Ameen, N.A., Figueroa, Y., and Salas, P.J. (2001). Anomalous apical plasma membrane phenotype in CK8-deficient mice indicates a novel role for intermediate filaments in the polarization of simple epithelia. J Cell Sci *114*, 563-575.

Apperson, M.L., Moon, I.S., and Kennedy, M.B. (1996). Characterization of densin-180, a new brain-specific synaptic protein of the O-sialoglycoprotein family. J Neurosci *16*, 6839-6852.

Arpin-Andre, C., and Mesnard, J.M. (2007). The PDZ domain-binding motif of the human T cell leukemia virus type 1 tax protein induces mislocalization of the tumor suppressor hScrib in T cells. J Biol Chem *282*, 33132-33141.

Assemat, E., Bazellieres, E., Pallesi-Pocachard, E., Le Bivic, A., and Massey-Harroche, D. (2008). Polarity complex proteins. Biochim Biophys Acta *1778*, 614-630.

Audebert, S., Navarro, C., Nourry, C., Chasserot-Golaz, S., Lecine, P., Bellaiche, Y., Dupont, J.L., Premont, R.T., Sempere, C., Strub, J.M., Van Dorsselaer, A., Vitale, N., and Borg, J.P. (2004). Mammalian Scribble forms a tight complex with the betaPIX exchange factor. Curr Biol *14*, 987-995.

Bacallao, R., Antony, C., Dotti, C., Karsenti, E., Stelzer, E.H., and Simons, K. (1989). The subcellular organization of Madin-Darby canine kidney cells during the formation of a polarized epithelium. J Cell Biol *109*, 2817-2832.

Balda, M.S., Garrett, M.D., and Matter, K. (2003). The ZO-1-associated Y-box factor ZONAB regulates epithelial cell proliferation and cell density. J Cell Biol *160*, 423-432.

Balda, M.S., and Matter, K. (2000). The tight junction protein ZO-1 and an interacting transcription factor regulate ErbB-2 expression. EMBO J *19*, 2024-2033.

Barros, C.S., Phelps, C.B., and Brand, A.H. (2003). Drosophila nonmuscle myosin II promotes the asymmetric segregation of cell fate determinants by cortical exclusion rather than active transport. Dev Cell *5*, 829-840.

Betanzos, A., Huerta, M., Lopez-Bayghen, E., Azuara, E., Amerena, J., and Gonzalez-Mariscal, L. (2004). The tight junction protein ZO-2 associates with Jun, Fos and C/EBP transcription factors in epithelial cells. Exp Cell Res *292*, 51-66.

Betschinger, J., Eisenhaber, F., and Knoblich, J.A. (2005). Phosphorylation-induced autoinhibition regulates the cytoskeletal protein Lethal (2) giant larvae. Curr Biol *15*, 276-282.

Bilder, D., Birnbaum, D., Borg, J.P., Bryant, P., Huigbretse, J., Jansen, E., Kennedy, M.B., Labouesse, M., Legouis, R., Mechler, B., Perrimon, N., Petit, M., and Sinha, P. (2000a). Collective nomenclature for LAP proteins. Nat Cell Biol *2*, E114.

Bilder, D., Li, M., and Perrimon, N. (2000b). Cooperative regulation of cell polarity and growth by Drosophila tumor suppressors. Science *289*, 113-116.

Bilder, D., and Perrimon, N. (2000). Localization of apical epithelial determinants by the basolateral PDZ protein Scribble. Nature *403*, 676-680.

Bissell, M.J., and Radisky, D. (2001). Putting tumours in context. Nat Rev Cancer *1*, 46-54.

Borg, J.P., Marchetto, S., Le Bivic, A., Ollendorff, V., Jaulin-Bastard, F., Saito, H., Fournier, E., Adelaide, J., Margolis, B., and Birnbaum, D. (2000). ERBIN: a basolateral PDZ protein that interacts with the mammalian ERBB2/HER2 receptor. Nat. Cell Biol. *2*, 407-414.

Borradori, L., and Sonnenberg, A. (1999). Structure and function of hemidesmosomes: more than simple adhesion complexes. J Invest Dermatol *112*, 411-418.

Bridges, D., and Moorhead, G.B. (2005). 14-3-3 proteins: a number of functions for a numbered protein. Sci STKE *296*, re10.

Brumby, A.M., and Richardson, H.E. (2003). scribble mutants cooperate with oncogenic Ras or Notch to cause neoplastic overgrowth in Drosophila. EMBO J *22*, 5769-5779.

Budnik, V., Koh, Y.H., Guan, B., Hartmann, B., Hough, C., Woods, D., and Gorczyca, M. (1996). Regulation of synapse structure and function by the Drosophila tumor suppressor gene dlg. Neuron *17*, 627-640.

Cau, J., and Hall, A. (2005). Cdc42 controls the polarity of the actin and microtubule cytoskeletons through two distinct signal transduction pathways. J Cell Sci *118*, 2579-2587.

Chang, L., and Goldman, R.D. (2004). Intermediate filaments mediate cytoskeletal crosstalk. Nat Rev Mol Cell Biol *5*, 601-613.

Chen, X., and Macara, I.G. (2005). Par-3 controls tight junction assembly through the Rac exchange factor Tiam1. Nat Cell Biol *7*, 262-269.

Chlenski, A., Ketels, K.V., Korovaitseva, G.I., Talamonti, M.S., Oyasu, R., and Scarpelli, D.G. (2000). Organization and expression of the human zo-2 gene (tjp-2) in normal and neoplastic tissues. Biochim Biophys Acta *1493*, 319-324.

Chou, Y.H., Flitney, F.W., Chang, L., Mendez, M., Grin, B., and Goldman, R.D. (2007). The motility and dynamic properties of intermediate filaments and their constituent proteins. Exp Cell Res *313*, 2236-2243.

Cohen, D., Musch, A., and Rodriguez-Boulan, E. (2001). Selective control of basolateral membrane protein polarity by cdc42. Traffic *2*, 556-564.

Colas, J.F., and Schoenwolf, G.C. (2001). Towards a cellular and molecular understanding of neurulation. Dev Dyn *221*, 117-145.

Colegio, O.R., Van Itallie, C.M., McCrea, H.J., Rahner, C., and Anderson, J.M. (2002). Claudins create charge-selective channels in the paracellular pathway between epithelial cells. Am J Physiol Cell Physiol *283*, C142-147.

Cory, G.O., Cramer, R., Blanchoin, L., and Ridley, A.J. (2003). Phosphorylation of the WASP-VCA domain increases its affinity for the Arp2/3 complex and enhances actin polymerization by WASP. Mol Cell *11*, 1229-1239.

Dalgarno, D.C., Botfield, M.C., and Rickles, R.J. (1997). SH3 domains and drug design: ligands, structure, and biological function. Biopolymers *43*, 383-400.

del Pozo, M.A., Price, L.S., Alderson, N.B., Ren, X.D., and Schwartz, M.A. (2000). Adhesion to the extracellular matrix regulates the coupling of the small GTPase Rac to its effector PAK. EMBO J *19*, 2008-2014.

Doudney, K., and Stanier, P. (2005). Epithelial cell polarity genes are required for neural tube closure. Am J Med Genet C Semin Med Genet *135C*, 42-47.

Dow, L.E., Brumby, A.M., Muratore, R., Coombe, M.L., Sedelies, K.A., Trapani, J.A., Russell, S.M., Richardson, H.E., and Humbert, P.O. (2003). hScrib is a functional homologue of the Drosophila tumour suppressor Scribble. Oncogene *22*, 9225-9230.

Dow, L.E., Elsum, I.A., King, C.L., Kinross, K.M., Richardson, H.E., and Humbert, P.O. (2008). Loss of human Scribble cooperates with H-Ras to promote cell invasion through deregulation of MAPK signalling. Oncogene *27*, 5988-6001.

Dow, L.E., and Humbert, P.O. (2007). Polarity regulators and the control of epithelial architecture, cell migration, and tumorigenesis. Int Rev Cytol *262*, 253-302.

Dow, L.E., Kauffman, J.S., Caddy, J., Zarbalis, K., Peterson, A.S., Jane, S.M., Russell, S.M., and Humbert, P.O. (2007). The tumour-suppressor Scribble dictates cell polarity during directed epithelial migration: regulation of Rho GTPase recruitment to the leading edge. Oncogene *26*, 2272-2282.

Doyle, D.A., Lee, A., Lewis, J., Kim, E., Sheng, M., and MacKinnon, R. (1996). Crystal structures of a complexed and peptide-free membrane protein-binding domain: molecular basis of peptide recognition by PDZ. Cell *85*, 1067-1076.

Drees, F., Pokutta, S., Yamada, S., Nelson, W.J., and Weis, W.I. (2005). Alpha-catenin is a molecular switch that binds E-cadherin-beta-catenin and regulates actin-filament assembly. Cell *123*, 903-915.

Ebnet, K., Suzuki, A., Horikoshi, Y., Hirose, T., Meyer Zu Brickwedde, M.K., Ohno, S., and Vestweber, D. (2001). The cell polarity protein ASIP/PAR-3 directly associates with junctional adhesion molecule (JAM). EMBO J *20*, 3738-3748.

Eckes, B., Colucci-Guyon, E., Smola, H., Nodder, S., Babinet, C., Krieg, T., and Martin, P. (2000). Impaired wound healing in embryonic and adult mice lacking vimentin. J Cell Sci *113 ( Pt 13)*, 2455-2462.

Eckes, B., Dogic, D., Colucci-Guyon, E., Wang, N., Maniotis, A., Ingber, D., Merckling, A., Langa, F., Aumailley, M., Delouvee, A., Koteliansky, V., Babinet, C., and Krieg, T. (1998). Impaired mechanical stability, migration and contractile capacity in vimentin-deficient fibroblasts. J Cell Sci *111 ( Pt 13)*, 1897-1907.

Erber, A., Riemer, D., Bovenschulte, M., and Weber, K. (1998). Molecular phylogeny of metazoan intermediate filament proteins. J Mol Evol *47*, 751-762.

Etienne-Manneville, S., and Hall, A. (2001). Integrin-mediated activation of Cdc42 controls cell polarity in migrating astrocytes through PKCzeta. Cell *106*, 489-498.

Etienne-Manneville, S., Manneville, J.B., Nicholls, S., Ferenczi, M.A., and Hall, A. (2005). Cdc42 and Par6-PKCzeta regulate the spatially localized association of Dlg1 and APC to control cell polarization. J Cell Biol *170*, 895-901.

Faigle, W., Colucci-Guyon, E., Louvard, D., Amigorena, S., and Galli, T. (2000). Vimentin filaments in fibroblasts are a reservoir for SNAP23, a component of the membrane fusion machinery. Mol Biol Cell *11*, 3485-3494.

Fanning, A.S., Jameson, B.J., Jesaitis, L.A., and Anderson, J.M. (1998). The tight junction protein ZO-1 establishes a link between the transmembrane protein occludin and the actin cytoskeleton. J Biol Chem *273*, 29745-29753.

Fogg, V.C., Liu, C.J., and Margolis, B. (2005). Multiple regions of Crumbs3 are required for tight junction formation in MCF10A cells. J Cell Sci *118*, 2859-2869.

Fukuhara, A., Irie, K., Yamada, A., Katata, T., Honda, T., Shimizu, K., Nakanishi, H., and Takai, Y. (2002). Role of nectin in organization of tight junctions in epithelial cells. Genes Cells *7*, 1059-1072.

Furuse, M., Fujita, K., Hiiragi, T., Fujimoto, K., and Tsukita, S. (1998a). Claudin-1 and -2: novel integral membrane proteins localizing at tight junctions with no sequence similarity to occludin. J Cell Biol *141*, 1539-1550.

Furuse, M., Sasaki, H., Fujimoto, K., and Tsukita, S. (1998b). A single gene product, claudin-1 or -2, reconstitutes tight junction strands and recruits occludin in fibroblasts. J Cell Biol *143*, 391-401.

Gardiol, D., Kuhne, C., Glaunsinger, B., Lee, S.S., Javier, R., and Banks, L. (1999). Oncogenic human papillomavirus E6 proteins target the discs large tumour suppressor for proteasome-mediated degradation. Oncogene *18*, 5487-5496.

Gardiol, D., Zacchi, A., Petrera, F., Stanta, G., and Banks, L. (2006). Human discs large and scrib are localized at the same regions in colon mucosa and changes in their expression patterns are correlated with loss of tissue architecture during malignant progression. Int J Cancer *119*, 1285-1290.

Garrod, D., and Chidgey, M. (2008). Desmosome structure, composition and function. Biochim Biophys Acta *1778*, 572-587.

Gateff, E. (1978). Malignant neoplasms of genetic origin in Drosophila melanogaster. Science *200*, 1448-1459.

Gateff, E., and Mechler, B.M. (1989). Tumor-suppressor genes of Drosophila melanogaster. Crit Rev Oncog *1*, 221-245.

Geiger, B., Bershadsky, A., Pankov, R., and Yamada, K.M. (2001). Transmembrane crosstalk between the extracellular matrix--cytoskeleton crosstalk. Nat Rev Mol Cell Biol *2*, 793-805.

Gilles, C., Polette, M., Zahm, J.M., Tournier, J.M., Volders, L., Foidart, J.M., and Birembaut, P. (1999). Vimentin contributes to human mammary epithelial cell migration. J Cell Sci *112 ( Pt 24)*, 4615-4625.

Godsel, L.M., Hobbs, R.P., and Green, K.J. (2008). Intermediate filament assembly: dynamics to disease. Trends Cell Biol *18*, 28-37.

Goldman, R.D., Khuon, S., Chou, Y.H., Opal, P., and Steinert, P.M. (1996). The function of intermediate filaments in cell shape and cytoskeletal integrity. J Cell Biol *134*, 971-983.

Gonzales, M., Weksler, B., Tsuruta, D., Goldman, R.D., Yoon, K.J., Hopkinson, S.B., Flitney, F.W., and Jones, J.C. (2001). Structure and function of a vimentin-associated matrix adhesion in endothelial cells. Mol Biol Cell *12*, 85-100.

Gonzalez-Mariscal, L., Betanzos, A., and Avila-Flores, A. (2000). MAGUK proteins: structure and role in the tight junction. Semin Cell Dev Biol *11*, 315-324.

Gorczyca, D., Ashley, J., Speese, S., Gherbesi, N., Thomas, U., Gundelfinger, E., Gramates, L.S., and Budnik, V. (2007). Postsynaptic membrane addition depends on the Discs-Large-interacting t-SNARE Gtaxin. J Neurosci *27*, 1033-1044.

Gottardi, C.J., Arpin, M., Fanning, A.S., and Louvard, D. (1996). The junction-associated protein, zonula occludens-1, localizes to the nucleus before the maturation and during the remodeling of cell-cell contacts. Proc Natl Acad Sci U S A *93*, 10779-10784.

Green, K.J., and Gaudry, C.A. (2000). Are desmosomes more than tethers for intermediate filaments? Nat Rev Mol Cell Biol *1*, 208-216.

Guillemot, L., Paschoud, S., Pulimeno, P., Foglia, A., and Citi, S. (2008). The cytoplasmic plaque of tight junctions: a scaffolding and signalling center. Biochim Biophys Acta *1778*, 601-613.

Gumbiner, B., Lowenkopf, T., and Apatira, D. (1991). Identification of a 160-kDa polypeptide that binds to the tight junction protein ZO-1. Proc Natl Acad Sci U S A *88*, 3460-3464.

Hall, A. (2005). Rho GTPases and the control of cell behaviour. Biochem Soc Trans *33*, 891-895.

Hanada, N., Makino, K., Koga, H., Morisaki, T., Kuwahara, H., Masuko, N., Tabira, Y., Hiraoka, T., Kitamura, N., Kikuchi, A., and Saya, H. (2000). NE-dlg, a mammalian homolog of Drosophila dlg tumor suppressor, induces growth suppression and impairment of cell adhesion: possible involvement of down-regulation of beta-catenin by NE-dlg expression. Int J Cancer *86*, 480-488.

Hanahan, D., and Weinberg, R.A. (2000). The hallmarks of cancer. Cell *100*, 57-70.

Harris, B.Z., and Lim, W.A. (2001). Mechanism and role of PDZ domains in signaling complex assembly. J. Cell Sci. *114*, 3219-3231.

Hartsock, A., and Nelson, W.J. (2008). Adherens and tight junctions: structure, function and connections to the actin cytoskeleton. Biochim Biophys Acta *1778*, 660-669.

Helfand, B.T., Mikami, A., Vallee, R.B., and Goldman, R.D. (2002). A requirement for cytoplasmic dynein and dynactin in intermediate filament network assembly and organization. J Cell Biol *157*, 795-806.

Herrmann, H., and Aebi, U. (2004). Intermediate filaments: molecular structure, assembly mechanism, and integration into functionally distinct intracellular Scaffolds. Annu Rev Biochem *73*, 749-789.

Herrmann, H., Bar, H., Kreplak, L., Strelkov, S.V., and Aebi, U. (2007). Intermediate filaments: from cell architecture to nanomechanics. Nat Rev Mol Cell Biol *8*, 562-573.

Herrmann, H., Hesse, M., Reichenzeller, M., Aebi, U., and Magin, T.M. (2003). Functional complexity of intermediate filament cytoskeletons: from structure to assembly to gene ablation. Int Rev Cytol *223*, 83-175.

Hirata, A., Higuchi, M., Niinuma, A., Ohashi, M., Fukushi, M., Oie, M., Akiyama, T., Tanaka, Y., Gejyo, F., and Fujii, M. (2004). PDZ domain-binding motif of human T-cell leukemia virus type 1 Tax oncoprotein augments the transforming activity in a rat fibroblast cell line. Virology *318*, 327-336.

Ho, C.L., Martys, J.L., Mikhailov, A., Gundersen, G.G., and Liem, R.K. (1998). Novel features of intermediate filament dynamics revealed by green fluorescent protein chimeras. J Cell Sci *111 ( Pt 13)*, 1767-1778.

Holmes, K.C., Popp, D., Gebhard, W., and Kabsch, W. (1990). Atomic model of the actin filament. Nature *347*, 44-49.

Hoover, K.B., Liao, S.Y., and Bryant, P.J. (1998). Loss of the tight junction MAGUK ZO-1 in breast cancer: relationship to glandular differentiation and loss of heterozygosity. Am J Pathol *153*, 1767-1773.

Hurd, T.W., Gao, L., Roh, M.H., Macara, I.G., and Margolis, B. (2003). Direct interaction of two polarity complexes implicated in epithelial tight junction assembly. Nat Cell Biol *5*, 137-142.

Hutterer, A., Betschinger, J., Petronczki, M., and Knoblich, J.A. (2004). Sequential roles of Cdc42, Par-6, aPKC, and Lgl in the establishment of epithelial polarity during Drosophila embryogenesis. Dev Cell *6*, 845-854.

Ikenouchi, J., Umeda, K., Tsukita, S., and Furuse, M. (2007). Requirement of ZO-1 for the formation of belt-like adherens junctions during epithelial cell polarization. J Cell Biol *176*, 779-786.

Inada, H., Izawa, I., Nishizawa, M., Fujita, E., Kiyono, T., Takahashi, T., Momoi, T., and Inagaki, M. (2001). Keratin attenuates tumor necrosis factor-induced cytotoxicity through association with TRADD. J Cell Biol *155*, 415-426.

Inoko, A., Itoh, M., Tamura, A., Matsuda, M., Furuse, M., and Tsukita, S. (2003). Expression and distribution of ZO-3, a tight junction MAGUK protein, in mouse tissues. Genes Cells *8*, 837-845.

Ishibe, S., Joly, D., Liu, Z.X., and Cantley, L.G. (2004). Paxillin serves as an ERK-regulated scaffold for coordinating FAK and Rac activation in epithelial morphogenesis. Mol Cell *16*, 257-267.

Ishidate, T., Matsumine, A., Toyoshima, K., and Akiyama, T. (2000). The APC-hDLG complex negatively regulates cell cycle progression from the G0/G1 to S phase. Oncogene *19*, 365-372.

Islas, S., Vega, J., Ponce, L., and Gonzalez-Mariscal, L. (2002). Nuclear localization of the tight junction protein ZO-2 in epithelial cells. Exp Cell Res *274*, 138-148.

Itoh, M., Furuse, M., Morita, K., Kubota, K., Saitou, M., and Tsukita, S. (1999a). Direct binding of three tight junction-associated MAGUKs, ZO-1, ZO-2, and ZO-3, with the COOH termini of claudins. J Cell Biol *147*, 1351-1363.

Itoh, M., Morita, K., and Tsukita, S. (1999b). Characterization of ZO-2 as a MAGUK family member associated with tight as well as adherens junctions with a binding affinity to occludin and alpha catenin. J Biol Chem *274*, 5981-5986.

Ivaska, J., Pallari, H.M., Nevo, J., and Eriksson, J.E. (2007). Novel functions of vimentin in cell adhesion, migration, and signaling. Exp Cell Res *313*, 2050-2062.

Ivaska, J., Vuoriluoto, K., Huovinen, T., Izawa, I., Inagaki, M., and Parker, P.J. (2005). PKCepsilon-mediated phosphorylation of vimentin controls integrin recycling and motility. EMBO J *24*, 3834-3845.

Izaurralde, E., and Adam, S. (1998). Transport of macromolecules between the nucleus and the cytoplasm. RNA *4*, 351-364.

Izawa, I., and Inagaki, M. (2006). Regulatory mechanisms and functions of intermediate filaments: a study using site- and phosphorylation state-specific antibodies. Cancer Sci *97*, 167-174.

Jaffe, A.B., and Hall, A. (2005). Rho GTPases: biochemistry and biology. Annu Rev Cell Dev Biol *21*, 247-269.

Jefferson, J.J., Leung, C.L., and Liem, R.K. (2004). Plakins: goliaths that link cell junctions and the cytoskeleton. Nat Rev Mol Cell Biol *5*, 542-553.

Jelen, F., Oleksy, A., Smietana, K., and Otlewski, J. (2003). PDZ domains - common players in the cell signaling. Acta Biochim Pol *50*, 985-1017.

Joberty, G., Petersen, C., Gao, L., and Macara, I.G. (2000). The cell-polarity protein Par6 links Par3 and atypical protein kinase C to Cdc42. Nat Cell Biol *2*, 531-539.

Johnston, J.A., Ward, C.L., and Kopito, R.R. (1998). Aggresomes: a cellular response to misfolded proteins. J. Cell Biol. *143*, 1883-1898.

Kajava, A.V. (1998). Structural diversity of leucine-rich repeat proteins. J Mol Biol *277*, 519-527.

Kallay, L.M., McNickle, A., Brennwald, P.J., Hubbard, A.L., and Braiterman, L.T. (2006). Scribble associates with two polarity proteins, Lgl2 and Vangl2, via distinct molecular domains. J Cell Biochem *99*, 647-664.

Kausalya, P.J., Phua, D.C., and Hunziker, W. (2004). Association of ARVCF with zonula occludens (ZO)-1 and ZO-2: binding to PDZ-domain proteins and cell-cell adhesion regulate plasma membrane and nuclear localization of ARVCF. Mol Biol Cell *15*, 5503-5515.

Kim, J.B., Islam, S., Kim, Y.J., Prudoff, R.S., Sass, K.M., Wheelock, M.J., and Johnson, K.R. (2000a). N-Cadherin extracellular repeat 4 mediates epithelial to mesenchymal transition and increased motility. J. Cell Biol. *151*, 1193-1206.

Kim, S., and Coulombe, P.A. (2007). Intermediate filament scaffolds fulfill mechanical, organizational, and signaling functions in the cytoplasm. Genes Dev *21*, 1581-1597.

Kim, S., Wong, P., and Coulombe, P.A. (2006). A keratin cytoskeletal protein regulates protein synthesis and epithelial cell growth. Nature *441*, 362-365.

Kim, S.H., Li, Z., and Sacks, D.B. (2000b). E-cadherin-mediated cell-cell attachment activates Cdc42. J Biol Chem *275*, 36999-37005.

Kiosses, W.B., Shattil, S.J., Pampori, N., and Schwartz, M.A. (2001). Rac recruits high-affinity integrin alphavbeta3 to lamellipodia in endothelial cell migration. Nat Cell Biol *3*, 316-320.

Klezovitch, O., Fernandez, T.E., Tapscott, S.J., and Vasioukhin, V. (2004). Loss of cell polarity causes severe brain dysplasia in Lgl1 knockout mice. Genes Dev *18*, 559-571.

Kostrewa, D., Brockhaus, M., D'Arcy, A., Dale, G.E., Nelboeck, P., Schmid, G., Mueller, F., Bazzoni, G., Dejana, E., Bartfai, T., Winkler, F.K., and Hennig, M. (2001). X-ray structure of junctional adhesion molecule: structural basis for homophilic adhesion via a novel dimerization motif. EMBO J *20*, 4391-4398.

Ku, N.O., and Omary, M.B. (2000). Keratins turn over by ubiquitination in a phosphorylation-modulated fashion. J Cell Biol *149*, 547-552.

Kupfer, A., Louvard, D., and Singer, S.J. (1982). Polarization of the Golgi apparatus and the microtubule-organizing center in cultured fibroblasts at the edge of an experimental wound. Proc. Natl. Acad. Sci. U. S. A. *79*, 2603-2607.

Lahuna, O., Quellari, M., Achard, C., Nola, S., Meduri, G., Navarro, C., Vitale, N., Borg, J.P., and Misrahi, M. (2005). Thyrotropin receptor trafficking relies on the hScrib-betaPIX-GIT1-ARF6 pathway. EMBO J *24*, 1364-1374.

Lauffenburger, D.A., and Horwitz, A.F. (1996). Cell migration: a physically integrated molecular process. Cell *84*, 359-369.

Lee, J.M., Dedhar, S., Kalluri, R., and Thompson, E.W. (2006). The epithelial-mesenchymal transition: new insights in signaling, development, and disease. J Cell Biol *172*, 973-981.

Legouis, R., Gansmuller, A., Sookhareea, S., Bosher, J.M., Baillie, D.L., and Labouesse, M. (2000). LET-413 is a basolateral protein required for the assembly of adherens junctions in Caenorhabditis elegans. Nat Cell Biol *2*, 415-422.

Legouis, R., Jaulin-Bastard, F., Schott, S., Navarro, C., Borg, J.P., and Labouesse, M. (2003). Basolateral targeting by leucine-rich repeat domains in epithelial cells. EMBO Rep *4*, 1096-1102.

Lehman, K., Rossi, G., Adamo, J.E., and Brennwald, P. (1999). Yeast homologues of tomosyn and lethal giant larvae function in exocytosis and are associated with the plasma membrane SNARE, Sec9. J Cell Biol *146*, 125-140.

Lemmers, C., Michel, D., Lane-Guermonprez, L., Delgrossi, M.H., Medina, E., Arsanto, J.P., and Le Bivic, A. (2004). CRB3 binds directly to Par6 and regulates the morphogenesis of the tight junctions in mammalian epithelial cells. Mol Biol Cell *15*, 1324-1333.

Lin, D., Edwards, A.S., Fawcett, J.P., Mbamalu, G., Scott, J.D., and Pawson, T. (2000). A mammalian PAR-3-PAR-6 complex implicated in Cdc42/Rac1 and aPKC signalling and cell polarity. Nat Cell Biol *2*, 540-547.

Liu, L.X., Liu, Z.H., Jiang, H.C., Qu, X., Zhang, W.H., Wu, L.F., Zhu, A.L., Wang, X.Q., and Wu, M. (2002). Profiling of differentially expressed genes in human gastric carcinoma by cDNA expression array. World J Gastroenterol *8*, 580-585.

Liu, Y., Nusrat, A., Schnell, F.J., Reaves, T.A., Walsh, S., Pochet, M., and Parkos, C.A. (2000). Human junction adhesion molecule regulates tight junction resealing in epithelia. J Cell Sci *113*, 2363-2374.

Lu, H., and Bilder, D. (2005). Endocytic control of epithelial polarity and proliferation in Drosophila. Nat Cell Biol *7*, 1232-1239.

Ludford-Menting, M.J., Oliaro, J., Sacirbegovic, F., Cheah, E.T., Pedersen, N., Thomas, S.J., Pasam, A., Iazzolino, R., Dow, L.E., Waterhouse, N.J., Murphy, A., Ellis, S., Smyth, M.J., Kershaw, M.H., Darcy, P.K., Humbert, P.O., and Russell, S.M. (2005). A network

of PDZ-containing proteins regulates T cell polarity and morphology during migration and immunological synapse formation. Immunity *22*, 737-748.

Magin, T.M., Vijayaraj, P., and Leube, R.E. (2007). Structural and regulatory functions of keratins. Exp Cell Res *313*, 2021-2032.

Manfruelli, P., Arquier, N., Hanratty, W.P., and Semeriva, M. (1996). The tumor suppressor gene, lethal(2)giant larvae (1(2)g1), is required for cell shape change of epithelial cells during Drosophila development. Development *122*, 2283-2294.

Manser, E., Loo, T.H., Koh, C.G., Zhao, Z.S., Chen, X.Q., Tan, L., Tan, I., Leung, T., and Lim, L. (1998). PAK kinases are directly coupled to the PIX family of nucleotide exchange factors. Mol Cell *1*, 183-192.

Marceau, N., Schutte, B., Gilbert, S., Loranger, A., Henfling, M.E., Broers, J.L., Mathew, J., and Ramaekers, F.C. (2007). Dual roles of intermediate filaments in apoptosis. Exp Cell Res *313*, 2265-2281.

Martys, J.L., Ho, C.L., Liem, R.K., and Gundersen, G.G. (1999). Intermediate filaments in motion: observations of intermediate filaments in cells using green fluorescent protein-vimentin. Mol Biol Cell *10*, 1289-1295.

Massimi, P., Gammoh, N., Thomas, M., and Banks, L. (2004). HPV E6 specifically targets different cellular pools of its PDZ domain-containing tumour suppressor substrates for proteasome-mediated degradation. Oncogene *23*, 8033-8039.

Massimi, P., Narayan, N., Thomas, M., Gammoh, N., Strand, S., Strand, D., and Banks, L. (2008). Regulation of the hDlg/hScrib/Hugl-1 tumour suppressor complex. Exp Cell Res *314*, 3306-3317.

Massimi, P., Shai, A., Lambert, P., and Banks, L. (2007). HPV E6 degradation of p53 and PDZ containing substrates in an E6AP null background. Oncogene.

Mathew, D., Gramates, L.S., Packard, M., Thomas, U., Bilder, D., Perrimon, N., Gorczyca, M., and Budnik, V. (2002). Recruitment of scribble to the synaptic scaffolding complex requires GUK-holder, a novel DLG binding protein. Curr Biol *12*, 531-539.

Matsuda, M., Kubo, A., Furuse, M., and Tsukita, S. (2004). A peculiar internalization of claudins, tight junction-specific adhesion molecules, during the intercellular movement of epithelial cells. J Cell Sci *117*, 1247-1257.

Matsumine, A., Ogai, A., Senda, T., Okumura, N., Satoh, K., Baeg, G.H., Kawahara, T., Kobayashi, S., Okada, M., Toyoshima, K., and Akiyama, T. (1996). Binding of APC to the human homolog of the Drosophila discs large tumor suppressor protein. Science *272*, 1020-1023.

McInroy, L., and Maatta, A. (2007). Down-regulation of vimentin expression inhibits carcinoma cell migration and adhesion. Biochem Biophys Res Commun *360*, 109-114.

Mechler, B.M., McGinnis, W., and Gehring, W.J. (1985). Molecular cloning of lethal(2)giant larvae, a recessive oncogene of Drosophila melanogaster. EMBO J *4*, 1551-1557.

Mertens, A.E., Rygiel, T.P., Olivo, C., van der Kammen, R., and Collard, J.G. (2005). The Rac activator Tiam1 controls tight junction biogenesis in keratinocytes through binding to and activation of the Par polarity complex. J Cell Biol *170*, 1029-1037.

Metais, J.Y., Navarro, C., Santoni, M.J., Audebert, S., and Borg, J.P. (2005). hScrib interacts with ZO-2 at the cell-cell junctions of epithelial cells. FEBS Lett. *579*, 3725-3730.

Michel, D., Arsanto, J.P., Massey-Harroche, D., Beclin, C., Wijnholds, J., and Le Bivic, A. (2005). PATJ connects and stabilizes apical and lateral components of tight junctions in human intestinal cells. J Cell Sci *118*, 4049-4057.

Montcouquiol, M., Rachel, R.A., Lanford, P.J., Copeland, N.G., Jenkins, N.A., and Kelley, M.W. (2003). Identification of Vangl2 and Scrb1 as planar polarity genes in mammals. Nature *423*, 173-177.

Montcouquiol, M., Sans, N., Huss, D., Kach, J., Dickman, J.D., Forge, A., Rachel, R.A., Copeland, N.G., Jenkins, N.A., Bogani, D., Murdoch, J., Warchol, M.E., Wenthold, R.J., and Kelley, M.W. (2006). Asymmetric localization of Vangl2 and Fz3 indicate novel mechanisms for planar cell polarity in mammals. J Neurosci *26*, 5265-5275.

Munger, K., Basile, J.R., Duensing, S., Eichten, A., Gonzalez, S.L., Grace, M., and Zacny, V.L. (2001). Biological activities and molecular targets of the human papillomavirus E7 oncoprotein. Oncogene *20*, 7888-7898.

Murdoch, J.N., Henderson, D.J., Doudney, K., Gaston-Massuet, C., Phillips, H.M., Paternotte, C., Arkell, R., Stanier, P., and Copp, A.J. (2003). Disruption of scribble (Scrb1) causes severe neural tube defects in the circletail mouse. Hum Mol Genet *12*, 87-98.

Murdoch, J.N., Rachel, R.A., Shah, S., Beermann, F., Stanier, P., Mason, C.A., and Copp, A.J. (2001). Circletail, a new mouse mutant with severe neural tube defects: chromosomal localization and interaction with the loop-tail mutation. Genomics *78*, 55-63.

Musch, A., Cohen, D., Yeaman, C., Nelson, W.J., Rodriguez-Boulan, E., and Brennwald, P.J. (2002). Mammalian homolog of Drosophila tumor suppressor lethal (2) giant larvae interacts with basolateral exocytic machinery in Madin-Darby canine kidney cells. Mol Biol Cell *13*, 158-168.

Nagasaka, K., Nakagawa, S., Yano, T., Takizawa, S., Matsumoto, Y., Tsuruga, T., Nakagawa, K., Minaguchi, T., Oda, K., Hiraike-Wada, O., Ooishi, H., Yasugi, T., and Taketani, Y. (2006). Human homolog of Drosophila tumor suppressor Scribble negatively regulates cell-cycle progression from G1 to S phase by localizing at the basolateral membrane in epithelial cells. Cancer Sci *97*, 1217-1225.

Nakagawa, M., Fukata, M., Yamaga, M., Itoh, N., and Kaibuchi, K. (2001). Recruitment and activation of Rac1 by the formation of E-cadherin-mediated cell-cell adhesion sites. J Cell Sci *114*, 1829-1838.

Nakagawa, S., and Huibregtse, J.M. (2000). Human scribble (Vartul) is targeted for ubiquitin-mediated degradation by the high-risk papillomavirus E6 proteins and the E6AP ubiquitin-protein ligase. Mol. Cell. Biol. *20*, 8244-8253.

Nakagawa, S., Yano, T., Nakagawa, K., Takizawa, S., Suzuki, Y., Yasugi, T., Huibregtse, J.M., and Taketani, Y. (2004). Analysis of the expression and localisation of a LAP protein, human scribble, in the normal and neoplastic epithelium of uterine cervix. Br J Cancer *90*, 194-199.

Nakanishi, H., and Takai, Y. (2004). Roles of nectins in cell adhesion, migration and polarization. Biol Chem *385*, 885-892.

Navarro, C., Nola, S., Audebert, S., Santoni, M.J., Arsanto, J.P., Ginestier, C., Marchetto, S., Jacquemier, J., Isnardon, D., Le Bivic, A., Birnbaum, D., and Borg, J.P. (2005). Junctional recruitment of mammalian Scribble relies on E-cadherin engagement. Oncogene *24*, 4330-4339.

Nayler, O., Stratling, W., Bourquin, J.P., Stagljar, I., Lindemann, L., Jasper, H., Hartmann, A.M., Fackelmayer, F.O., Ullrich, A., and Stamm, S. (1998). SAF-B protein couples transcription and pre-mRNA splicing to SAR/MAR elements. Nucleic Acids Res *26*, 3542-3549.

Nieminen, M., Henttinen, T., Merinen, M., Marttila-Ichihara, F., Eriksson, J.E., and Jalkanen, S. (2006). Vimentin function in lymphocyte adhesion and transcellular migration. Nat Cell Biol *8*, 156-162.

Nishiya, N., Kiosses, W.B., Han, J., and Ginsberg, M.H. (2005). An alpha4 integrin-paxillin-Arf-GAP complex restricts Rac activation to the leading edge of migrating cells. Nat Cell Biol *7*, 343-352.

Nogales, E., Wolf, S.G., and Downing, K.H. (1998). Structure of the alpha beta tubulin dimer by electron crystallography. Nature *391*, 199-203.

Nola, S., Sebbagh, M., Marchetto, S., Osmani, N., Nourry, C., Audebert, S., Navarro, C., Rachel, R., Montcouquiol, M., Sans, N., Etienne-Manneville, S., Borg, J.P., and Santoni,

M.J. (2008). Scrib regulates PAK activity during the cell migration process. Hum Mol Genet *17*, 3552-3565.

O'Brien, L.E., Jou, T.S., Pollack, A.L., Zhang, Q., Hansen, S.H., Yurchenco, P., and Mostov, K.E. (2001). Rac1 orientates epithelial apical polarity through effects on basolateral laminin assembly. Nat Cell Biol *3*, 831-838.

Omary, M.B., Coulombe, P.A., and McLean, W.H. (2004). Intermediate filament proteins and their associated diseases. N Engl J Med *351*, 2087-2100.

Oriolo, A.S., Wald, F.A., Ramsauer, V.P., and Salas, P.J. (2007). Intermediate filaments: a role in epithelial polarity. Exp Cell Res *313*, 2255-2264.

Osmani, N., Vitale, N., Borg, J.P., and Etienne-Manneville, S. (2006). Scrib controls Cdc42 localization and activity to promote cell polarization during astrocyte migration. Curr Biol *16*, 2395-2405.

Ozdamar, B., Bose, R., Barrios-Rodiles, M., Wang, H.R., Zhang, Y., and Wrana, J.L. (2005). Regulation of the polarity protein Par6 by TGFbeta receptors controls epithelial cell plasticity. Science *307*, 1603-1609.

Pagliarini, R.A., and Xu, T. (2003). A genetic screen in Drosophila for metastatic behavior. Science *302*, 1227-1231.

Parry, D.A., Strelkov, S.V., Burkhard, P., Aebi, U., and Herrmann, H. (2007). Towards a molecular description of intermediate filament structure and assembly. Exp Cell Res *313*, 2204-2216.

Peng, C.Y., Manning, L., Albertson, R., and Doe, C.Q. (2000). The tumour-suppressor genes lgl and dlg regulate basal protein targeting in Drosophila neuroblasts. Nature *408*, 596-600.

Perlson, E., Hanz, S., Ben-Yaakov, K., Segal-Ruder, Y., Seger, R., and Fainzilber, M. (2005). Vimentin-dependent spatial translocation of an activated MAP kinase in injured nerve. Neuron *45*, 715-726.

Petit, M.M., Crombez, K.R., Vervenne, H.B., Weyns, N., and Van de Ven, W.J. (2005a). The tumor suppressor Scrib selectively interacts with specific members of the zyxin family of proteins. FEBS Lett *579*, 5061-5068.

Petit, M.M., Meulemans, S.M., Alen, P., Ayoubi, T.A., Jansen, E., and Van de Ven, W.J. (2005b). The tumor suppressor Scrib interacts with the zyxin-related protein LPP, which shuttles between cell adhesion sites and the nucleus. BMC Cell Biol *6*, 1.

Phillips, H.M., Rhee, H.J., Murdoch, J.N., Hildreth, V., Peat, J.D., Anderson, R.H., Copp, A.J., Chaudhry, B., and Henderson, D.J. (2007). Disruption of planar cell polarity

signaling results in congenital heart defects and cardiomyopathy attributable to early cardiomyocyte disorganization. Circ Res *101*, 137-145.

Plant, P.J., Fawcett, J.P., Lin, D.C., Holdorf, A.D., Binns, K., Kulkarni, S., and Pawson, T. (2003). A polarity complex of mPar-6 and atypical PKC binds, phosphorylates and regulates mammalian Lgl. Nat Cell Biol *5*, 301-308.

Prahlad, V., Yoon, M., Moir, R.D., Vale, R.D., and Goldman, R.D. (1998). Rapid movements of vimentin on microtubule tracks: kinesin-dependent assembly of intermediate filament networks. J Cell Biol *143*, 159-170.

Qin, Y., Capaldo, C., Gumbiner, B.M., and Macara, I.G. (2005). The mammalian Scribble polarity protein regulates epithelial cell adhesion and migration through E-cadherin. J Cell Biol *171*, 1061-1071.

Rajasekaran, A.K., Hojo, M., Huima, T., and Rodriguez-Boulan, E. (1996). Catenins and zonula occludens-1 form a complex during early stages in the assembly of tight junctions. J Cell Biol *132*, 451-463.

Redfield, A., Nieman, M.T., and Knudsen, K.A. (1997). Cadherins promote skeletal muscle differentiation in three-dimensional cultures. J. Cell Biol. *138*, 1323-1331.

Reichert, M., Muller, T., and Hunziker, W. (2000). The PDZ domains of zonula occludens-1 induce an epithelial to mesenchymal transition of Madin-Darby canine kidney I cells. Evidence for a role of beta-catenin/Tcf/Lef signaling. J Biol Chem *275*, 9492-9500.

Ridley, A.J., Schwartz, M.A., Burridge, K., Firtel, R.A., Ginsberg, M.H., Borisy, G., Parsons, J.T., and Horwitz, A.R. (2003). Cell migration: integrating signals from front to back. Science *302*, 1704-1709.

Roche, J.P., Packard, M.C., Moeckel-Cole, S., and Budnik, V. (2002). Regulation of synaptic plasticity and synaptic vesicle dynamics by the PDZ protein Scribble. J Neurosci *22*, 6471-6479.

Rodriguez-Boulan, E., Kreitzer, G., and Musch, A. (2005). Organization of vesicular trafficking in epithelia. Nat Rev Mol Cell Biol *6*, 233-247.

Roh, M.H., Liu, C.J., Laurinec, S., and Margolis, B. (2002a). The carboxyl terminus of zona occludens-3 binds and recruits a mammalian homologue of discs lost to tight junctions. J Biol Chem *277*, 27501-27509.

Roh, M.H., Makarova, O., Liu, C.J., Shin, K., Lee, S., Laurinec, S., Goyal, M., Wiggins, R., and Margolis, B. (2002b). The Maguk protein, Pals1, functions as an adapter, linking mammalian homologues of Crumbs and Discs Lost. J Cell Biol *157*, 161-172.

Rosevear, E.R., McReynolds, M., and Goldman, R.D. (1990). Dynamic properties of intermediate filaments: disassembly and reassembly during mitosis in baby hamster kidney cells. Cell Motil Cytoskeleton *17*, 150-166.

Saito, H., Santoni, M.J., Arsanto, J.P., Jaulin-Bastard, F., Le Bivic, A., Marchetto, S., Audebert, S., Isnardon, D., Adelaide, J., Birnbaum, D., and Borg, J.P. (2001). Lano, a novel LAP protein directly connected to MAGUK proteins in epithelial cells. J Biol Chem *276*, 32051-32055.

Salas, P.J. (1999). Insoluble gamma-tubulin-containing structures are anchored to the apical network of intermediate filaments in polarized CACO-2 epithelial cells. J Cell Biol *146*, 645-658.

Santoni, M.J., Pontarotti, P., Birnbaum, D., and Borg, J.P. (2002). The LAP family: a phylogenetic point of view. Trends Genet *18*, 494-497.

Schmidt, A., Utepbergenov, D.I., Mueller, S.L., Beyermann, M., Schneider-Mergener, J., Krause, G., and Blasig, I.E. (2004). Occludin binds to the SH3-hinge-GuK unit of zonula occludens protein 1: potential mechanism of tight junction regulation. Cell Mol Life Sci *61*, 1354-1365.

Senda, T., Iizuka-Kogo, A., Onouchi, T., and Shimomura, A. (2007). Adenomatous polyposis coli (APC) plays multiple roles in the intestinal and colorectal epithelia. Med Mol Morphol *40*, 68-81.

Shen, L., Weber, C.R., and Turner, J.R. (2008). The tight junction protein complex undergoes rapid and continuous molecular remodeling at steady state. J Cell Biol *181*, 683-695.

Sheth, B., Nowak, R.L., Anderson, R., Kwong, W.Y., Papenbrock, T., and Fleming, T.P. (2008). Tight junction protein ZO-2 expression and relative function of ZO-1 and ZO-2 during mouse blastocyst formation. Exp Cell Res *314*, 3356-3368.

Shin, K., Straight, S., and Margolis, B. (2005). PATJ regulates tight junction formation and polarity in mammalian epithelial cells. J Cell Biol *168*, 705-711.

Shin, K., Wang, Q., and Margolis, B. (2007). PATJ regulates directional migration of mammalian epithelial cells. EMBO Rep *8*, 158-164.

Sieburth, D.S., Sun, Q., and Han, M. (1998). SUR-8, a conserved Ras-binding protein with leucine-rich repeats, positively regulates Ras-mediated signaling in C. elegans. Cell *94*, 119-130.

Snapper, S.B., Takeshima, F., Anton, I., Liu, C.H., Thomas, S.M., Nguyen, D., Dudley, D., Fraser, H., Purich, D., Lopez-Ilasaca, M., Klein, C., Davidson, L., Bronson, R., Mulligan, R.C., Southwick, F., Geha, R., Goldberg, M.B., Rosen, F.S., Hartwig, J.H., and

Alt, F.W. (2001). N-WASP deficiency reveals distinct pathways for cell surface projections and microbial actin-based motility. Nat Cell Biol *3*, 897-904.

Sone, K., Nakagawa, S., Nakagawa, K., Takizawa, S., Matsumoto, Y., Nagasaka, K., Tsuruga, T., Hiraike, H., Hiraike-Wada, O., Miyamoto, Y., Oda, K., Yasugi, T., Kugu, K., Yano, T., and Taketani, Y. (2008). hScrib, a human homologue of Drosophila neoplastic tumor suppressor, is a novel death substrate targeted by caspase during the process of apoptosis. Genes Cells *13*, 771-785.

Sotillos, S., Diaz-Meco, M.T., Caminero, E., Moscat, J., and Campuzano, S. (2004). DaPKC-dependent phosphorylation of Crumbs is required for epithelial cell polarity in Drosophila. J Cell Biol *166*, 549-557.

Sourisseau, T., Georgiadis, A., Tsapara, A., Ali, R.R., Pestell, R., Matter, K., and Balda, M.S. (2006). Regulation of PCNA and cyclin D1 expression and epithelial morphogenesis by the ZO-1-regulated transcription factor ZONAB/DbpA. Mol Cell Biol *26*, 2387-2398.

Stevenson, B.R., Siliciano, J.D., Mooseker, M.S., and Goodenough, D.A. (1986). Identification of ZO-1: a high molecular weight polypeptide associated with the tight junction (zonula occludens) in a variety of epithelia. J Cell Biol *103*, 755-766.

Straight, S.W., Shin, K., Fogg, V.C., Fan, S., Liu, C.J., Roh, M., and Margolis, B. (2004). Loss of PALS1 expression leads to tight junction and polarity defects. Mol Biol Cell *15*, 1981-1990.

Strand, D., Jakobs, R., Merdes, G., Neumann, B., Kalmes, A., Heid, H.W., Husmann, I., and Mechler, B.M. (1994). The Drosophila lethal(2)giant larvae tumor suppressor protein forms homo-oligomers and is associated with nonmuscle myosin II heavy chain. J Cell Biol *127*, 1361-1373.

Strand, D., Unger, S., Corvi, R., Hartenstein, K., Schenkel, H., Kalmes, A., Merdes, G., Neumann, B., Krieg-Schneider, F., Coy, J.F., and et al. (1995). A human homologue of the Drosophila tumour suppressor gene l(2)gl maps to 17p11.2-12 and codes for a cytoskeletal protein that associates with nonmuscle myosin II heavy chain. Oncogene *11*, 291-301.

Strelkov, S.V., Herrmann, H., and Aebi, U. (2003). Molecular architecture of intermediate filaments. Bioessays *25*, 243-251.

Strelkov, S.V., Kreplak, L., Herrmann, H., and Aebi, U. (2004). Intermediate filament protein structure determination. Methods Cell Biol *78*, 25-43.

Styers, M.L., Salazar, G., Love, R., Peden, A.A., Kowalczyk, A.P., and Faundez, V. (2004). The endo-lysosomal sorting machinery interacts with the intermediate filament cytoskeleton. Mol Biol Cell *15*, 5369-5382.

Sugimoto, M., Inoko, A., Shiromizu, T., Nakayama, M., Zou, P., Yonemura, S., Hayashi, Y., Izawa, I., Sasoh, M., Uji, Y., Kaibuchi, K., Kiyono, T., and Inagaki, M. (2008). The keratin-binding protein Albatross regulates polarization of epithelial cells. J Cell Biol *183*, 19-28.

Suzuki, A., Ishiyama, C., Hashiba, K., Shimizu, M., Ebnet, K., and Ohno, S. (2002). aPKC kinase activity is required for the asymmetric differentiation of the premature junctional complex during epithelial cell polarization. J Cell Sci *115*, 3565-3573.

Suzuki, T., Ohsugi, Y., Uchida-Toita, M., Akiyama, T., and Yoshida, M. (1999). Tax oncoprotein of HTLV-1 binds to the human homologue of Drosophila discs large tumor suppressor protein, hDLG, and perturbs its function in cell growth control. Oncogene *18*, 5967-5972.

Takai, E., Tan, X., Tamori, Y., Hirota, M., Egami, H., and Ogawa, M. (2005). Correlation of translocation of tight junction protein Zonula occludens-1 and activation of epidermal growth factor receptor in the regulation of invasion of pancreatic cancer cells. Int J Oncol *27*, 645-651.

Takizawa, S., Nagasaka, K., Nakagawa, S., Yano, T., Nakagawa, K., Yasugi, T., Takeuchi, T., Kanda, T., Huibregtse, J.M., Akiyama, T., and Taketani, Y. (2006). Human scribble, a novel tumor suppressor identified as a target of high-risk HPV E6 for ubiquitin-mediated degradation, interacts with adenomatous polyposis coli. Genes Cells *11*, 453-464.

Tang, V.W. (2006). Proteomic and bioinformatic analysis of epithelial tight junction reveals an unexpected cluster of synaptic molecules. Biol Direct *1*, 37.

ten Klooster, J.P., Jaffer, Z.M., Chernoff, J., and Hordijk, P.L. (2006). Targeting and activation of Rac1 are mediated by the exchange factor beta-Pix. J Cell Biol *172*, 759-769.

Thiery, J.P., and Sleeman, J.P. (2006). Complex networks orchestrate epithelial-mesenchymal transitions. Nat Rev Mol Cell Biol *7*, 131-142.

Thomas, M., Pim, D., and Banks, L. (1999). The role of the E6-p53 interaction in the molecular pathogenesis of HPV. Oncogene *18*, 7690-7700.

Thomas, U., Phannavong, B., Muller, B., Garner, C.C., and Gundelfinger, E.D. (1997). Functional expression of rat synapse-associated proteins SAP97 and SAP102 in Drosophila dlg-1 mutants: effects on tumor suppression and synaptic bouton structure. Mech Dev *62*, 161-174.

Toivola, D.M., Tao, G.Z., Habtezion, A., Liao, J., and Omary, M.B. (2005). Cellular integrity plus: organelle-related and protein-targeting functions of intermediate filaments. Trends Cell Biol *15*, 608-617.

Traweger, A., Fuchs, R., Krizbai, I.A., Weiger, T.M., Bauer, H.C., and Bauer, H. (2003). The tight junction protein ZO-2 localizes to the nucleus and interacts with the heterogeneous nuclear ribonucleoprotein scaffold attachment factor-B. J Biol Chem *278*, 2692-2700.

Tsukita, S., Furuse, M., and Itoh, M. (2001). Multifunctional strands in tight junctions. Nat Rev Mol Cell Biol *2*, 285-293.

Tsuruta, D., and Jones, J.C. (2003). The vimentin cytoskeleton regulates focal contact size and adhesion of endothelial cells subjected to shear stress. J Cell Sci *116*, 4977-4984.

Umeda, K., Ikenouchi, J., Katahira-Tayama, S., Furuse, K., Sasaki, H., Nakayama, M., Matsui, T., Tsukita, S., and Furuse, M. (2006). ZO-1 and ZO-2 independently determine where claudins are polymerized in tight-junction strand formation. Cell *126*, 741-754.

Utepbergenov, D.I., Fanning, A.S., and Anderson, J.M. (2006). Dimerization of the scaffolding protein ZO-1 through the second PDZ domain. J Biol Chem *281*, 24671-24677.

Vaccari, T., and Bilder, D. (2005). The Drosophila tumor suppressor vps25 prevents nonautonomous overproliferation by regulating notch trafficking. Dev Cell *9*, 687-698.

Van Itallie, C.M., and Anderson, J.M. (1997). Occludin confers adhesiveness when expressed in fibroblasts. J Cell Sci *110*, 1113-1121.

Vikstrom, K.L., Lim, S.S., Goldman, R.D., and Borisy, G.G. (1992). Steady state dynamics of intermediate filament networks. J Cell Biol *118*, 121-129.

Virtanen, I., Lehto, V.P., Lehtonen, E., Vartio, T., Stenman, S., Kurki, P., Wager, O., Small, J.V., Dahl, D., and Badley, R.A. (1981). Expression of intermediate filaments in cultured cells. J Cell Sci *50*, 45-63.

Wada, H., Iwasaki, M., Sato, T., Masai, I., Nishiwaki, Y., Tanaka, H., Sato, A., Nojima, Y., and Okamoto, H. (2005). Dual roles of zygotic and maternal Scribble1 in neural migration and convergent extension movements in zebrafish embryos. Development *132*, 2273-2285.

Wald, F.A., Oriolo, A.S., Casanova, M.L., and Salas, P.J. (2005). Intermediate filaments interact with dormant ezrin in intestinal epithelial cells. Mol Biol Cell *16*, 4096-4107.

Wang, B., Wylie, F.G., Teasdale, R.D., and Stow, J.L. (2005). Polarized trafficking of E-cadherin is regulated by Rac1 and Cdc42 in Madin-Darby canine kidney cells. Am J Physiol Cell Physiol *288*, C1411-1419.

Wang, H.R., Zhang, Y., Ozdamar, B., Ogunjimi, A.A., Alexandrova, E., Thomsen, G.H., and Wrana, J.L. (2003). Regulation of cell polarity and protrusion formation by targeting RhoA for degradation. Science *302*, 1775-1779.

Wang, Q., Chen, X.W., and Margolis, B. (2007). PALS1 regulates E-cadherin trafficking in mammalian epithelial cells. Mol Biol Cell *18*, 874-885.

Watson, R.A., Rollason, T.P., Reynolds, G.M., Murray, P.G., Banks, L., and Roberts, S. (2002). Changes in expression of the human homologue of the Drosophila discs large tumour suppressor protein in high-grade premalignant cervical neoplasias. Carcinogenesis *23*, 1791-1796.

Welch, M.D., and Mullins, R.D. (2002). Cellular control of actin nucleation. Annu Rev Cell Dev Biol *18*, 247-288.

Werme, K., Wigerius, M., and Johansson, M. (2008). Tick-borne encephalitis virus NS5 associates with membrane protein scribble and impairs interferon-stimulated JAK-STAT signalling. Cell Microbiol *10*, 696-712.

Wilson, P.D. (1997). Epithelial cell polarity and disease. Am J Physiol *272*, F434-442.

Windoffer, R., Kolsch, A., Woll, S., and Leube, R.E. (2006). Focal adhesions are hotspots for keratin filament precursor formation. J Cell Biol *173*, 341-348.

Windoffer, R., and Leube, R.E. (2001). De novo formation of cytokeratin filament networks originates from the cell cortex in A-431 cells. Cell Motil Cytoskeleton *50*, 33-44.

Windoffer, R., Woll, S., Strnad, P., and Leube, R.E. (2004). Identification of novel principles of keratin filament network turnover in living cells. Mol Biol Cell *15*, 2436-2448.

Wittchen, E.S., Haskins, J., and Stevenson, B.R. (2000). Exogenous expression of the amino-terminal half of the tight junction protein ZO-3 perturbs junctional complex assembly. J Cell Biol *151*, 825-836.

Wittchen, E.S., Haskins, J., and Stevenson, B.R. (2003). NZO-3 expression causes global changes to actin cytoskeleton in Madin-Darby canine kidney cells: linking a tight junction protein to Rho GTPases. Mol Biol Cell *14*, 1757-1768.

Wodarz, A., and Nathke, I. (2007). Cell polarity in development and cancer. Nat Cell Biol *9*, 1016-1024.

Woods, D.F., and Bryant, P.J. (1989). Molecular cloning of the lethal(1)discs large-1 oncogene of Drosophila. Dev Biol *134*, 222-235.

Woods, D.F., Hough, C., Peel, D., Callaini, G., and Bryant, P.J. (1996). Dlg protein is required for junction structure, cell polarity, and proliferation control in Drosophila epithelia. J Cell Biol *134*, 1469-1482.

Xu, J., Kausalya, P.J., Phua, D.C., Ali, S.M., Hossain, Z., and Hunziker, W. (2008). Early embryonic lethality of mice lacking ZO-2, but Not ZO-3, reveals critical and nonredundant roles for individual zonula occludens proteins in mammalian development. Mol Cell Biol *28*, 1669-1678.

Yamanaka, T., Horikoshi, Y., Izumi, N., Suzuki, A., Mizuno, K., and Ohno, S. (2006). Lgl mediates apical domain disassembly by suppressing the PAR-3-aPKC-PAR-6 complex to orient apical membrane polarity. J Cell Sci *119*, 2107-2118.

Yamanaka, T., Horikoshi, Y., Sugiyama, Y., Ishiyama, C., Suzuki, A., Hirose, T., Iwamatsu, A., Shinohara, A., and Ohno, S. (2003). Mammalian Lgl forms a protein complex with PAR-6 and aPKC independently of PAR-3 to regulate epithelial cell polarity. Curr Biol *13*, 734-743.

Yamanaka, T., Horikoshi, Y., Suzuki, A., Sugiyama, Y., Kitamura, K., Maniwa, R., Nagai, Y., Yamashita, A., Hirose, T., Ishikawa, H., and Ohno, S. (2001). PAR-6 regulates aPKC activity in a novel way and mediates cell-cell contact-induced formation of the epithelial junctional complex. Genes Cells *6*, 721-731.

Yeh, J.H., Sidhu, S.S., and Chan, A.C. (2008). Regulation of a late phase of T cell polarity and effector functions by Crtam. Cell *132*, 846-859.

Yokoyama, S., Tachibana, K., Nakanishi, H., Yamamoto, Y., Irie, K., Mandai, K., Nagafuchi, A., Monden, M., and Takai, Y. (2001). alpha-catenin-independent recruitment of ZO-1 to nectin-based cell-cell adhesion sites through afadin. Mol Biol Cell *12*, 1595-1609.

Yoon, M., Moir, R.D., Prahlad, V., and Goldman, R.D. (1998). Motile properties of vimentin intermediate filament networks in living cells. J Cell Biol *143*, 147-157.

Yu, W., Datta, A., Leroy, P., O'Brien, L.E., Mak, G., Jou, T.S., Matlin, K.S., Mostov, K.E., and Zegers, M.M. (2005). Beta1-integrin orients epithelial polarity via Rac1 and laminin. Mol Biol Cell *16*, 433-445.

Zallen, J.A. (2007). Planar polarity and tissue morphogenesis. Cell *129*, 1051-1063.
Zeitler, J., Hsu, C.P., Dionne, H., and Bilder, D. (2004). Domains controlling cell polarity and proliferation in the Drosophila tumor suppressor Scribble. J Cell Biol *167*, 1137-1146.

Zhang, Y., Yeh, S., Appleton, B.A., Held, H.A., Kausalya, P.J., Phua, D.C., Wong, W.L., Lasky, L.A., Wiesmann, C., Hunziker, W., and Sidhu, S.S. (2006). Convergent and

divergent ligand specificity among PDZ domains of the LAP and zonula occludens (ZO) families. J Biol Chem *281*, 22299-22311.

Zhao, Y., Yan, Q., Long, X., Chen, X., and Wang, Y. (2008). Vimentin affects the mobility and invasiveness of prostate cancer cells. Cell Biochem Funct *26*, 571-577.

Zohn, I.E., Chesnutt, C.R., and Niswander, L. (2003). Cell polarity pathways converge and extend to regulate neural tube closure. Trends Cell Biol *13*, 451-454.